University of Siena

PhD in Medical Genetics

Molecular work-up of patients with the congenital variant of Rett syndrome: analysis of the 14q12 region

Ariele Spanhol Rosseto

Supervisor: Prof. Alessandra Renieri

Thesis suitable for the title of *"Doctor Europaeus"*

Academic year 2009-2010
cycle XXII

Ph.D. dissertation board

Prof. Mandich Paola
Department of Oncology, Biology and Genetics, University of Genova and U.O. Medical Genetics of Azienda Ospedaliera, Universitaria S. Martino di Genova, Italy

Prof. V.Kucinskas
Dept. Human and Medical Genetics, Faculty of Medicine
Vilnius University, Director Center for Medical Genetics
Vilnius University Hospital Vilnius, Lithuania.

Prof. Tecce Mario
Professor of Biochemistry,
Department of Pharmaceutical Sciences,
University of Salerno, Italy

Ph.D. thesis reviewers:

Prof. Jon J. Jonsson
Dept. of Genetics and Molecular Medicine
Landspitali - University Hospital
On Hringbraut, Reykjavik
Iceland

Prof. Suzanna. Frints
Associate Professor, Clinical Geneticist
Department of Clinical Genetics,
Prenatal Diagnosis and Therapy,
Maastricht University Medical Center,
Maastricht, The Netherlands

Abstract

Rett syndrome is a severe neurodevelopmental disorder and it is the second most common cause of mental retardation in females. Beside the most common classic form, due to *MECP2* mutations, a number of variants have been observed. For some of these variants mutations in *MECP2* or in a second gene, *CDKL5*, have been identified. However, for other variants, such as the congenital, the molecular defect remained unknown. During my Ph.D program, I worked on a project aimed to dissect the molecular bases of Rett Syndrome (RTT) cases negative for mutations in *MECP2* and *CDKL5* genes. In particular, by candidate gene approach, we have identified *FOXG1* as the gene responsible for the congenital variant of RTT. More recently, we identified mutations in this gene also in patients with the milder forme fruste variant. *FOXG1* gene, located in 14q12, encodes for a brain-specific transcriptional factor. A total of 22 cases have been reported to date with a *FOXG1* alteration: eight deletions, one duplication, one inversion and twelve point mutations. Even though the reported cases are still few and genotype phenotype correlation cannot be performed, there seems to be no difference in the neurological phenotype between patients with chromosome alteration on and patients with point mutations. In conclusion, this work underlines the importance to perform *FOXG1* mutation analysis for both deletions and point mutations in patients with a phenotype resembling the congenital RTT

prior to the analysis of *MECP2* gene, and in patients with RTT features, negative for mutations in the other genes.

Index

1. Introduction

1. Introduction

Rett syndrome (RTT, OMIM#312750) is a neurodevelopmental disorder that represents one of the most common genetic causes of mental retardation in girls. It was first described by Andreas Rett, an Austrian pediatrician, in 1966, but it only became known worldwide in 1983 with the publication by Hagberg et al. in Annals of Neurology [1, 2]. RTT is now recognized as a distinct clinical entity with an estimated prevalence of 1 in 10.000 female births [3]. RTT phenotype is broad and, in addition to a classic form, a number of variants have been described including the congenital, the early onset seizures, the forme fruste and the Zappella variant [4, 5]. Since more than 99% of RTT cases are sporadic, it was very hard to map the disease locus by traditional linkage analysis. Using information from rare familial cases, exclusion mapping identified the Xq28 candidate region, and subsequent screening of candidate genes in RTT patients revealed mutations in *MECP2* gene (Methyl-CpG-binding Protein 2) [6]. *MECP2* mutations account for approximately 95% of cases with classic RTT [3]. However, a large degree of phenotypic variability has been observed in individuals with *MECP2* mutations. In fact, soon after the discovery of *MECP2* as the gene causing classic RTT, we and others demonstrated that the milder preserved speech variant ”PSV” (now renamed Zappella variant) is allelic to the classic form [6, 7]. Furthermore, in our Italian cohort of patients, we have described a “highly functioning PSV” associated with acquisition of more complex language functions

including use of first person phrases also due to *MECP2* mutations [5]. However, the percentage of variant patients with *MECP2* mutations is lower compared to the classic form (about 20-40%). *MECP2* mutations have been identified also in male patients with variable phenotypes. In 2000, our group described a family in which a *MECP2* mutation segregated in male patients with recessive X-linked mental retardation (XLMR) and spasticity [8]. Other studies identified *MECP2* mutations in patients with non specific mental retardation, with severe neonatal encephalopathy, with language disorder and schizophrenia, with psychosis, pyramidal signs, and macro-orchidism (PPM-X), with Angelman syndrome (AS) and with infantile autism[8-12]. The spectrum of mutations in Rett patients includes missense, nonsense, and frameshift mutations, with over 300 unique pathogenic nucleotide changes described (http://mecp2.chw.edu.au/; http://www.biobank.unisi.it) [13]. Deletions and inactivating mutations of *MECP2* have been associated with a Rett-like syndrome characterized by hypotonia, irritability, developmental delay, hand stereotypies, and deceleration of head growth [14].

Subsequently, another X–linked gene, *CDKL5* (Cyclin-dependent Kinase like 5; OMIM #300203; also known as serine threonine kinase 9-STK9) has been shown to be responsible for a variant of RTT, namely the early onset seizures variant [9, 15, 16]. Mutations in this gene have been also shown to cause other severe neurodevelopmental disorders including infantile spasms, encephalopathy, and West-syndrome.

In spite of the intense research efforts that resulted in the identification of *MECP2* and *CDKL5* genes, for many RTT variant patients the molecular defect is still unknown. In particular, for some variants, such as the congenital variant, no mutations in *MECP2* or *CDKL5* have been identified, suggesting the involvement of one or more additional genes. Recently, our group identified by array–CGH analysis a *de novo* interstitial deletion of chromosome 14 in a patient with a complex phenotype including severe neurological impairment, dyspraxia, stereotypies, gastro esophageal reflux, constipation, scoliosis and cold extremities together with a normal perinatal period. Only five genes were included in the region: *FOXG1B, PRKD1, SCFD1, COCH* and *STRN3*. The clinical history and the neurological features of the patient were evocative of a Rett spectrum disorder, we thus decided to screen these genes, and in particular *FOXG1B*, for mutations in RTT patients without a molecular diagnosis [17].

1.1 Clinical features

The current guidelines for the diagnosis of RTT are based on the criteria established by Hagberg, [11, 18-20]. For classic RTT these criteria include a period of normal development, during which girls reach motor, language and social milestones at the expected rate and age. Their neurological development is then arrested and begins to regress according to a predictable course that comprises four stages. During **Stage I** (6-18 months), patients cease to acquire new skills; they show decelerating head growth and autistic features. In **Stage II** (1-4 years), RTT girls lose the ability to speak and the purposeful use of the hands. During this stage, patients show the classic 'hand-washing' stereotypic activity, irregular breathing patterns, truncal and gait ataxia/apraxia; about half of them also develop seizures. In **Stage III** (4-7 years), girls become more alert and interested both in people and their surroundings; however inability to speak, hand apraxia and stereotypic hand activities persist. Other somatic and neurologic handicaps, such as severe scoliosis, reduced somatic growth and epilepsy, become evident during this period. During **Stage IV** (5-15 years and older), seizures become less frequent, but somatic and neurologic deterioration continues, resulting in spastic quadriparesis.

In addition to the classic form described above, several RTT variants have been described. These variants have some, but not all diagnostic features of RTT and can be milder or more severe. In particular, five distinct categories of atypical cases have been delineated on the bases of clinical criteria i) the

Zappella variant (previously known as the Preserved Speech Variant- “PSV”), in which girls recover the ability to speak in single words and third person phrases and display an improvement of purposeful hand movements at Stage 3 of disease progression; ii) the early-onset seizure variant, with seizure onset before regression; iii) "forme fruste" with a milder and incomplete clinical course (regression between 1 and 3 years); iv) the congenital variant, in which affected girls appear floppy and retarded since the very first months of life and thus lack the normal perinatal period typical of classic RTT; v) the late regression variant, which is rare and still controversial. Furthermore, we have described a “highly functioning PSV” associated with acquisition of more complex language function including use of first person phrases [4, 18, 21]. In this variant, girls acquire a better control of their hands and they are able to draw figures and write simple words. The degree of mental retardation in these girls is also milder than in the Zappella variant and their I.Q. can be as high as 50 [22, 23].

For my project I focused mainly on patients with variant phenotypes.

1.2 Genes involved in Rett Syndrome

1.2.1 MECP2

MeCP2 protein is encoded by a four-exon gene located in Xq28 [7] (Fig.1 and 2A). Two MeCP2 isoforms that differ in the N-terminus are generated by alternative splicing of exon 2. The first identified isoform, MeCP2A, uses a translational start site within exon 2, whereas the other isoform, MeCP2B results from an mRNA in which exon 2 is excluded, and a new in-frame ATG located within exon 1 is used (Fig.2b) [24, 25]. Interestingly, MeCP2B is predominantly expressed in brain, while MeCP2A is more abundant in other tissues, such as fibroblast and lymphoblast cells [25].

MeCP2 protein has different functional domains (Fig.2a and Fig.3): a nuclear localization signal; the methyl-CpG binding domain (MBD), that binds to symmetrically methylated CpGs islands; and the transcriptional repression domain (TRD), which is able to recruit co-repressor complexes, that mediate gene silencing through deacetylation of core histones [26, 27]. In particular, MeCP2-mediated gene silencing occurs through chromatin modifications mediated by its interaction with Sin3A/HDACI or Ski/NcoR/HDACII repression complexes that remodel chromatin, which become inaccessible to the transcriptional machinery [27, 28]. Furthermore, the interaction of MeCP2 with the basal transcriptional machinery suggest its involvement also in chromatin-independent transcriptional repression [29]. Considering these data MeCP2 has been long considered to be essentially a global transcriptional repressor [30]. However, MeCP2 involvement in other

processes has been demonstrated. In fact, it has been also implicated in maintaining imprinting through chromatin looping [31]. Moreover, in 2005, it has been demonstrated that MeCP2 acts as a splicing regulator [32]. In fact, authors identified the RNA-binding protein Y box-binding protein 1 (YB1), a principal component of messenger ribonucleoprotein particles that controls multiple step of mRNA processing, as a MeCP2 binding partner [32]. They also showed that in MeCP2-deficient neurons, splicing is altered, and aberrantly spliced transcripts can be produced [33]. More recently expression profiling studies demonstrated that MeCP2 activates and represses transcription [34].

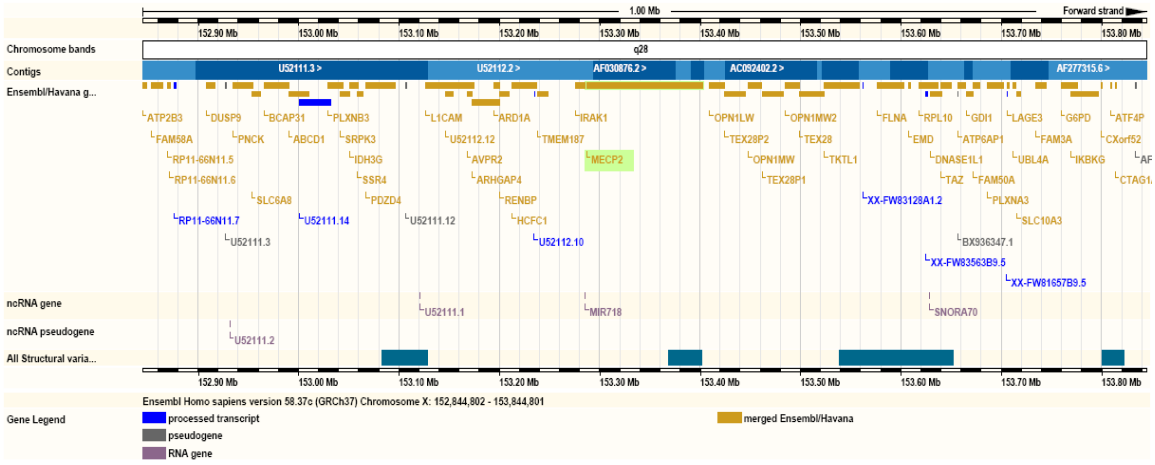

Figure 1. *MECP2* gene localization according to Ensembl data-base, *MECP2* gene (in green) is located on the X chromosome in Xq28 [153,287,024-153,402,578].

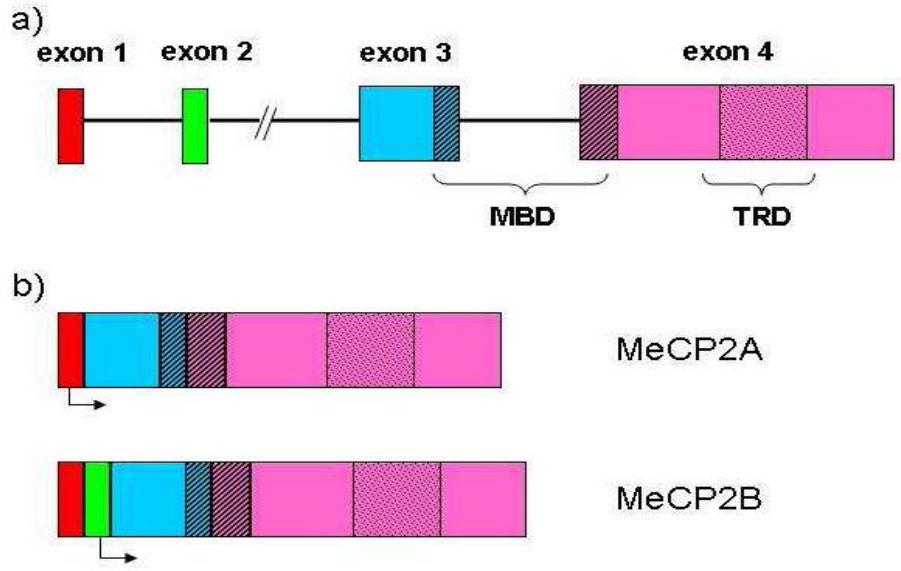

Figure 2. *MECP2* gene and its splicing isoforms:
a) Structure of *MECP2* gene with its 4 exons (outlined in different colours). The regions encoding the MBD (Methyl-CpG Binding Domain) and the TRD (Trascriptional Repression Domain) are indicated.
b) The two alternatively spliced *MECP2* trancripts, excluding or including exon 2 (in green), corresponding to MeCP2A and MeCP2B protein isoforms, respectively. The arrows show the position of the translationn initiation codons.

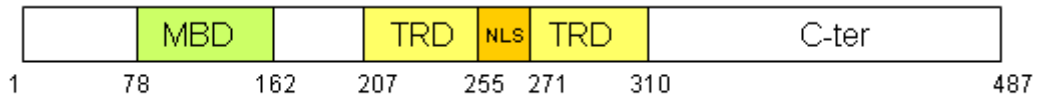

Figure 3. MeCP2 protein structure with its functional domains is shown: MBD: methyl binding domain; TRD: transcription repression domain; NLS: nuclear localisation signal; C-ter: C-terminal domain. The numbers refer to the aminoacid positions.

1.2.2 CDKL5

Cyclin-dependent kinase-like 5 (*CDKL5/STK9*, OMIM#300203) is an X–linked gene located at Xp22. The gene contains 21 exons and it encodes for a large protein of 1030 amino acids with an estimated molecular mass of 116 kDa. It is responsible for a variant of RTT, namely the early onset seizures variant [9, 35].

Mutations in *CDKL5* have been reported also in patients with X-linked infantile spasms (ISSX) (OMIM#308350). Patients with a deleterious mutation in *CDKL5* share the common features of mental retardation, early-onset seizures and very often Rett-like features [36]. The seizure disorder is polymorphic and is mainly characterized by complex partial seizures, infantile spasms, myoclonic, generalized tonic–clonic seizures and tonic seizures. No unique EEGs pattern was identified, since it seems to vary with age and seizures type, as recently described by Bahi-Buisson [37]. Psychomotor development results severely impaired since the first clinical or neurological examinations, usually performed at the epilepsy onset. Severe neurological impairment is reported [9].

CDKL5 is a kinase protein that shuttles between the cytoplasm and the nucleus; accordingly, a nuclear export signal, responsible for protein localization to the cytoplasm, has been identified in the the C-terminal tail (Fig. 4). Two putative nuclear localization signals have also been identified [38].

A direct interaction of CDKL5 with MeCP2 has been demonstrated [15]. Moreover, the 2 proteins have overlapping expression in the nervous system. This fact, toghether with CDKL5 ability to to mediate MeCP2 phosphorylation, suggests that they belong to the same molecular pathway [15]. In line with this hypothesis, it has been recently demonstrated that, like MeCP2, also CDKL5 can bind to the N-terminal domain of Dnmt1. However, MeCP2 and CDKL5 bind to different regions of this domain. Specifically, MeCP2 binds to the Zn-finger-like sequence, while CDKL5 binds to the very N-terminal domain. This difference indicates that MeCP2 and CDKL5 may be able to bind simultaneously to Dnmt1 and form a multiprotein complex with this protein. The interactions of Dnmt1 with both MeCP2 and CDKL5 suggest that Dnmt1 might be involved in the pathogenic processes of RTT [39].

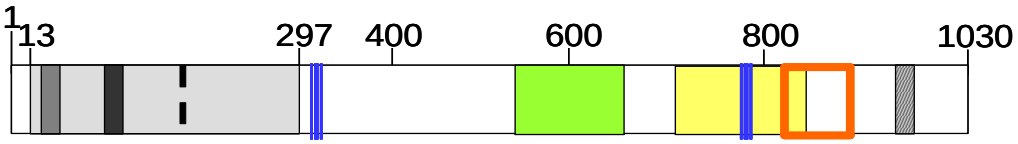

Figure 4. Schematic representation of the CDKL5 protein, the catalytic kinase domain (gray box) contains an ATP binding site (dark gray box) and the serine–threonine protein kinase active site (black box). The Thr-Glu-Tyr (TEY) motif in this domain is indicated by a black dashed line. The Putative NLS are indicated with blue lines. The MECP2 interaction domain (green box), and the DNMT1 interaction domain (yellow box) are also indicated. The orange square corresponds to the nuclear export signal. The signal peptidases I Serine active site, located in the C-terminal region of the protein, is represented by the striped box. Numbers at the top refer to the amino acid positions.

1.3 FOXG1B

FOXG1B gene (OMIM#164874), located on chromosome 14, encodes forkhead box protein G1, *FoxG1* (formerly brain factor 1 [BF-1]). FoxG1 is a transcription factor. Three functional domains have been identified in the protein (Figure 5): 1- A Fork-Head Domain allows the protein to directly bind DNA; 2- A JARID1B-binding domain. JARID1B is a demethylase that plays an important role in regulating chromatin dynamics; it is capable of removing three methyl groups from histone H3 lysine 4 and it can regulate gene transcription either alone or as part of a multimolecular complex together with FoxG1. 3- A Groucho-binding domain that allows the interaction with global transcriptional co-repressors of the Groucho family that act as both a corepressor and an adapter.

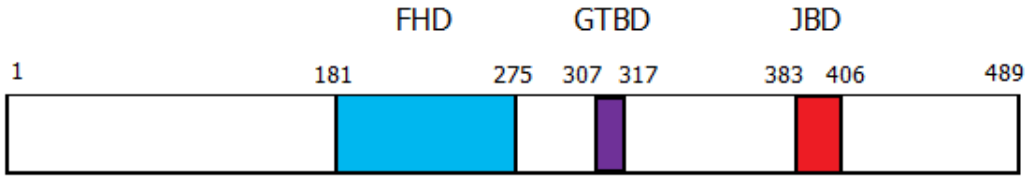

Figure 5. FoxG1 protein Functional Domains:
The three main functional domains of FoxG1 protein are shown: the DNA binding fork-head domain in light blue (FHD), the Groucho-binding domain in violet (GTBD), and the JARID1B binding domain in red (JBD). The numbers at the top refer to amino acid positions.

FoxG1 also indirectly associates with the histone deacetylase 1 protein [34, 64, 65].

Foxg1 is potentially a strong candidate gene for determining forebrain size in vertebrates due to its role in the development of the telencephalon, where it promotes progenitor proliferation and suppresses premature neurogenesis [11]. It is one of the earliest transcription factors to be expressed in the part of the neural plate from which telencephalon develops. It is strongly expressed in the proliferating neuroepitelium other than the developing retina, optic stalks and superior culliculus. In particular, several studies have implicated FoxG1 in regulating cortical arealization, expansion of the cortical progenitor pool and regulation of progenitor cell–cycle length [40-45]. Accordingly, *Foxg1* mutant brains show a remarkable reduction of the telencephalic vesicles due to a severely compromised growth of the telencephalon and absence of ventral tissue [40, 44, 46, 47]. On the contrary, Foxg1 overexpression results in the proliferation of progenitor cells and suppression of neuronal differentiation [40]. The observed telencephalic hypoplasia of Foxg1 KO mice seem to be due to a are 2-fold reduced progenitor cell proliferation and an increased rate of differentiation [42].

The telencephalon arises from the rostral end of the neural tube; the dorsal and ventral telencephalic domains are patterned by the activities of a number of secreted molecules that produced by specific signalling centres [47, 48]: Sonic hedgehog (Shh) is produced ventrally; fibroblast growth factor 8 (Fgf8) is produced by the rostral center; bone morphogenetic proteins (Bmps) and Wnt proteins are produced caudo-medially. These signalling molecules in turn activate the graded expression of transcription factors that control the development of telencephalic cells, including their

molecular and cellular identities. Foxg1 plays an essential role in this processes [49]. In fact, FoxG1 probably coordinates the activity of the different signaling centers: i- it is a key downstream effector of the Shh pathway during induction of subpallial (ventral) identity. Moreover, it probably directly or indirectly regulate Shh expression, since Shh is reduced in *Foxg1–/–* telencephalon [50]. ii- it seem to regulate fgf8 expression, since rostral telencephalic Fgf8 expression is reduced in *Foxg1–/–* embryos [44]. iii- It inhibits Wnt/b-catenin signaling through direct transcriptional repression of Wnt ligands. This inhibition restricts the dorsal Wnt signaling center to the roof plate and consequently limits pallial identities. Accordingly, Foxg1 absence results in a ventral expansion of roof plate wnt and bmp expression [45, 51], correlated with increased BMP activity inside the telencephalon, [42, 44, 50, 52]. Concomitantly to these roles, Foxg1 controls the formation of the compartment boundary between telencephalon and basal diencephalon. These data explain the absence of ventral telencephalic tissue in Foxg1 KO mice. This is partially due to reduced production of the morphogens Shh and fgf8. However, it seems that Foxg1 seem to have a wider role, that enables cells to develop the competence to adopt ventral identities. In fact, experiment in chimeric embryos between Foxg1+/+ and Foxg1-/- cells demonstrated that the cells lacking Foxg1 could contribute to ventral telencephalon, but they expressed dorsal rather than ventral telencephalic markers [49].

Foxg1 proliferative effects rely on its ability to inhibit the FoxO–Smad transcriptional complex and, therefore, to block p21Cip1 induction by

TGF–beta signals in neuroepithelial cells [41, 53]. In fact, Smad proteins, activated by TGF-beta signaling, form a complex with FoxO proteins to turn on p21Cip1 gene. This gene in turn mediate cell cycle arrest at G1. The blockage of p21Cip1 activation by Foxg1 thus result in release of from this arrest and cell cycle progression.

The function of *FOXG1B* in the developing human brain presumably parallels that of FoxG1 in the mouse. Several splicing variants of *FOXG1B* are expressed exclusively in fetal brain tissue, suggesting that they play an important role specifically in early development, perhaps through regulation of the function of the predominant *FOXG1B* transcript, which is expressed in both fetal and adult brain [54].

In accordance with its important role in brain development, a potential involvement of FOXG1B alterations in mental impairment had been reported . In fact, 3 patients with large deletions of 14q region, including FOXG1 gene had been identified [54, 55]. A fourth patient presented a complex rearrangement with a translocation between chromosomes 2 and 14 and an inversion on the chromosome 14 breakpoint adjacent to FOXG1 gene affecting fetal isoforms of the gene (46,XX,t(2;14)(p.22;q12) [17].

2.Rationale

and

aims of this work

2. Rationale

Rett Syndrome (RTT) is a severe neurodevelopment disorder representing one of the most common genetic causes of mental retardation in girls. The classic form is caused by mutations in *MECP2* gene. Since its first description by Andreas Rett 40 years ago, the syndrome has been the object of extensive investigations, revealing a wide spectrum of clinical phenotypes and resulting in the identification of a second X-linked gene, *CDKL5*, as the responsible for the early onset seizures variant of the syndrome [1, 9, 18].

However, there are still patients, especially with variant form of the disorder, that do not have a molecular diagnosis. We thus thought that there could be other genes involved. In this context, the aim of my PhD project has been the search and mutation screening of new genes responsible for Rett syndrome. To this aim we took advantage of the identification by our group of a 3Mb deletion in 14q12 in a girl with severe encephalopathy, postnatal microcephaly and Rett-like features [17]. The region included only 5 genes: *FOXG1B, PRKD1, SCFD1, COCH* and *STRN3*. We reasoned that one of these genes might be responsible for the RTT-like phenotype of the patient and it might thus be a new RTT gene. Among the 5 genes, we concentrated our attention on *FOXG1* since it encodes for a brain-specific transcriptional repressor already potentially involved in mental impairment [9, 54, 56].

2.1 Specific aims of the thesis

Aim#1. Molecular Analysis of the *FOXG1* gene**.**

The entire coding region of *FOXG1B* gene was analyzed in order to identify new *FOXG1B* point mutations. Patients that resulted negative for point mutations were subsequently screened for copy number variations (deletion/duplication).

Aim#2. Clarification of clinical phenotype of congenital variant of Rett

Following the identification of *FOXG1B* mutations in girls with a congenital RTT phenotype from our first cohort of patients, cases with a phenotype reminiscent of this RTT variant were selected for subsequent screenings. We selected in total a cohort of 115 patients. To better clarify the clinical phenotype we established an international collaboration with the following European medical genetics groups:

- N Bahi-Buisson, J Nectoux, R Rubinsztajn and T Bienvenu of Université Paris Descartes, Institut Cochin, Inserm U567, Paris, France
- A Moncla and B Chabrol of Inserm U910, Université de la Méditerranée, Assistance Publique Hôpitaux de Marseille, Hôpital de La Timone, Marseille, France
- L Villard of Inserm U910, Université de la Méditerranée, Faculté de Médecine de La Timone, Marseille, France

- Z Krumina of Medical Genetics Clinic of Latvian State, Children's University Hospital, Latvia
- J Armstrong, A Roche and M Pineda of Hospital Sant Joan de Déu, Esplugues, Barcelona, Spain
- E Gak of Sagol Neuroscience Center, Sheba Medical Center, Tel Hashomer affiliated to the Sackler School of Medicine, Tel Aviv University, Tel Aviv, Israel
- A Superti-Furga, B Zabel, S Unger and E Lausch of Medical Genetics Clinic and laboratory of Freiburg im Breisgau Children's University Hospital, Germany

Aim#3. Genotype/phenotype correlation.

Patients clinical data were carefully collected and compared with those of patients reported in literature (see Table 1). Patients with deletions involving additional genes were analysed separately.

3. Materials and methods

3. Methods

3.1 Patients' collection

Patients enrolled in this study have been selected from those admitted to the Medical Genetics Unit (University Hospital of Siena) during the last four years and thanks of the collaboration european medical genetics groups we collected a cohort of 108 European patients (56 patients from France, 49 from Spain and 2 from Latvia and 1 from Germany) with the following clinical classification: 61 RTT girls (34 classic, 16 congenital, 7 with early onset seizures, 2 late regression, 1 Z-RTT and1 'forme fruste'), 43 patients with encephalopathy with early onset seizures (40 females and 3 males), and 4 RTT-like patients (1 female and 3 males with microcephaly, hand stereotypies and autistic features). Patients with classic and variant RTT were diagnosed according to the international criteria [57]. 7 RTT-like cases are patients who show some RTT clinical features but who do not fulfil all diagnostic criteria for classic or variant RTT. Phenotypic scores have been calculated using the severity score system previously reported by Renieri et al. [4]. All patients have been tested negative for *MECP2* and *CDKL5* mutations by a combination of denaturing high performance liquid chromatography (DHPLC) and multiplex ligation dependent probe amplification/quantitative polymerase chain reaction (MLPA/qPCR) analysis. One of this patients from Germany we collected and work with collaboration of the Centre for Paediatrics and Adolescent Medicine of Freiburg University during this year. Informed consent was obtained for

each patient/family. Genomic DNA of the patient was isolated from peripheral blood sample in EDTA by using a QIAamp DNA Blood Kit according to manufacturer protocol (Qiagen, www.qiagen.com). Genomic DNA of a female and a male control have been obtained from Promega.

3.2 Point mutations analysis

PCR amplification of fragments was carried out in a 50-µl reaction volume containing 100 ng of genomic DNA, 0.2 µM each primer , 0.2 mM dNTPs, 1X Go Taq Buffer with 1.5mM MgCl2 and 1,5U/50µl Gold Taq polymerase (Applied). Primers for the amplification of *FOXG1* coding sequence are listed in table 3. Cycling conditions were as follows: 95 °C 5 minutes, 35 cycles of 95 °C 60 seconds, primer-specific temperature 60 seconds (see table 3) and 72 °C 60 seconds, and a final elongation step at 72 °C for 10 minutes.

Amplicon size and purity were verified on a 1,2% agarose gel containing 0.5 µg/ml ethidium bromide. Mutation analysis was performed by DHPLC using the Transgenomic WAVE™ apparatus (Transgenomic, San Jose, CA, USA). To this aim, PCR products were denatured at 96°C, re-annealed at 65°C for 10 minutes, and cooled to 4°C to generate heteroduplexes. The optimal column temperature for the analysis of each fragment was calculated using the WaveMaker Software (Transgenomic, San Jose, CA, USA). Samples with abnormal DHPLC profiles were sequenced on an ABI PRISM 310 genetic analyzer (Applied Biosystems) using the big dye terminator kit. For exon 1A the analysis was performed by direct sequencing.

Table 3. *FOXG1* primers' sequences

EXON	Primer Sequence (5'- 3')	Annealing temperature
Ex 1A-F	TTTCCCCCCGACGACTG	58°C
Ex 1A-R	GCT TTAGCCCCGTCCAG	
Ex 1B-F	ACGACAAGGGCCCCCAGC	not amplified
Ex 1B-R	TGCCGGATGGCCATCATGA	
Ex 1C-F	AACGGCAAGTACGAGAAGC	62°C
Ex 1C-R	ACGGGTCCAGCATCCAGTA	
Ex 1D-F	CCACAATCTGTCCCTCAAC	60°C
Ex 1D-R	TGAGTCAACACGGAGCTGT	
Ex 1E-F	TTCCTGTCCCTGCACCAC	64°C
Ex 1E-R	CTCTGCGAAGTCATTGAC	
Ex 1F-F	CTGCTCTGGGACCTACTC	58°C
Ex 1F-R	TGCAAATGTGTGTAAAACGTT	

3.3 Real-Time qPCR analysis

Real-time PCR was carried out as previously described with the fluorescent Taqman method [58]. Probes and primers for *FOXG1* were designed using the "File Builder 3.1" software Applied Biosystems. I use the qPCR Real-Time *FOXG1* Probe: TTGACTTCCAAACCTTATATTCT and Primers' sequence forward GTCAGCGAGGTGCAATGTG and Reverse GGCAAAGCAGTCACTATTTAGATACACA. Real-time PCR experiments PCR were carried out using an ABI prism 7000 (Applied Biosystems, https://products.appliedbiosystems.com) in a 96-well optical plate with a final reaction volume of 50 µl. A total of 100 ng DNA were dispensed in each of the four sample wells for quadruplicate reactions. Thermal cycling conditions included a pre-run of 2 min at 50°C and 10 min at 95°C. Cycle conditions were composed of 40 cycles at 95°C for 15 sec and 60°C for 1 min according to the TaqMan Universal PCR Protocol (ABI). The TaqMan

Universal PCR Master Mix and Microamp reaction tubes were purchased from Applied Biosystems. The starting copy number of the unknown samples were determined using the comparative Ct method as previously described [58].

3.4 Multiplex Ligation-dependent Probe Amplification (MLPA)

MLPA analysis was performed according to the provider's protocol with a set of probes specifically designed for testing regions relevant for Rett syndrome (MRC-Holland, Amsterdam, Netherlands; http://www.mrcholland.com). In particular, SALSA kit P075A1 was used (table 4). Ligation products were amplified by PCR using a common primer set with the 6-FAM label distributed by the supplier. Briefly, 100 ng of genomic DNA were diluted with TE buffer to 5 µl, denatured at 98°C for 5 minutes and hybridized with SALSA Probe-mix at 60°C overnight. Ligase-65 mix was then added and ligation was performed at 54°C for 15 minutes. The ligase was successively inactivated by heat (98°C for 5 minutes). PCR reaction was performed in a 50 µl volume. Primers, dNTPs and polymerase were added and amplification was carried out for 35 cycles (30 seconds at 95°C, 30 seconds at 60°C and 60 seconds at 72°C). Amplification products were identified and quantified by capillary electrophoresis on an ABI 310 genetic analyzer, using GENESCAN software (version 3.7) from Applied Biosystems (Foster City, CA, USA). Peak areas of the PCR products were determined by GENOTYPER software (Applied Biosystems). A spreadsheet was developed in MicrosoftTM Excel

files (Office for Windows) in order to process the sample data efficiently. Data were normalized by dividing each probe's peak area by the average peak area of the sample. This normalized peak pattern was divided by the average normalized peak pattern of all the samples in the same experiment using Coffalyser software (MRC Holland) [14]. Dosage alterations were considered significant if sample values deviated more than 30% from the control. Real Time quantitative PCR was used to confirm MLPA results and to analyze parent's DNA [58].

3.4.1 Data analysis

The P075-A1 *TCF4-FOXG1* probe-mix contains 45 MLPA probes with amplification products between 130 and 481 nt. In addition, it contains 9 control fragments generating an amplification product smaller than 120 nt: four DNA Quantity fragments (Q-fragments) at 64-70-76-82 nt, three DNA denaturation control fragments (D-fragments) at 88-92-96 nt, one X-fragment at 100 nt and one Y-fragment at 105 nt. More information on how to interpret observations on these control fragments can be found in the MLPA protocol MRC-Holland. Data generated by this probemix can first be normalised intra-sample by dividing the peak area of each probe's amplification product by the total area of only the reference probes in this probemix (block normalisation). Secondly, inter-sample normalisation can be achieved by dividing the intra-normalised probe ratio in a sample by the average intra-normalised probe ratio of all reference samples.

Length (nt)	SALSA MLPA probe	FOXG1 exon	Ligation site NM_005249.3	Partial sequence (24 nt adjacent to ligation site)	Distance to next probe
337	13753-L15240	upstream	900 nt before exon 1, reverse	CCTTTGTAGGTA-ATAGTCTAGCGC	0.3 kb
190	13756-L15243	upstream	643 nt before exon 1	GAGGAAGCCGGA-AATGTGAGCTAT	0.9 kb
		start codon	*200-202*		
301	13757-L15244	exon 1	231-232	GAAAGAGGTGAA-AATGATCCCCAA	1.4 kb
274	13755-L15242	exon 1	1613-1612 reverse	GAAATAATCAGA-CAGTCCCCCAGA	0.2 kb
463	13754-L15241	exon 1	1807-1808	TCTAGGGTTGTT-TATTATTCTAAC	
		stop codon	*1667-1669*		

Table 4. P075 probes arranged according to chromosomal location FOXG1 gene 14q12.

3.5 Array-CGH analysis

Array-based CGH analysis was performed using commercially available oligonucleotide microarrays containing about 75.000-60-mer probes with an estimated average resolution of about ≥50kb (Human Genome CGH Microarray, Agilent Technologies). The OD260/280 method on a photometer was used to determine DNA concentration. DNA (10 ug) from the patient and sex-matched controls (Promega) was sonicated and subsequently purified using DNA Clean and Concentrator kit (Zymo Research, Orange, CA). After purification, DNA concentration was determined by a DyNA Quant_200 Fluorometer (GE Healthcare, www.gehealthcare.com). DNA labeling was carried out according to the Agilent protocol (Oligonucleotide Array-Based CGH for Genomic DNA Analysis 2.0v) using the Bioprime DNA labelling system (Invitrogen). Briefly, genomic DNA (2 ug) was mixed with 20 ul of 2.5X Random primer solution (Invitrogen) and water to a total volume of 41 ul. The mix was denaturated at 95 °C for 7 min and then incubated in ice for 5 min. Five ul of 10X dUTP nucleotide mix (1.2 mM dATP, dGTP, dCTP, 0.6 mM dTTP in 10

mM Tris, pH 8, and 1 mM EDTA), 2.5ul of Cy5-dUTP (test sample) or 2.5ul of Cy3-dUTP (reference sample) and 1.5 ul of Exo-Klenow (40 U/ml, Invitrogen) were added to each sample. Labeled samples were subsequently purified using CyScribe GFX Purification kit (Amersham Biosciences) according to manufacturer protocol. Test and reference DNA were pooled and mixed with 5ug of Human Cot I DNA (Invitrogen), 11ul of Blocking buffer (Agilent Technologies) and 55ul of hybridization buffer (Agilent Technologies). The mix was denatured at 95 °C for 7 min and then pre-associated at 37 °C for 30 min. Probes were then applied to the slide using an Agilent microarray hybridization station. Hybridization was carried out for 24h at 65°C in a rotating oven (20 rpm). The array was subsequently disassembled and washed according to the manufacturer protocol with wash buffers supplied by Agilent. The slides were dried and scanned using an Agilent G2565BA DNA microarray scanner.

Array results were analyzed using the Feature Extraction software (v8.1). The software determines automatically the fluorescence intensities of the spots for both fluorochromes performing background extraction and data normalization, and compiles the data into a spreadsheet that links the fluorescent signal of every probe on the array to the oligonucleotide name, its position on the array and its position in the genome. Graphical overview can be obtained using the CGH analytics software (v3.2.32) with default settings. The linear order of the oligonucleotides is reconstituted in the ratio plots consistent with an ideogram. Gains and losses in DNA copy number at a

particular locus can be observed as a deviation of the ratio plot from a modal value of 1.0.

3.5.1 In silico analysis

Gene content of the deletion/duplication can be determined using the published working draft sequence of the human genome (http://genome.ucsc.edu), and the map of EST maintained at NCBI (http://www.ncbi.nlm.nih.gov/).

4. Results

Result 4.1

FOXG1 is responsible for the congenital variant of Rett syndrome.

Francesca Ariani, Giuseppe Hayek, Dalila Rondinella, Rosangela Artuso, Maria Antonietta Mencarelli, Ariele Spanhol-Rosseto, Marzia Pollazzon, Sabrina Buoni, Ottavia Spiga, Sara Ricciardi, Ilaria Meloni, Ilaria Longo, Francesca Mari, Vania Broccoli,
Michele Zappella and Alessandra Renieri

A. Am J Hum Genet. 2008 Jul;83(1):89-93

FOXG1 Is Responsible for the Congenital Variant of Rett Syndrome

Francesca Ariani,[1] Giuseppe Hayek,[2] Dalila Rondinella,[1] Rosangela Artuso,[1] Maria Antonietta Mencarelli,[1] Ariele Spanhol-Rosseto,[1] Marzia Pollazzon,[1] Sabrina Buoni,[2] Ottavia Spiga,[3] Sara Ricciardi,[4] Ilaria Meloni,[1] Ilaria Longo,[1] Francesca Mari,[1] Vania Broccoli,[4] Michele Zappella,[2] and Alessandra Renieri[1,*]

Rett syndrome is a severe neurodevelopmental disease caused by mutations in the X-linked gene encoding for the methyl-CpG-binding protein MeCP2. Here, we report the identification of *FOXG1*-truncating mutations in two patients affected by the congenital variant of Rett syndrome. *FOXG1* encodes a brain-specific transcriptional repressor that is essential for early development of the telencephalon. Molecular analysis revealed that Foxg1 might also share common molecular mechanisms with MeCP2 during neuronal development, exhibiting partially overlapping expression domain in postnatal cortex and neuronal subnuclear localization.

In the classic form of Rett syndrome (RTT [MIM 312750]), females are heterozygous for mutations in the X-linked *MECP2* gene (MIM 300005) and the few reported males have an XXY karyotype or *MECP2* mutations in a mosaic state.[1] A number of variants have been described including the congenital, the early-onset seizures, and the preserved speech variant.[2] Soon after the discovery of *MECP2* as the RTT gene, we demonstrated that the preserved speech variant is allelic to the classic form.[3] More recently, we and others showed that *CDKL5* (MIM 300203) is responsible for atypical RTT, namely the early-onset seizures variant.[4,5] The congenital variant was initially described by Rolando in 1985.[6] In this form, girls are floppy and retarded from the very first months of life. The majority of congenital variants do not bear *MECP2* or *CDKL5* mutations,[7,8] with only four cases being reported with *MECP2* mutations.[9–11]

Using oligo array CGH, we recently identified a de novo 3 Mb interstitial deletion of chromosome 14q12 in a 7 year-old girl.[12] She showed dysmorphic features and a Rett-like clinical course, including normal perinatal period, postnatal microcephaly, seizures, and severe mental retardation. The deleted region was gene poor and contained only five genes. Among them, *FOXG1* (MIM 164874) turned out to be a very interesting gene because it encodes a brain-specific transcriptional repressor. We analyzed this gene with a combination of both DHPLC and real-time quantitative PCR in a cohort of 53 *MECP2*/*CDKL5* mutation-negative RTT patients, including seven classic, 21 preserved speech, seven early-onset seizures, one "forme fruste," two congenital variants and 15 Rett-like cases.[13] For real-time qPCR analysis, we designed primers and TaqMan probe complementary to a segment located in the middle of the single exon of the gene using Primer Express software (Applied Biosystems). Sequences of primers and probe (FAM labeled) are listed in Table S1 available online. We used an RNAase P kit as an internal reference (VIC-labeled probe, Applied Biosystems). PCR was carried out as previously described.[14] The starting copy number of the unknown samples was determined with the comparative Ct method, as reported by Livak.[15] By DHPLC, we identified a different de novo *FOXG1* truncating mutation in the two congenital variant patients. Real-time qPCR failed to identify any microdeletion in the 53 patients.

FOXG1 encodes forkhead box protein G1, FoxG1 (formerly brain factor 1 [BF-1]), a transcriptional factor with expression restricted to fetal and adult brain and testis. FoxG1 interacts with the transcriptional repressor JARID1B and with global transcriptional corepressors of the Groucho family. The interaction with these proteins is of functional importance for early brain development.[16,17] Like MeCP2, FoxG1 also indirectly associates with the histone deacetylase 1 protein.[1,17] Both mutations disrupted the protein at different levels (Figure 1). In case 1, a stop-codon mutation p.W255X (c.765G→A) impaired the DNA binding because of the disruption of the forkhead domain (Figure 1D, left). Case 2 showed a 1 bp deletion c.969 delC (p.S323fsX325) causing the loss of JARID1B-interacting domain and the misfolding of the motif responsible for the Groucho binding (Figure 1D, right). Lastly, both *FOXG1* mutations affected all the four brain fetal isoforms that lack the last 37 amino acids and have different C-terminal domains.[18]

The two mutated individuals, aged 22 (case 1) and 7 years (case 2), fulfilled the international criteria for RTT variants.[19] Pregnancy, delivery, and auxological parameters at birth were normal. Neurological and behavioral neonatal evaluations were reported as normal, but at three

[1]Medical Genetics, Molecular Biology Department, University of Siena, 53100 Siena, Italy; [2]Child Neuropsychiatry University Hospital AOUS, 53100 Siena, Italy; [3]Biochemistry and Molecular Biology, Molecular Biology Department, University of Siena, 53100 Siena, Italy; [4]San Raffaele Scientific Institute, Dibit, 20132 Milano, Italy
*Correspondence: renieri@unisi.it
DOI 10.1016/j.ajhg.2008.05.015.

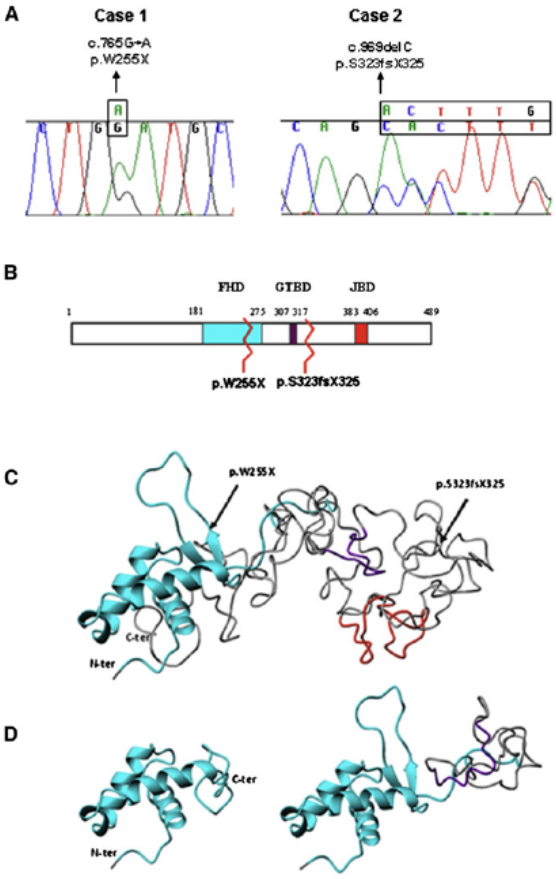

Figure 1. *FOXG1* Mutations and Alterations of the Functional Domains

(A) Sequence tracing of *FOXG1* mutations in the two patients. Mutated bases are indicated above the line.

(B) Schematic representation of FoxG1 protein. The three main functional domains are shown: the DNA binding fork-head domain in light blue (FHD), the Groucho-binding domain in violet (GTBD), and the JARID1B binding domain in red (JBD). The numbers at the top refer to the amino acid positions. Mutations are indicated by zigzag lines.

(C and D) Ribbon representation of the tertiary structure obtained with Phyre v.0.2 software. (C) shows the structure of the region containing the three functional domains of wild-type protein (amino acids 180–489). Arrows highlight the two mutations. The FHD domain (cyan) consists of three alpha helices and one beta hairpin (two beta strands and one loop), whereas the GTBD (violet) and JBD (red) domains are random coiled. (D) shows structural modification after p.W255X (left) and p.S323fsX325 (right) mutations. The p.W255X mutation determines a protein truncation just after the second beta strand leading to the loss of the beta hairpin and thus preventing DNA binding. The p.S323fsX325 mutation leaves the FHD domain intact and truncates the protein just after GTBD, inducing conformational changes that lead to its misfolding.

months, an abnormal head-circumference growing was noticed in the patients. These patients appeared to weep inconsolably, and they did not respond when called and were unable to lift their heads. Case 1 was never able to sit unaided and laid permanently in bed, whereas case 2 was barely able to sit. They were always apraxic and from 1 year of age, they showed peculiar jerky movements of the upper limbs and midline stereotypic activities, typical of RTT syndrome (Figure 2). They never acquired spoken language. Generalized convulsions appeared at 14 years in case 1 and at 2 1/2 years in case 2. Ever since cases 1 and 2 were 3 and 5 years old, respectively, an EEG showed features often found in RTT patients: a multifocal pattern with spikes and sharp waves and occasional paroxysmal activity. In both patients brain MRI showed corpus callosum hypoplasia, a finding which has already been reported in RTT.[20] Currently, they show microcephaly (OFC of 49 cm in case 1, and 47 cm in case 2). They have occasional periods of deep breathing with exaggerated inspirations. Sialorrhoea, bruxism, scoliosis, and cold lower extremities as well as stypsis are present in both patients who are currently fed by mouth.

These two girls show neurological and neurovegetative symptoms as well as somatic features consistent with a diagnosis of congenital RTT variant. It should only be noted that a retrospective assessment concerning the possible presence of a regression was not feasible. We attempted to compare their phenotype with the four other *MECP2*-mutated girls described as congenital variants.[9–11] However, they have been reported with very little detail, thereby hampering a posteriori clinical re-evaluation according to the revised criteria.[19] According to the new criteria, in the classic form, psychomotor development may have been delayed from birth; thus, a re-evaluation of these four patients would have lead to their reclassification as classic form. Alternatively, the disruption of either MeCP2 or FoxG1 may lead to a phenotype, namely the congenital variant, indistinguishable at the level of the clinical and instrumental investigations performed.

A translocation with inversion affecting fetal isoforms of *FOXG1* was recently described in a 7-year-old girl.[18] She had acquired microcephaly, alalia, inability to sit and walk, and epilepsy in common with the present cases. Corpus callosum was absent, whereas in our cases, it was hypoplasic. Stereotypic hand activities were not mentioned, and tetraplegia was described.[18] The clinical features of this patient have something in common with a RTT phenotype. The impairment of only fetal *FOXG1* isoforms and the possible contribution of genes at the other two breakpoints of the complex rearrangement might explain the phenotypic differences.

The mouse ortholog *Foxg1* has a restricted expression domain in the central nervous system coinciding with the emergence of the telencephalic structures of the brain. Its function has been extensively characterized and found to promote telencephalon development by sustaining proliferation of the progenitor pool and preventing

Figure 2. Pictures of the Two Congenital RTT Patients

Case 1 (#156) is shown on the left; case 2 (#868) is shown on the right. They show peculiar jerky movements of the upper limbs frequently pushed in different directions accompanied by continuous flexion-extension, wringing movements of the fingers of the hands. The hands were brought together in hand-washing and hand-mouth stereotypic activities, which were intense and present all the time they were awake. Similar flexion-extension movements of the toes were noticed in the feet. The double scoliosis of case 1 is clearly evident, whereas the other girl maintained a straight vertebral column as often occurs in RTT in the first decade. Teeth grinding was present, and the tongue often protruded out from the mouth.

premature cortical neural differentiation.[21,22] In agreement, FoxG1 expression is found in the proliferating neuroepithelium starting from early development onward.[23] This expression profile might explain the particular early onset of the neurological symptoms displayed by the patients.

Despite its early expression in telencephalon development, in this study we found that *Foxg1* expression is detectable in the differentiating cortical compartment in the postnatal stages, although at lower levels with respect to the early embryonic phases (Figure 3A). This expression profile overlaps with the described MeCP2 expression

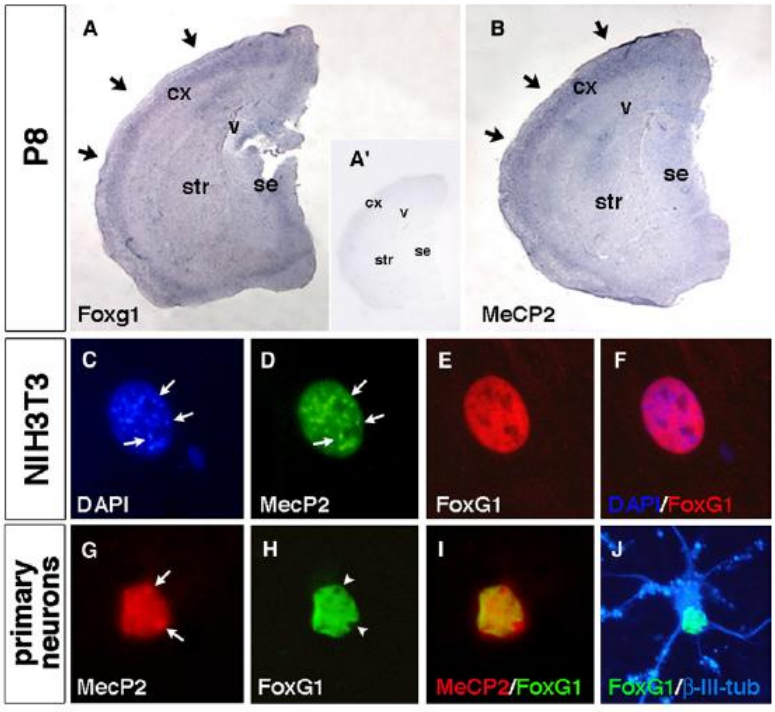

Figure 3. FoxG1 and MeCP2 Expression Domain in Postnatal Cortex and Neuronal Subnuclear Localization

(A and B) Expression analysis by in situ hybridization of Foxg1 and MeCP2 on P8 postnatal forebrain tissue. As shown in (A), Foxg1 expression is found in differentiating and mature cortical neurons in the definitive cortical plate (indicated by arrows in [A]) similar to the MeCP2 expression pattern (indicated by arrows in [B]). In (A′), the inset shows background staining with a sense cRNA for Foxg1 in the same in situ hybridization conditions used for (A) and (B).

(C–J) FoxG1 and MeCP2 sub-cellular localization in non-neural and primary neurons. As shown in (C)–(F), in NIH 3T3 cells, MeCP2-GFP exogenous protein has a diffuse nuclear localization with accumulation in the heterochromatic foci (indicated by arrows in [D]) as identified when compared with DAPI staining (indicated by arrows in [C]). (E) and (F) show that conversely, FoxG1-flag exogenous protein displays a widespread nuclear localization without enrichment in heterochromatic sites. (G)–(J) show FoxG1 and MeCP2 localization in 12DIV (days in vitro) primary hippocampal neurons. In (G), MeCP2 endogenous protein is accumulated in heterochromatic foci (indicated by arrows). As shown in (H), FoxG1-flag exogenous nuclear localization is excluded from heterochromatic puncta (indicated by arrowheads). As shown in (I), MeCP2 and FoxG1-flag colocalize in the nuclear compartment outside the heterochromatic foci. As shown in (J), Nuclear FoxG1-flag localization is detected in a differentiated β-III-tubulin-positive neuron. The following abbreviations are used: cx, cerebral cortex; se, septum; str, striatum; and v, ventricle.

domain in cortical tissues, in differentiating and mature neurons (Figures 3A and 3B). *Foxg1* homozygote-mutant mice die shortly after birth with severe brain defects.[24–26] Unfortunately, the severe compromised development of *Foxg1* mutant telencephali has prevented the analysis of its function in more differentiated neurons. At the single-cell level, FoxG1 localizes in the nuclear compartment but is excluded from the MeCP2-positive heterochromatic foci both in nonneural and primary neurons (Figures 3C–3J). These findings suggest that, differently from MeCP2, FoxG1 is not a transcriptional repressor stably associated with heterochromatin. However, both proteins have a large colocalization domain in other nuclear compartments (Figure 3I).

Overall, these data suggest that FoxG1 may exert some additional functions in differentiating and mature neurons, thus sharing similarities with those described for MeCP2. These findings may provide some biological evidence for the development of similar clinical manifestations in disorders affecting the two genes. However, it is also possible that the two transcriptional regulators act on different stages of the process that leads to proper cortical development, from early cell-fate decisions to later circuit connectivity and dendritic development.

FoxG1 shares some interesting analogies with MeCP2 in its molecular functions, raising the question whether the two protein networks may interact in some circumstances and on selective common targets. Future studies will address this intriguing hypothesis. Recently, heterozygous *Foxg1*$^{+/-}$ mice were found to display subtler defects including a reduction in size of the corpus callosum together with specific patterning defects.[25,27] Furthermore, heterozygous *Foxg1*$^{+/-}$ exhibit learning deficits based on fear-condition behavioral tests associated with a loss of postnatal neurogenesis in the hippocampus.[27] These mice represent a very interesting animal model for further investigation about how *Foxg1* haploinsufficiency may impact on brain development and neuronal maturation and function.

In conclusion, we demonstrated that *FOXG1* is a previously unrecognized gene responsible for variant Rett syndrome. It is worth noting that in the revised criteria for Rett syndrome the female sex is no longer present as inclusion criteria.[19] This seemed to open the door to the discovery of an autosomal gene.

Supplemental Data

One table listing primers and probes for real-time qPCR is available at http://www.ajhg.org/.

Acknowledgments

We would first like to thank the Rett patients and their families. This work was supported by Telethon grants GTB07001 to A.R. and GGP07181 to V.B., by the EuroRETT E-RARE network to A.R. and to V.B, and by the Emma and Ernesto Rulfo Foundation to A.R.

Received: April 2, 2008
Revised: May 9, 2008
Accepted: May 23, 2008
Published online: June 19, 2008

Web Resources

The URLs for data presented herein are as follows:

Italian Rett database and biobank, http://www.biobank.unisi.it/
Online Mendelian Inheritance in Man (OMIM), http://www.ncbi.nlm.nih.gov/Omim/

References

1. Chahrour, M., and Zoghbi, H.Y. (2007). The story of Rett syndrome: from clinic to neurobiology. Neuron *56*, 422–437.
2. Hagberg, B.A., and Skjeldal, O.H. (1994). Rett variants: A suggested model for inclusion criteria. Pediatr. Neurol. *11*, 5–11.
3. De Bona, C., Zappella, M., Hayek, G., Meloni, I., Vitelli, F., Bruttini, M., Cusano, R., Loffredo, P., Longo, I., and Renieri, A. (2000). Preserved speech variant is allelic of classic Rett syndrome. Eur. J. Hum. Genet. *8*, 325–330.
4. Tao, J., Van Esch, H., Hagedorn-Greiwe, M., Hoffmann, K., Moser, B., Raynaud, M., Sperner, J., Fryns, J., Schwinger, E., Gecz, J., et al. (2004). Mutations in the X-linked cyclin-dependent kinase-like 5 (CDKL5/STK9) gene are associated with severe neurodevelopmental retardation. Am. J. Hum. Genet. *75*, 1149–1154.
5. Scala, E., Ariani, F., Mari, F., Caselli, R., Pescucci, C., Longo, I., Meloni, I., Giachino, D., Bruttini, M., Hayek, G., et al. (2005). CDKL5/STK9 is mutated in Rett syndrome variant with infantile spasms. J. Med. Genet. *42*, 103–107.
6. Rolando, S. (1985). Rett syndrome: report of eight cases. Brain Dev. *7*, 290–296.
7. Erlandson, A., Samuelsson, L., Hagberg, B., Kyllerman, M., Vujic, M., and Wahlstrom, J. (2003). Multiplex ligation-dependent probe amplification (MLPA) detects large deletions in the MECP2 gene of Swedish Rett syndrome patients. Genet. Test. *7*, 329–332.
8. Scala, E., Longo, I., Ottimo, F., Speciale, C., Sampieri, K., Katzaki, E., Artuso, R., Mencarelli, M.A., D'Ambrogio, T., Vonella, G., et al. (2007). MECP2 deletions and genotype-phenotype correlation in Rett syndrome. Am. J. Med. Genet. A. *143*, 2775–2784.
9. Huppke, P., Laccone, F., Kramer, N., Engel, W., and Hanefeld, F. (2000). Rett syndrome: Analysis of *MECP2* and clinical characterization of 31 patients. Hum. Mol. Genet. *9*, 1369–1375.
10. Monros, E., Armstrong, J., Aibar, E., Poo, P., Canos, I., and Pineda, M. (2001). Rett syndrome in Spain: Mutation analysis and clinical correlations. Brain Dev. Suppl. *1*, S251–S253.
11. Smeets, E., Schollen, E., Moog, U., Matthijs, G., Herbergs, J., Smeets, H., Curfs, L., Schrander-Stumpel, C., and Fryns, J.P. (2003). Rett syndrome in adolescent and adult females: Clinical and molecular genetic findings. Am. J. Med. Genet. A. *122*, 227–233.
12. Papa, F.T., Mencarelli, M.A., Caselli, R., Katzaki, E., Sahpieri, K., Meloni, I., Ariani, F., Longo, I., Maggio, A., Balestri, P., et al. (2008). A 3 Mb deletion in 14912 causes severe mental retardation, mild facial dysmorphisms and Rett-like features. Am. J. Med. Genet. A., in press.

13. Sampieri, K., Meloni, I., Scala, E., Ariani, F., Caselli, R., Pescucci, C., Longo, I., Artuso, R., Bruttini, M., Mencarelli, M.A., et al. (2007). Italian Rett database and biobank. Hum. Mutat. *28*, 329–335.
14. Ariani, F., Mari, F., Pescucci, C., Longo, I., Bruttini, M., Meloni, I., Hayek, G., Rocchi, R., Zappella, M., and Renieri, A. (2004). Real-time quantitative PCR as a routine method for screening large rearrangements in Rett syndrome: Report of one case of MECP2 deletion and one case of MECP2 duplication. Hum. Mutat. *24*, 172–177.
15. Livak, K. (1997). *ABI Prism 7700 Sequence Detection System*.
16. Tan, K., Shaw, A.L., Madsen, B., Jensen, K., Taylor-Papadimitriou, J., and Freemont, P.S. (2003). Human PLU-1 Has transcriptional repression properties and interacts with the developmental transcription factors BF-1 and PAX9. J. Biol. Chem. *278*, 20507–20513.
17. Yao, J., Lai, E., and Stifani, S. (2001). The winged-helix protein brain factor 1 interacts with groucho and hes proteins to repress transcription. Mol. Cell. Biol. *21*, 1962–1972.
18. Shoichet, S.A., Kunde, S.A., Viertel, P., Schell-Apacik, C., von Voss, H., Tommerup, N., Ropers, H.H., and Kalscheuer, V.M. (2005). Haploinsufficiency of novel FOXG1B variants in a patient with severe mental retardation, brain malformations and microcephaly. Hum. Genet. *117*, 536–544.
19. Hagberg, B., Hanefeld, F., Percy, A., and Skjeldal, O. (2002). An update on clinically applicable diagnostic criteria in Rett syndrome. Comments to Rett Syndrome Clinical Criteria Consensus Panel Satellite to European Paediatric Neurology Society Meeting, Baden Baden, Germany, 11 September 2001. Eur. J. Paediatr. Neurol. *6*, 293–297.
20. Murakami, J.W., Courchesne, E., Haas, R.H., Press, G.A., and Yeung-Courchesne, R. (1992). Cerebellar and cerebral abnormalities in Rett syndrome: a quantitative MR analysis. AJR Am. J. Roentgenol. *159*, 177–183.
21. Hanashima, C., Shen, L., Li, S.C., and Lai, E. (2002). Brain factor-1 controls the proliferation and differentiation of neocortical progenitor cells through independent mechanisms. J. Neurosci. *22*, 6526–6536.
22. Seoane, J., Le, H.V., Shen, L., Anderson, S.A., and Massague, J. (2004). Integration of Smad and forkhead pathways in the control of neuroepithelial and glioblastoma cell proliferation. Cell *117*, 211–223.
23. Tao, W., and Lai, E. (1992). Telencephalon-restricted expression of BF-1, a new member of the HNF-3/fork head gene family, in the developing rat brain. Neuron *8*, 957–966.
24. Martynoga, B., Morrison, H., Price, D.J., and Mason, J.O. (2005). Foxg1 is required for specification of ventral telencephalon and region-specific regulation of dorsal telencephalic precursor proliferation and apoptosis. Dev. Biol. *283*, 113–127.
25. Xuan, S., Baptista, C.A., Balas, G., Tao, W., Soares, V.C., and Lai, E. (1995). Winged helix transcription factor BF-1 is essential for the development of the cerebral hemispheres. Neuron *14*, 1141–1152.
26. Hanashima, C., Fernandes, M., Hebert, J.M., and Fishell, G. (2007). The role of Foxg1 and dorsal midline signaling in the generation of Cajal-Retzius subtypes. J. Neurosci. *27*, 11103–11111.
27. Shen, Q., Wang, Y., Dimos, J.T., Fasano, C.A., Phoenix, T.N., Lemischka, I.R., Ivanova, N.B., Stifani, S., Morrisey, E.E., and Temple, S. (2006). The timing of cortical neurogenesis is encoded within lineages of individual progenitor cells. Nat. Neurosci. *9*, 743–751.

Result 4.2

Novel *FOXG1* mutations associated with the congenital variant of Rett syndrome

M A Mencarelli, A Spanhol-Rosseto, R Artuso, D Rondinella, R De Filippis, N Bahi-Buisson, J Nectoux, R Rubinsztajn, T Bienvenu, A Moncla, B Chabrol, L Villard, Z Krumina, J Armstrong, A Roche, M Pineda, E Gak, F Mari, F Ariani, A Renieri

J Med Genet 2010;47:49e53. doi:10.1136/jmg.2009.067884

Novel *FOXG1* mutations associated with the congenital variant of Rett syndrome

M A Mencarelli,[1] A Spanhol-Rosseto,[1] R Artuso,[1] D Rondinella,[1] R De Filippis,[1] N Bahi-Buisson,[2] J Nectoux,[2] R Rubinsztajn,[2] T Bienvenu,[2] A Moncla,[3] B Chabrol,[3] L Villard,[4] Z Krumina,[5] J Armstrong,[6] A Roche,[6] M Pineda,[6] E Gak,[7] F Mari,[1] F Ariani,[1] A Renieri[1]

[1]Medical Genetics, Department of Molecular Biology, University of Siena, Siena, Italy [2]Université Paris Descartes, Institut Cochin, Inserm U567, Paris, France [3]Inserm U910, Université de la Méditerranée, Assistance Publique Hôpitaux de Marseille, Hôpital de La Timone, Marseille, France [4]Inserm U910, Université de la Méditerranée, Faculté de Médecine de La Timone, Marseille, France [5]Medical Genetics Clinic of Latvian State, Children's University Hospital, Latvia [6]Hospital Sant Joan de Déu, Esplugues, Barcelona, Spain [7]Sagol Neuroscience Center, Sheba Medical Center, Tel Hashomer affiliated to the Sackler School of Medicine, Tel Aviv University, Tel Aviv, Israel

Correspondence to
Alessandra Renieri, Medical Genetics, Molecular Biology Department, University of Siena, Viale Bracci, 2, 53100 Siena, Italy; renieri@unisi.it

Received 16 March 2009
Revised 21 May 2009
Accepted 30 May 2009
Published Online First 2 June 2009

ABSTRACT

Background Rett syndrome is a severe neurodevelopmental disorder representing one of the most common genetic causes of mental retardation in girls. The classic form is caused by *MECP2* mutations. In two patients affected by the congenital variant of Rett we have recently identified mutations in the *FOXG1* gene encoding a brain specific transcriptional repressor, essential for early development of the telencephalon.

Methods 60 *MECP2/CDKL5* mutation negative European Rett patients (classic and variants), 43 patients with encephalopathy with early onset seizures, and four atypical Rett patients were analysed for mutations in *FOXG1*.

Results and conclusions Mutations have been identified in four patients, independently classified as congenital Rett variants from France, Spain and Latvia. Clinical data have been compared with the two previously reported patients with mutations in *FOXG1*. In all cases hypotonia, irresponsiveness and irritability were present in the neonatal period. At birth, head circumference was normal while a deceleration of growth was recognised soon afterwards, leading to severe microcephaly. Motor development was severely impaired and voluntary hand use was absent. In contrast with classic Rett, patients showed poor eye contact. Typical stereotypic hand movements with hand washing and hand mouthing activities were present continuously. Some patients showed abnormal movements of the tongue and jerky movements of the limbs. Brain magnetic resonance imaging showed corpus callosum hypoplasia in most cases, while epilepsy was a variable sign. Scoliosis was present and severe in the older patients. Neurovegetative symptoms typical of Rett were frequently present.

INTRODUCTION

Rett syndrome (RTT) is characterised by a serious and global developmental disorder affecting the central nervous system. First described by Andreas Rett 40 years ago, the syndrome has been the object of extensive investigations, revealing a wide spectrum of clinical phenotypes including the classic form, the early onset seizure variant, the Zappella variant (Z-RTT), the congenital variant, the 'forme fruste' variant, and the late regression variant.[1–3] Mutations in the *MECP2* gene, located in Xq28, are responsible for 95% of classic RTT and for 50% of Z-RTT[4]; while the early onset seizure variant results from mutations in the *CDKL5* gene, in Xp22.[5] We have recently used a candidate gene approach to demonstrate that the *FOXG1* gene, located in 14q12, is responsible for the congenital variant of RTT.[3] In this variant, initially described by Rolando in 1985, the affected girls present the same clinical features as in classic RTT, but in addition they are floppy and retarded from the very first months of life.[6]

We report the identification of *FOXG1* mutations in four additional congenital RTT girls, through mutation screening of a cohort of 107 European patients: 60 RTT patients (classic and variants), 43 patients with epileptic encephalopathy, and four RTT-like patients. Clinical data of these four patients were compared with the two previously reported girls in order to improve the characterisation of the phenotype associated with *FOXG1* mutations.[3]

PATIENTS AND METHODS

Patients and phenotype definitions

We collected a cohort of 107 European patients (56 patients from France, 49 from Spain and 2 from Latvia) with the following clinical classification: 60 RTT girls (33 classic, 16 congenital, 7 with early onset seizures, 2 late regression, 1 Z-RTT and 1 'forme fruste'), 43 patients with encephalopathy with early onset seizures (40 females and 3 males), and 4 RTT-like patients (1 female and 3 males with microcephaly, hand stereotypies and autistic features). Patients with classic and variant RTT were diagnosed according to the international criteria.[7] RTT-like cases are patients who show some RTT clinical features but who do not fulfil all diagnostic criteria for classic or variant RTT. Phenotypic scores have been calculated using the severity score system previously reported by Renieri *et al*.[2] All patients have been tested negative for *MECP2* and *CDKL5* mutations by a combination of denaturing high performance liquid chromatography (DHPLC) and multiplex ligation dependent probe amplification/quantitative polymerase chain reaction (MLPA/qPCR) analysis.

Molecular analysis

Blood samples were obtained after informed consent. DNA was extracted from peripheral blood using a QIAamp DNA Blood Kit (Qiagen GmbH QIAGEN strasse 1, 40724 Hilden, Germany). To determine the appropriate DNA concentration, we used the OD260/280 method on a photometer.[8] DNA samples were screened for mutations in *FOXG1* gene using Transgenomic WAVE DHPLC. The entire

coding portion of *FOXG1* was analysed as previously reported.[3] PCR products resulting in abnormal DHPLC profiles were sequenced on both strands using PCR primers with fluorescent dye terminators on an ABI PRISM 310 genetic analyser (PE Applied Biosystems, Foster City, California, USA).

Clinical score

For each patient a severity score was assigned through the evaluation of 22 different clinical signs.[2] Results were compared with the severity score of 128 classic and 25 Z-RTT patients with mutation in the *MECP2* gene, and nine patients with the early onset seizures variant of RTT with a *CDKL5* mutation.[2 9] Statistical analysis was performed using the median test.

RESULTS

Molecular analysis

A mutation in the *FOXG1* gene was identified in four patients clinically classified as congenital RTT. The *de novo* origin of the mutation was confirmed in three cases (cases 2–4), while in one case (case 1) parents were not available. Cases 3 and 4 bear the truncating mutations p. S185fsX454 (c.551_552insC) and p.Y208X (c.624C>G). The remaining two cases have missense mutations that lie within the forkhead domain and affect residues highly conserved in different species (including *Tetraodon nigroviridis*—CAF93027; *Xenopus tropicalis*—NN_001116933; and *Xenopus laevis*—NP_001079165): p.N227K (c.681C>G) in case 1 and p.F215L (c.643T>C) in case 2.

Clinical description

Case 1 (1091) is a female from Latvia, presently aged 17 years; she is in the fourth stage of RTT with spastic paraparesis (table 1; figure 1B). Since the age of 16 months she has grown up in an orphanage and her parents are presently unavailable. The girl was her mother's first child and was born after a normal pregnancy. Birth weight was 3900 g with an Apgar score 8/9. Psychomotor delay was appreciated from the age of 6–7 months. The time of occurrence of the first seizures is unknown. The girl has been examined only once, at the age of 13 years 2 months.

Case 2 (RTT00967) is a female from France, presently aged 8 years 6 months (table 1, figure 1C). She is the second child of a non-consanguineous couple; another child was born afterwards. She was born at 39 weeks after a normal pregnancy. Auxological parameters at birth were normal. In the neonatal period sleep disturbance and severe distress (crying) were noticed. She was referred to a clinical unit at 6 months because of psychomotor retardation. At this age, examination revealed severe hypotonia with sleep disturbances and no dysmorphic features except strabismus and hypermetropia. A re-evaluation at 2 years showed normal weight and height (height 81 cm, weight 12 kg), while the occipitofrontal circumference (OFC) was at −2 SD (45 cm), with developmental delay, hypotonia, very poor social contact, manual stereotypies and dystonia of the extremities. At 6.5 years, she could only stand up with support and did not walk; could hold an object (feeding bottle) with a simple grasp; and showed trunk rocking and tongue chewing. On last examination, at 8 years of age, the clinical phenotype was unchanged; she was only able to pronounce two disyllabic words (mama, papa) and brain magnetic resonance imaging (MRI) showed microcephaly with abnormal development of the frontal lobes without gyration defect.

Case 3 (RTT01158) is a female from France, presently aged 3 years (table 1). The patient is the first child of non-consanguineous parents from Benin, without a relevant family history. She was born at term and showed normal auxological parameters. She developed severe microcephaly at an early stage. Brain MRI performed in the first months showed isolated ventricular dilatation. Subsequently, she developed severe epileptic encephalopathy. In addition she had a disturbed sleep pattern from 2 years. When last examined, she was able to hold her head steadily but showed asymmetric spastic tetraplegia and scoliosis. Brain MRI performed at 2 years showed delayed myelination with hypoplasia/hypomyelination of the corpus callosum.

Case 4 (60719368) is a female from Spain, presently aged 3 years 2 months (table 1, figure 1A). The mother has a normal boy of 9 years and has had three spontaneous abortions. At birth she showed very severe hypotonia and normal auxological parameters. Subsequently microcephaly became evident. At 4 months OFC was at −2SD, at 9 months at −3.5, and since the age of 2 years at −5SD. She developed hand stereotypies at 12 months: she used to bring her hands to the mouth and pat her fingers on her lips. Protruding tongue movements have been constant from the age of 4 months.

Clinical comparison of the six patients with *FOXG1* mutations

We compared the clinical picture of these four additional patients with a *FOXG1* mutation to the two previously reported.[3] These six patients, with age ranging from 3–22 years, present a distinct clinical phenotype (table 1).

In order to recognise the clinical differences among the RTT phenotypes, we compared the clinical scores of four patients with mutations in *FOXG1* for whom we could obtain complete clinical information (patients 3–6) to the scores of classic and Z-RTT patients with *MECP2* mutations and those of early onset seizure variant patients with *CDKL5* mutations. In patients with a *FOXG1* mutation the clinical score median value is 31.5, with total score ranging from 28–38. Among the classic RTT cases the median value is 27, with a range from 13–39.[9] In the nine patients with *CDKL5* mutation, the median value is 27, with total score ranging from 22–30.[9] In the Z-RTT the median value is 13, with values ranging from 4–24.[2]

DISCUSSION

This work confirms that the *FOXG1* gene is responsible for the congenital variant of RTT. In fact, *FOXG1* mutations (figure 2) have so far been identified only in patients originally classified by different clinical centres as affected by this variant of RTT.

The overall clinical phenotype is characterised by normal pregnancy and delivery, normal auxological parameters at birth, followed by hypotonia, irresponsiveness and irritability in the neonatal period. Deceleration of head growth represents one of the most important diagnostic signs: in the four cases for whom the OFC had been recorded in the first months of life, microcephaly was evident already before the fourth month. Apparently microcephaly is more severe than in classic RTT (mean −4.32 SD compared with a mean of −2.4 SD in classic RTT). All five patients bearing a rearrangement on chromosome 14q12 involving *FOXG1* presented with microcephaly: in the first reported case the onset was not defined[10]; in three patients microcephaly was evident between 5–8 months[11–13]; while in the fifth patient head circumference was below the third centile at the age of 11 months.[14]

In the two girls previously described with *FOXG1* mutations, a retrospective assessment as to whether there had been a period of normal development was not feasible, although the parents noted a delay only at 3 months. In patient 3, who presented with the earliest onset, a real regression period was not identifiable, while the other three cases (patients 1, 2 and 4) presented a regression before 6 months of age, more precocious than in classic RTT, in

Table 1 Clinical features of patients with *FOXG1* mutations

	Patient 1 (1091)	Score	Patient 2 (RTT00967)	Score	Patient 3 (RTT01158)	Score	Patient 4 (60718368)	Score	Patient 5 Ariani *et al*[3]	Score	Patient 6 Ariani *et al*[3]	Score
Age/sex	13 y 2 m/female		8 y/female		3 y/female		3 y 2 m/female		22 y/female		7 y/female	
Inheritance	Parents not available (NA)		De novo		Parents' DNA requested		De novo		De novo		De novo	
Mutation	c.681C>G; p.N227K		c.643T>C; p.F215L		c.551_552insC; p.S185fsX454		c.624C>G; p.Y208X		c.765G>A; p.W255X		c.969delC; p.S323fsX325	
OFC at birth	NA		34 cm 50–75th cnt		32.5 cm 3–10th cnt		33.5 cm 25–50th cnt		34 cm 50th cnt		34 cm 50th cnt	
Weight at birth	3900 g 90th cnt		3300 g 50–75th cnt		2800 g 10th cnt		3150 g 50th cnt		3150 g 25–50th cnt		3350 g 50th cnt	
Length at birth	NA		49 cm 50th cnt		48 cm 50th cnt		50 cm 50th cnt		49 cm 50th cnt		50 cm 50th cnt	
Perinatal signs	NA		Inconsolable crying		Hypotonia, psychomotor retardation		Sleepiness, cries only if hungry		Inconsolable crying		Inconsolable crying	
Age of regression	6 months	2	6 months	2	3 months	2	3 months	2	3 months	2	3 months	2
Present OFC	46 cm −6 SD	2	48 cm −2.24 SD	2	43 cm −5 SD	2	42 cm −5 SD	2	49 cm −4 SD	2	47 cm −3.7 SD	2
Present weight	NA		NA		13.4 kg 3rd cnt	1	10 kg <5th cnt	2	38 kg <5th cnt BMI 19.1	2	18.5 kg <5th cnt BMI 15.3	2
Present height	NA		NA		97 cm 75th cnt	0	87 cm <3rd cnt	2	141 cm <<5th cnt	2	110 cm <5th cnt	2
Hand stereotypy	NA		Intermittent: hand to mouth, washing	1	Intermittent	1	Constant: hand to mouth	2	Constant: clapping, hand to mouth	1	Constant: clapping, hand to mouth	2
Age of stereotypy onset	NA		NA		NA		12 months		NA		12 months	
Jerky movements	NA		Yes		Yes		Occasional		Yes		Yes	
Rocking	Yes		NA		Absent		No		Yes		No	
Voluntary hand use	NA		Poor	1	Absent	2	Poor	1	Absent	2	Absent	2
Sitting	NA		15 months	0	Not acquired	2	No sitting alone	2	Not acquired	2	10 months	1
Walking	Not acquired	2	Not acquired	2	Not acquired	2	Not acquired	2	Not acquired	2	Not acquired	2
Age at walk	Never		Never	2	Never	2	Never	2	Never	2	Never	2
Speech	Not acquired	2	Not acquired	2	Not acquired	2	Not acquired	2	Not acquired	2	Not acquired	2
Age of increasing words	Never	2	Never	2	Never	2	Never	2	Never	2	Never	2
Level of speech	Absent	2	Absent	2	Absent	2	Absent	2	Absent	2	Absent	2
Level of phrases	Absent	2	Absent	2	Absent	2	Absent	2	Absent	2	Absent	2
Epilepsy	Not controlled by therapy	2	No epilepsy	0	Recurrent status epilepticus controlled by treatment	1	No epilepsy (3 years)	0	Not controlled by therapy	2	Controlled by therapy	1
Seizure onset	NA		Never		17 months		Never (3 years)		14 years		30 months	
Sleep disturbances	NA		Yes		Yes, severe		No		Yes		Yes	
Eye contact	NA		Poor		Poor		Good at 12 months		Poor		Poor	
Gastro-intestinal disturbances	NA		Moderate constipation	1	Severe, reflux and constipation	2	Constipation	1	Constipation	1	Constipation	1
Breathing disorders	NA		No	0	No	0	Apnoeas	1	Sporadic hyperventilation episodes	1	Prolonged inspirations	1
Cold extremities	NA		Yes	1	No	0	No	0	Mild	1	Mild	1
Tongue protruding movements	NA		Yes		No		Yes		Yes		Yes	
Bruxism	Yes		No		Yes		Yes, teeth chattering		Yes		Teeth beating/ teeth-chattering	
Sialorrhea	NA		No		Yes		Yes		Yes		Yes	
Pain threshold	NA		Normal		Normal		High				High	
Joint rigidity	NA		No		No		No		Yes, large and small joints		Small joints	
Strabismus	NA		Yes		Yes		Yes		Yes		Yes	
Sphincter control	NA		No	2	Absent	2	Absent	2	Absent	2	Absent	2
Genu valgu	NA		NA		No	0	Absent		Severe	2	Absent	0
Pes planus	NA		Absent	0	NA		Mild	1	NA		NA	

Continued

Table 1 Continued

	Patient 1 (1091)	Score	Patient 2 (RTT00967)	Score	Patient 3 (RTT01158)	Score	Patient 4 (60718368)	Score	Patient 5 Ariani *et al*[3]	Score	Patient 6 Ariani *et al*[3]	Score
Scoliosis	Severe	2	No	0	No	0	Absent	0	Severe	2	Absent	0
Kyphosis	NA		No	0	Yes	1	Severe	2	Severe	2	Absent	0
Corpus callosum thinning at brain MRI	NA		No		Yes		Yes		Yes, mild		Yes, mild	
Total score		–		–		28		32		38		31

accordance with the diagnosis of the congenital variant. Motor development is severely impaired: no girl with a mutation could either walk with support or speak, although cases 2 and 6 can stand up with assistance (figure 1C). Voluntary hand use was absent in the majority of patients (3/5) and poor in two (cases 2 and 4). Poor eye contact and absence of response to social interaction were evident in five out of six patients, in contrast with classic RTT where eye contact is intense, and this feature represents a supportive criterion for diagnosis.

Stereotypic hand movements are typical as in classic RTT, with intense and continuous hand washing and hand mouthing activities. In addition, all girls showed constant thrusting of the tongue. These repetitive movements are not so typical of classic RTT, where ineffective chewing movements (seen in one of our patients) are found rather than thrusting of the tongue. Similar tongue protruding movements were present in the girl with the 14q12 deletion, which led to the identification of *FOXG1* mutations in the first patients with congenital RTT.[12] Also, in 4/5 patients jerky movements are often seen in the upper limbs, that are frequently pushed in different directions, while in classic RTT such movements are rarely reported.

In this small cohort of patients, epilepsy was a variable sign: two girls, aged 3 years and 6.5 years respectively, have never presented with epileptic seizures (cases 2 and 4); in four patients epilepsy was present with an onset between 14 and 30 months. In two the epilepsy was well controlled by antiepileptic drugs (patients 3 and 6), while in the remaining two, seizures recurred despite treatment.

Neurological and neurovegetative symptoms are consistent with a diagnosis of RTT: constipation is reported in 4/6 patients; breathing abnormalities in 4/6; cold extremities in 3/6; bruxism in 4/6; sialorrhea in 4/6. Skeletal alterations such as scoliosis and kyphosis, genu valgu and pes planus are severe in the older cases.

Brain MRI showed corpus callosum hypoplasia in four patients, and this has been excluded in only one of the remaining two cases. Moreover, complete agenesis of the corpus callosum has been identified in patients with chromosomal rearrangements involving *FOXG1*.[11 15] All these findings are in accord with the phenotype of heterozygous *Foxg1*$^{+/-}$ mice, showing a corpus callosum defect.[3]

Our results contribute to the clarification of the phenotype associated with *FOXG1*, confirming its role in the RTT spectrum. In particular, they seem to be associated with the most severe end of this spectrum. In fact, the median of the total clinical score in this group of patients is higher in comparison with patients affected by classic or early onset seizure variant of RTT.

All the patients reported to date with *FOXG1* mutations are female. This is probably due to an ascertainment bias and we expect that further mutations will be identified in male cases, given that *FOXG1* is an autosomal gene.

In conclusion, we suggest that *FOXG1* gene mutation analysis should be performed in female and male patients showing RTT features but lacking the typical early normal period due to the

Figure 1 Pictures of three of the new patients with *FOXG1* mutations. Panel A, case 4; panel B, case 1; panel C, case 2. Note in patient 4 the constant and intense hand to mouth stereotypic activities. The severe microcephaly of case 1 is clearly evident. Patient 2, presently aged 6 years 6 months, is able to stand up only with support but she cannot walk. Parental/guardian consent has been obtained.

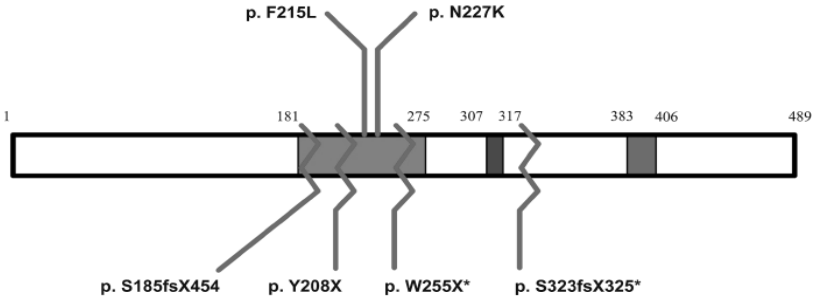

Figure 2 *FOXG1* mutations and alterations of the functional domains. Schematic representation of FoxG1 protein. The three main functional domains are shown: the DNA binding fork-head domain, the Groucho binding domain and the JARID1B binding domain is red. The numbers at the top refer to the amino acid positions. The frameshift and stop mutations are showed below by zigzag lines. The missense mutations are indicated at the top. The asterisks indicate the two mutations previously reported in Ariani *et al*.[3]

Key points

- *FOXG1* gene, located in 14q12, is responsible for the congenital variant of RTT.
- Mutation analysis should be performed in female and male patients showing RTT features but lacking the typical early normal period due to the precocious onset of symptoms.
- Major signs possibly indicating a *FOXG1* mutation are severe psychomotor delay with inability to walk, severe postnatal microcephaly evident before the age of 4 months, poor eye contact, tongue stereotypies, jerky movements of limbs, and corpus callosum hypoplasia.

precocious onset of symptoms. Besides other features typical of classic RTT, major signs possibly indicating a *FOXG1* mutation are severe psychomotor delay with inability to walk, severe postnatal microcephaly evident before the age of 4 months, poor eye contact, tongue stereotypies, jerky movements of limbs, and corpus callosum hypoplasia.

Acknowledgements We would first like to thank the Rett patients and their families. This work was supported by Telethon grants GTB07001, by the EuroRETT E-RARE network and by the Emma and Ernesto Rulfo Foundation to A.R. This work was also supported by A.I.R. (Associazione Italiana Rett) to M.A.M and by PAR 06 of University of Siena to F.M.

Competing interest None.

Patient consent Obtained.

Provenance and peer review Not commissioned; externally peer reviewed.

REFERENCES

1. **Chahrour M,** Zoghbi HY. The story of Rett syndrome: from clinic to neurobiology. *Neuron* 2007;**56**:422—37.
2. **Renieri A,** Mari F, Mencarelli MA, Scala E, Ariani F, Longo I, Meloni I, Cevenini G, Pini G, Hayek G, Zappella M. Diagnostic criteria for the Zappella variant of Rett syndrome (the preserved speech variant). *Brain Dev* 2009;**31**:208—16.
3. **Ariani F,** Hayek G, Rondinella D, Artuso R, Mencarelli MA, Spanhol-Rosseto A, Pollazzon M, Buoni S, Spiga O, Ricciardi S, Meloni I, Longo I, Mari F, Broccoli V, Zappella M, Renieri A. FOXG1 is responsible for the congenital variant of Rett syndrome. *Am J Hum Genet* 2008;**83**:89—93.
4. **Scala E,** Longo I, Ottimo F, Speciale C, Sampieri K, Katzaki E, Artuso R, Mencarelli MA, D'Ambrogio T, Vonella G, Zappella M, Hayek G, Battaglia A, Mari F, Renieri A, Ariani F. MECP2 deletions and genotype-phenotype correlation in Rett syndrome. *Am J Med Genet A* 2007;**143**:2775—84.
5. **Mari F,** Azimonti S, Bertani I, Bolognese F, Colombo E, Caselli R, Scala E, Longo I, Grosso S, Pescucci C, Ariani F, Hayek G, Balestri P, Bergo A, Badaracco G, Zappella M, Broccoli V, Renieri A, Kilstrup-Nielsen C, Landsberger N. CDKL5 belongs to the same molecular pathway of MeCP2 and it is responsible for the early-onset seizure variant of Rett syndrome. *Hum Mol Genet* 2005;**14**:1935—46.
6. **Rolando S.** Rett syndrome: report of eight cases. *Brain Dev* 1985;**7**:290—296.
7. **Hagberg B,** Hanefeld F, Percy A, Skjeldal O. An update on clinically applicable diagnostic criteria in Rett syndrome. Comments to Rett Syndrome Clinical Criteria Consensus Panel Satellite to European Paediatric Neurology Society Meeting, Baden Baden, Germany, 11 September 2001. *Eur J Paediatr Neurol* 2002;**6**:293—7.
8. **Sambrook J,** Fritsch EF, Maniatis T. *Molecular cloning: a laboratory manual*. 2nd edn. Cold Spring Harbor Laboratory Press, Woodbury, New York, USA. 1989.
9. **Artuso R,** Mencarelli MA, Polli R, Sartori S, Ariani F, Pollazzon M, Marozza A, Cilio MR, Specchio N, Vigevano F, Vecchi M, Boniver C, Bernardina BD, Parmeggiani A, Buoni S, Hayek G, Mari F, Renieri A, Murgia A. Early-onset seizure variant of Rett syndrome: definition of the clinical diagnostic criteria. *Brain Dev* Published Online First: 2009 doi:10.1016/j.braindev.2009.02.004.
10. **Grammatico P,** de Sanctis S, di Rosa C, Cupilari F, del Porto G. First case of deletion 14q11.2q13: clinical phenotype. *Ann Genet* 1994;**37**:30—2.
11. **Shoichet SA,** Kunde SA, Viertel P, Schell-Apacik C, von Voss H, Tommerup N, Ropers HH, Kalscheuer VM. Haploinsufficiency of novel FOXG1B variants in a patient with severe mental retardation, brain malformations and microcephaly. *Hum Genet* 2005;**117**:536—44.
12. **Papa FT,** Mencarelli MA, Caselli R, Katzaki E, Sampieri K, Meloni I, Ariani F, Longo I, Maggio A, Balestri P, Grosso S, Farnetani MA, Berardi R, Mari F, Renieri A. A 3 Mb deletion in 14q12 causes severe mental retardation, mild facial dysmorphisms and Rett-like features. *Am J Med Genet A* 2008;**146A**:1994—8.
13. **Mencarelli MA,** Kleefstra T, Katzaki E, Papa FT, Cohen M, Pfundt R, Ariani F, Meloni I, Mari F, Renieri A. 14q12 Microdeletion syndrome and congenital variant of Rett syndrome. *Eur J Med Genet* 2009;**52**:148—52.
14. **Bisgaard AM,** Kirchhoff M, Tumer Z, Jepsen B, Brondum-Nielsen K, Cohen M, Hamborg-Petersen B, Bryndorf T, Tommerup N, Skovby F. Additional chromosomal abnormalities in patients with a previously detected abnormal karyotype, mental retardation, and dysmorphic features. *Am J Med Genet A* 2006;**140**:2180—7.
15. **Schuffenhauer S,** Leifheit HJ, Lichtner P, Peters H, Murken J, Emmerich P. De novo deletion (14)(q11.2q13) including PAX9: clinical and molecular findings. *J Med Genet* 1999;**36**:233—6.

Result 4.3

FOXG1 **mutation leading to reduced chromatin affinity causes *"Rett fruste"* overlapping with *EHMT1* phenotype**.

De Filippis R 1*, Pancrazi 2,3 *, Bjørgo K 4, Rosseto A 1, Kleefstra T 5, Grillo E 1, Panighini A 2, Meloni I 1, Ariani F 1, Mencarelli MA 1, Hayek J 6, Renieri A 1, Costa M 2, Mari F 1.

* *This manuscript submitted to Human Mutation.*

***FOXG1* mutation leading to reduced chromatin affinity causes *"Rett fruste"* overlapping with *EHMT1* phenotype.**

De Filippis R 1*, Pancrazi 2,3 *, Bjørgo K 4, Rosseto A 1, Kleefstra T 5, Grillo E 1, Panighini A 2, Meloni I 1, Ariani F 1, Mencarelli MA 1, Hayek J 6, Renieri A 1, Costa M 2, Mari F 1.

*both authors contributed equally to the work

1 Medical Genetics, Dept. Molecular Biology, University of Siena, Italy

2 CNR, Pisa, Italy

3 Scuola Normale Superiore, Pisa, Italy

4 Medical Genetics, University of Oslo, Norway

5 Department of Human Genetics, Radboud University Nijmegen, Netherlands

6 Child Neupsychiatry University Hospital AOUS Siena, Italy

Corresponding authors

Mario Costa, CNR Pisa, mario.costa@in.cnr.it

Alessandra Renieri, Medical Genetics, University of Siena, renieri@unisi.it

Abstract

The Forkhead box G1 (*FOXG1*) gene, a brain specific transcriptional factor essential for the early development of telencephalon, located in 14q12, has been recently implicated in the congenital variant of Rett Syndrome (RTT). Until now only 10 patients with *FOXG1* point mutations have been reported with a quite homogeneous phenotype including a severe neurological impairment in accordance with a clinical diagnosis of congenital variant RTT. These patients do not show peculiar facial features in contrast with those with the 14q12 microdeletion syndrome. Here we report on two unrelated patients with a *de novo FOXG1* point mutation, p.Gln46X and p.Tyr400X respectively, having a milder RTT phenotype according with RTT "*forme fruste"* and sharing strikingly similar facial features resembling the Kleefstra syndrome due to *EHMT1* gene. Although FoxG1 action as well as EHMT1 depends critically on its binding to chromatin, very little is known about the dynamics of this process. Here we apply photobleaching strategies within the nucleus comparing the wild type GFP tagged FoxG1 with the protein carrying pathological mutations. We report for the first time that most of the FoxG1 fusion protein is transiently associated with chromatin *in vivo* and that mutations caused a mislocalization of FoxG1 and a dramatic alteration in chromatin affinity which is particularly high in the two mutations reported here. Interestingly both FoxG1 and EHMT1 proteins interact with members of JARID1 family and are involved in modulation of the chromatin structure. In this perspective, the overlapping phenotype described in this paper could not be completely unexpected.

Introduction

Rett Syndrome is a neurodevelopmental disorder that represents one of the most common causes of mental retardation in girls. This syndrome is characterized by high clinical variability revealing a wide spectrum of clinical variants. Besides the classical form due to *MECP2* mutations, other three variants have been associated with a quite specific molecular defect [1]. They include the early-onset seizure variant mostly due to *CDKL5* mutations, the congenital variant mostly due to *FOXG1* mutations and the Zappella variant (Z-RTT) mostly due to *MECP2* mutations [1]. Gene phenotype association is not so strict and *MECP2* mutated early onset seizure variant cases as well as *MECP2* mutated congenital variant cases can be rarely found [2], [3], [4]. At the same time a *FOXG1* mutation has been identified in one case with a classic phenotype [5]. In the late 80 s Hagberg described also the *"form fruste"* of RTT for cases partially fulfilling the classic inclusion

criteria (Hagberg 1986; Hagberg B, ed Rett syndrome-Clinical and biological aspects. Clinics in developmental medicine No 127. London: Mac Keith Press, 1993;21-5). The cases reported as *"forme fruste"* form a clinically heterogeneous group. Some patients are described as not microcephalic and with normal build, in some others stereotypies never developed and in other patients some degree of hand use is retained [6], [7]. Some cases affected by this variant have been reported associated with *MECP2* mutation (www.biobank.unisi.it). The association between *FOXG1* gene and the congenital variant of RTT is relatively recent [8]. From 2008 to now 10 patients with *FOXG1* point mutations have been reported [8], [9], [5],

[10]. Among these, 9 patients are reported as affected by the congenital variant of RTT and 1 by the classic form. All these *FOXG1* mutated patients showed a quite homogeneous phenotype presenting the same clinical features of classic RTT but appearing floppy and with developmental delay from the very first months of life. Beside the congenital RTT due to *FOXG1* point mutation a 14q12 microdeletion syndrome has been described [11], [12]. These patients show in addition to the severe neurological phenotype peculiar facial features including downslanting palpebral fessures, bilateral epicantal folds, depressed nasal bridge, bulbous nasal tip, tended upper lip, everted lower lip and large ears [13]. The *FOXG1* gene encodes a forkhead box protein G1, a DNA-binding transcription factor essential for the development of the ventral telencephalon in embryonic mammalian forebrain. The protein acts by maintaining telencephalic progenitor status and ensuring that these progenitors maintain appropriate cell cycle kinetics [14]. Despite its early expression in telencephalon development, Ariani *et al.* demonstrated that *FOXG1* expression is detectable in the differentiating cortical compartment in the postnatal stages, although at lower levels respect to the early embryonic phases. At the single cell level, *FOXG1* is localized widespread in the nuclear compartment, outside the heterochromatic foci, suggesting that it is not stably associated with heterochromatin [8]. The FoxG1 protein is composed by 489 aminoacids organized in three main functional domains: the DNA-binding forkhead domain, the GROUCHO-binding domain and the JARID1B binding domain. The interaction with these two proteins is required for early brain development. Groucho protein

is coexpressed with FoxG1 in telencephalic neuronal progenitor cells and participates to the transcriptional function of FoxG1 by acting as both a corepressor and an adapter [15]. JARID1B is a demethylase capable of removing three methyl groups from histone H3 lysine 4. It plays an important role in regulating chromatin dynamics and can directly regulate gene transcription either alone or as part of a multimolecular complex together with FoxG1 [16]. Given MecP2 important involvement in the interpretation of chromatin modifications, Rett syndrome has been considered an epigenetic disorder. Indeed, we and others [17], [18] recently provided evidence indicating that in Rett syndrome different pathological mutations of *MECP2* regulate its chromatin – binding dynamics *in vivo*. The epigenetic nature of this syndrome is further supported by the identification of *FOXG1* mutations in patients with this syndrome. *FOXG1* is in fact known to be involved in global chromatin organization and displays a key role in regulating neuronal differentiation: the relationship between FoxG1 and chromatin and its functional role in the nucleus have as yet not been elucidated [16]. To address this issue we herein employed photobleaching strategies, a well accepted assay to study the *in vivo* properties of chromatin binding proteins. The subcellular localization and dynamics of FoxG1 binding to chromatin in living cells were then investigated using fluorescence recovery after photobleaching (FRAP). In particular, we compared the localization and mobility of a GFP-tagged wild type FoxG1 (GFP-FoxG1 WT), with that of nonsense derivatives mimicking diverse pathological mutations. Our findings demonstrate that: (1) FoxG1 binds strongly to chromatin and

this binding is partially irreversible as demonstrated by the presence of the immobile fraction; (2) the nuclear or cytoplasmatic localization of FoxG1 depends on its dramatic change in chromatin affinity; (3) the chromatin affinity as well as the capability of FoxG1 to maintain a nuclear or cytoplasmatic localization, decreases with progressive deletion of *FOXG1*; (4) the amount of immobile fraction is not in relation with the progressive deletion of *FOXG1*. Our data suggest that alterations in chromatin binding of FoxG1 might contribute to the pathological effects of mutations causing Rett syndrome and may explain the milder phenotype of the two patients described here.

Material and Methods

Molecular analysis

Blood samples were obtained from patients and available parents after informed consent: DNA was extracted from peripheral blood using a QIAmp DNA Blood Kit (Qiagen, Hilden, Germany). To determine the appropriate DNA concentration, we used the OD260/280 method on a photometer. The entire coding sequence was amplified by polymerase chain reaction (PCR) in six overlapping fragments. Primers and PCR conditions used for single exons analysis were as described previously [8], [5]. The analysis of fragments 1C-1F DNA was performed using Transgenomic WAVE Denaturing High Performance Liquid Chromatography (DHPLC). PCR products resulting in abnormal DHPLC profiles together with fragments 1A and 1B were sequenced on both strands using PCR primers with fluorescent dye

terminators on an ABI PRIMSM 310 genetic analyzer (Applied Biosystem, Foster City, CA). The analysis was performed using the Collection and Sequence Analysis software package (Applied Biosystems).The results were compared with the reference RTT genomic sequence (GeneBank accession n°NM_005249.3).

DNA enzymatic digestion

In order to confirm the mutation c.136C>T (p.Gln46X) introducing the restriction site CTAG, we performed an enzyme digestion of DNA using BfaI. A 50 µl reaction containing 1 µg of DNA and 200 units of BfaI incubated for 16 hours at 37° C resulted in a DNA pattern free of detectable nuclease degradation as determined by agarose gel electrophoresis.

Cell culture and transfection.

NIH3T3 cell line was cultured according to ATCC indications. The cells were plated at 60–70% confluence, in a glass chamber for the Leica confocal microscope, and transfected using Lipofectamine 2000 (Invitrogen) according to the manufacture's instructions. After transfection, cells were left undisturbed for 24 hours before any further experimental manipulation. All experiments have been performed at 37°C.

Plasmid construction.

pGFP-FoxG1 wt vector, containing the entire cDNA of mouse *FoxG1* except the start codon (480 amino acids), was generated by PCR and the HindIII / BamHI digested product inserted into the HindIII /BamHI sites of pEGFP-C3 (Clontech). The vector containing FoxG1 cDNA was kindly provided by

Dr. Vania Broccoli. The pathological derivatives constructs are shown in figure 3A and they were obtained as
follows:

GFP-*Foxg1* Ser315fsX317 (homologue to human Ser323fsX325 mutation) *Foxg1* mouse cDNA was amplified by PCR using a forward primer incorporating XhoI site (underlined) and the *FOXG1* ATG start codon (bold). Forward primer: 5'-CTCGAGAA**ATG**CTGGACATGGGAGATAGG-3'. The reverse primer was 5'- GGATCC**TCA**AAGT(G)CTGCTGGCGCGG-3' incorporating BamHI site (underlined) and the *FOXG1* deletion (G) that activates the stop codon shown in bold. The amplification product was purified and cleaved with XhoI/BamHI, and ligated to the corresponding restriction sites in the vector pEGFP-C1 (Clontech, USA).

GFP-*Foxg1* Tyr392X (homologue to human Tyr400X mutation) *Foxg1* mouse cDNA was amplified by PCR using GFP-*Foxg1* Ser323fsX325 as DNA template and a forward primer incorporating the KpnI restriction site that occurs in the mouse *FOXG1* cDNA (underlined) Forward primer: 5'-GAAGGTACCGCGCCACTACGAC-3'. The reverse primer was 5'-GGATCCTAGGTCCCGGAGCAGGGCAC-3', incorporating BamHI site (underlined) and annealing until base 1175, the point corresponding to the site of the non sense mutation Tyr400X in human. The amplification product was purified and cleaved with XhoI/BamHI, and ligated to the corresponding restriction sites in the vector pEGFP-C1 (Clontech, USA).

GFP-*Foxg1* Gln46X *Foxg1* mouse cDNA was amplified by PCR using GFP-*Foxg1* Ser323fsX325 as DNA template and the same forward primer used for

GFP-*Foxg1* Ser315fsX317; the reverse primer was 5'-GGATC*CTA***A**GGGGTGGTGGCTGTTG-3', incorporating BamHI site (underlined)

and the non sense mutation (bold) originating a stop codon (italics) . The amplification product was purified and cleaved with XhoI/BamHI, and ligated to the corresponding restriction sites in the vector pEGFP-C1 (Clontech, USA).

Imaging

Strip FRAP were performed on a Leica TCS NT confocal microscope with an oil immersion lens (Leica HCX PL APO 40X, NA 1.25-0.75). GFP fluorescence was excited at 488 nm with an Ar/K laser. Quantification of fluorescence was performed on the Leica platform Average fluorescence background was evaluated on non-transfected cells and was subtracted from all measurements. We did not mask the presence of fluorescence artefacts in any of the images accompanying the paper. In average, the laser power employed during imaging was about 30 □W. Data plotting and statistical testing (one or two ways t-test as appropriate) has been performed with the Origin 7.5 package.

Strip-FRAP.

Photobleaching was preceded by the acquisition of 64 lines necessary for data normalisation. The total fluorescence bleached in the imaging run was estimated by comparing a pre-bleach image of the whole cell with an image acquired at the end of the line scans. Bleaching was performed by scanning the line at high power (about 50 times larger than during pre bleach and

recovery) for 160 ms. The line was chosen to intersect the nucleus and the cytoplasm (Fig 4A and 5A). Line scan was performed at a frequency of 400 Hz and the recovery was evaluated for 30 s (Fig 4B and 5B). Fluorescence is corrected for background and normalised for the corresponding prebleached regions. Recovery curves were fitted by a double exponential function. The immobile fraction was computed by the asymptotic value of the recovery corrected for the total amount of fluorescence loss, as estimated by the comparison of the pre-bleach and post-bleach images.

Results

Clinical description

Patient 1. She is 12.5 year old female patient. She is the only child of unrelated and healthy parents. She was born at the 38th week of gestation after an uneventful pregnancy. At birth the weight was 3.050 Kg (50° cnt), length was 49 cm (50°-75° cnt), OFC 33 cm (25°-50° cnt), Apgar score was 10 at 1' and 5'. She was referred as a infant extremely peaceful in the first months of life. Deceleration of head growth and developmental delay were apparent from the age of 4 months. She acquired the ability to sit at 9 months and she was able to walk independently at 2.5 years. Febrile convulsions appeared at the age of 5 months followed (at 7 months) by atonic afebrile convulsions that were not completely controlled by therapy. Parents referred that she showed hand-mouthing stereotypies during the first year of life. At 6 years bilateral strabismus was surgically corrected. Brain MRI performed at 6 years and 10 years were normal. At the age of our first

examination she was 7.5 years, she showed an ataxic gait and no language. She presented postnatal microcephaly (48 cm), midface hypoplasia, downslanting palpebral fissures, bulbous nasal tip and anteverted nares, prognatism, diastasis of teeth, thick and everted lower lip and straight hair. A wrist X-ray performed at 9.5 years demonstrated a delayed skeletal maturation (7.3 years). First menses appeared at 12 years. At the last examination she was 12.5 years, language was absent, she was still able to walk unsupported with broad base and flexed upper and lower limbs and she still presented atonic seizures. She showed rocking of the trunk, an hyperactive behavior and hand apraxia. She had stereotypies of the tongue that she always protruded out of the mouth and hand stereotypies. She continuously grasped paper and she tore it in little pieces. Hyperventilation was apparent and sleep disturbances and constipation were referred. She showed microcephaly (49.8 cm) with normal height and weight. All specific facial feature present at the first examination were more pronounced resulting in a coarse facial appearance (Fig. 1A and 1C). Karyotype, methylation analysis of the 15q11.2 region and molecular analysis of *UBE3A* resulted normal. The *UBE3A* analysis revealed the presence of the p.Lys466Asp variant also present in mother's and grandmother's DNA. *MECP2* and *CDKL5* analysis resulted normal. Following the clinical suspicion of 9q34 deletion syndrome an array-CGH analysis (Agilent 44K) and the *EHMT1* molecular analysis (point mutations and deletions) have been performed and both resulted normal.

Patient 2. The patient is a 31 years old woman with severe mental retardation. She is the third child of healthy unrelated parents. No relevant information in the family history. Older siblings are healthy. The pregnancy was normal, but the mother noticed less fetal movements than in earlier pregnancies. She was born at 42 weeks of gestation by cesarean sectio because of abruptio placenta. At birth she showed normal auxological parameters and had hip dysplasia on the right side that was diagnosed later. Development was noticed to be delayed already at four weeks of age by her mother because she did not give normal eye contact and smiled later than her siblings. She was hypotonic and had to have supplementary feeding by bottle. By one year of age a visual impairment was hypothesized since she gave eye contact only for short moments of time. She was able to sit at 3 years, she was able to stand with support at 5 years. At the time of our observation she could walk only with support. She wore a corset for scoliosis. The patient did have some slight hand washing stereotypies and sleep disturbances as a child. She has never had seizures. EEG has not been performed. Cerebral CT performed in the first year of life was normal. At the examination she knew about 30 words, but she pronounced them unclearly and she did not always use them appropriately. She was also able to use some handsigns. Her growth parameters were in the normal range with OFC of 54 cm (10°-25° percentile). She has coarse facial features with midface hypoplasia, bulbous nose and broad nasal bridge, thick lower lip, prognatism, dark, thick and straight hair (Fig. 1B and 1D). Karyotype, array-

CGH (Agilent 105K), and *MECP2* and *UBE3A* molecular analysis were all normal.

Molecular analysis

The molecular analysis of *FOXG1* gene revealed one *de novo* mutation in both patients (Fig 2). In patient 1, the mutation c.136C>T was identified. This mutation introduces a premature stop-codon (p.Gln46X) that disrupts the protein at the N-terminal, causing the loss of the three main functional domains: the DNA binding fork-head domain, the GROUCHO-binding domain and JARID1B binding domain. In patient 2, the mutation c.1200C>A (p.Tyr400X) interrupts the protein at the level of the JARID1B binding domain.

GFP-FoxG1 Fluorescently tagged mutants and subcellular localization The cellular localization of FoxG1 is controlled by a sophisticate signalling network that results in the nuclear or cytoplasmatic localization of the protein [19].To examine the effects caused by pathological mutations on FoxG1 cellular localization, we generated a series of mutants corresponding to the two mutations reported here and to a previously described mutation associated with RTT congenital variant (Fig 3A) [8]. These constructs were

inserted into the pEGFP vector (Clontech) and transiently transfected into NIH3T3. 24 hours after the transfection we could clearly identify two classes of cells: cells presenting a predominant amount of FoxG1 in the nuclear compartment and cell in which FoxG1 is visibly cytoplasmatic (Fig 3C). In

order to distinguish in a quantitative manner the two classes of cells and compare the wild type FoxG1 localization with the pathological derivatives we calculated the nuclear/cytoplasmic (Nuc/Cyt) ratios of fluorescence intensity (Fig 3B). This ratios were determined by dividing the intensity of the GFP fluorescence from the nucleus by that in the cytoplasm. In the cells expressing wild type FoxG1 the two classes of cell presents respectively a Nuc/Cyt average ratio of 9.14+/- 2.33 in the case of FoxG1 nuclear localization and 0.37 +/-0.038 in the case of cytoplasmatic localization (Fig 3B). As concerns the pathological mutants Gln46X, Ser323fsX325 and Tyr400X, the two classes of cell present progressive decrease capability of FoxG1 segregation in the nuclear or in the cytoplasmatic compartment (Fig 3C). In the case of the shorter N-terminal phatological mutation Gln46X the Nuc/Cyt ratio decrease near to 1 (1.38+/-0,02) and the two classes of cells are undistinguishable. On the contrary, in cells expressing Ser323fsX325 pathological FoxG1 mutant the two classes of cell present a Nuc/Cyt average ratio 2.42+/-0.6 and 0.63 +/-0.15 in the case of FoxG1 nuclear and cytoplasmic localization respectively. Finally, cells expressing the Tyr400X pathological FoxG1 mutant show respectively a Nuc/Cyt average ratio of 3.91+/-0.52 in case of FoxG1 nuclear localization and 0.38 +/-0.07 in case of FoxG1 cytoplasmic localization (Fig 3B).

Foxg1 is dynamically bound to the chromatin

In order to study the stability of the binding of FoxG1 to chromatin and in the cytoplasmatic compartment we adopted a photobleaching strategy called strip FRAP. In the FRAP experiments, a powerful light beam is used to

irreversibly photobleach the fluorescent molecules in a micron-sized area of the sample (Fig 4A and 5A). After photobleaching, photobleached molecules will gradually move out of the photobleached area and will be replaced by unbleached molecules from the surroundings. Due to this diffusional exchange, the fluorescence inside the photobleached area recovers, and this process is monitored as a function of time (Fig. 4 and 5).

GFP-Foxg1 WT expressing cells:

Cells with nuclear localization of FoxG1: As shown in figure 4 the recovery of fluorescence outside of the nucleus is much faster (t2= 0.79 s versus 3.08 s) and the immobile fraction is smaller (0.1 versus 0.17) than within the nuclear compartment indicating that the binding is stronger and less reversible in the nuclear compartment.

Cells with the cytoplasmatic localization of FoxG1: The same measure performed on this class of cells demonstrated that the recovery of fluorescence inside and outside of the nucleus is similar (t2=1.13+/-0.15 s versus 1.05+/-0.09 s) as well as the immobile fraction (0.1+/-0.018 versus 0.093+/-0.02) (Fig 5C and 5D). As a consequence of this dramatic loss in chromatin affinity the ratio t2 chromatin/t2 cytoplasm was definitely higher in the cells presenting FoxG1 in the nuclear compartment (4.24+/-0.51) respect to the cells in which the protein is predominantly cytoplasmatic (1.16+/-0.17), indicating that the protein localization depends primarily on the affinity for chromatin.

GFP-FoxG1 Tyr400X expressing cells:

Cells with nuclear localization of FoxG1: When the strip-FRAP protocol was applied to cells transfected with GFP-Tyr400X we found that the recovery of fluorescence outside of the nucleus is still faster (t2= 0,67+/-0.06 s versus 0.9 3+/-0.09s) and the immobile fraction is smaller (0.09+/-0.08 versus 0.7+/-0.02) than within the nuclear compartment indicating that still in the mutant Tyr400X the binding is stronger and less reversible in the nuclear compartment (Fig 4E). The binding to chromatin of Tyr400X was much lower than that of the GFP-FoxG1WT (t2=0.9+/-0.09 s versus 3.08+/-0.3 s); and a slight but not significative decrease was apparent also in the cytoplasm (t2=0.67+/-0.06 s compared to 0,79+/-0.06 s). Interestingly, we found that the ratio t2 chromatin/t2 cytoplasm was higher for the full length protein than for the mutant (4.24+/-0.51 versus 1.35+/- 0.18), indicating that the deletion affects primarily the affinity for the chromatin.

Cells with the cytplasmatic localization of FoxG1: The same measure performed on this class of cells demonstrated that the recovery of fluorescence inside and outside of the nucleus is similar (0.73+/-0.05 s versus 0.65+/-0.04 s) but significantly faster than in the corresponding class of cells transfected with GFP-FoxG1WT (0.73+/-0.05 s versus 1.13+/-0.15 s in the nucleus and 0.65+/-0.04 s versus 1.05+/-0.09 s in the cytoplasm). No difference can be observed in the immobile fraction inside and outside the nucleus (0.076+/-0.013 versus 0.082+/-0.018) and between the same cellular compartments in the corresponding class of cells transfected with GFP-FoxG1WT (0.076+/-0.013 versus 0.1+/-0.018 in the nucleus and

0.082+/-0.018 versus 0.093+/-0.02 in the cytoplasm) (Fig.5E). In this class of cells the ratio t2 chromatin/t2 cytoplasm was similar for the full length proteinand for the mutant (1.16+/-0.17 versus 1.15+/-0,11), indicating that the deletion affects the affinity for the chromatin only in those cells with a Nuc/Cyt ratio mag 1.

GFP-FoxG1 Ser323fsX325 expressing cells:

Cells with nuclear localization of FoxG1: In cells transfected with Ser323fsX325 we found that therecovery of fluorescence outside and inside the nucleus is similar (t2= 0.64+/-0.03 s versus 0,73+/-0.06 s) and the immobile fraction is smaller (0,11.+/-0,005 in the cytoplasm versus 0,14+/-0,01 in the nucleus) (Fig 4E). An important difference respect to the other two mutants is the significantly higher immobile fraction. The binding to chromatin of Ser323fsX325 was much lower than that of the GFP-FoxG1WT (t2=0.73+/-0.06 s versus 3.08 +/-0.31 s); and a significative decrease was apparent also in the cytoplasm (t2= 0.64 +/-0.03 s compared to 0,79 +/-0.06 s) (Fig 4E). Also in this case we found that the ratio t2 chromatin/t2 cytoplasm was higher for the full length protein than for the mutant (4.24+/-0.51 versus 1,07+/-0.05), indicating also this deletion affects primarily the affinity for the chromatin.

Cells with the cytplasmatic localization of FoxG1: The same measure performed on this class of cells demonstrated that the recovery of fluorescence inside the nucleus is still faster than outside (0.79+/-0.07 s versus 0.62+/-0.04 s), as observed in GFP-FoxG1 WT; in addition, the recovery of fluorescence in the nucleus and the cytoplasm is significantly

faster than in the corresponding classes of cells transfected with GFP-FoxG1 WT (0.73+/-0.05 s versus 1.13+/-0.15 s in the nucleus and 0.65+/-0.04 s versus 1.05+/-0.09 s in the cytoplasm). No difference can be observed in the immobile fraction inside and outside the nucleus (0.076+/-0.013 versus 0.082+/-0.018) and between the same cellular compartments in the corresponding classes of cells transfect with GFPFoxG1WT (0.076+/-0.013 versus 0.1+/-0.018 in the nucleus and 0.082+/-0.018 versus 0.093+/-0.02 in the cytoplasm) (Fig 5E). In this class of cells the ratio t2 chromatin/t2 cytoplasm was similar for the full length protein and for the mutant (1.16+/-0.17 versus 1.15+/-0,11) indicating that, as in the case of Tyr400X mutation, this truncation affects the affinity for the chromatin only in those cells with a Nuc/Cyt ratio > 1.

GFP-FoxG1 Gln46X expressing cells:

Transfection with GFP-FoxG1 Gln46X, produce a fusion protein excluding the FHD, the GROUCHO and the JARID1B domain (Fig 3A). This construct revealed that FoxG1 did not accumulate in the nuclear or in the cytoplasmatic compartment but was distributed rather uniformly in the cell (Fig 3C). Indeed, strip-FRAP experiments showed that fluorescence recovery of GFPFoxG1 Gln46X was faster than that of the full length protein (0.471+/-0.013 s in the nucleus and 0.46+/-0.014 s in the cytoplasm) and similar to that of the GFP alone (0.471+/-0.013 s versus 0,450.471+/-0.018 s in the nucleus and 0.46+/-0.014 s versus 0,4490.46+/-0.01 s in the cytoplasm) (Fig.4E and 5E).

However, it has to be noted that the immobile fraction of GFP-FoxG1 Gln46X was significantly higher than the nearly negligible immobile fraction of GFP alone (0.065+/-0.008 s versus 0.014+/- 0.007 s in the nucleus and 0,027+/-0.008 s versus 0 in the cytoplasm). These values are considerably lower than the corresponding values found in cells transfected with GFP-FoxG1 WT or the other two mutant constructs. The ratio t2 chromatin/t2 cytoplasm was 1.03+/-0.03, not significantly different to the ratio measured in cells transfected with GFP alone (1.004+/-0.037).

Discussion

Since the first description in 2008, 10 patients with *FOXG1* point mutations have been reported with a quite homogeneous phenotype characterized by a severe neurological impairment in accordance with a clinical diagnosis of congenital variant of RTT. These patients have a very severe microcephaly, severely impaired motor development and absence of voluntary hand use, constant hand stereotypies and brain abnormalities [9], [1]. We reported here two unrelated patients with a *de novo FOXG1* point mutation, p.Gln46X and p.Tyr400X respectively. These patients have RTT features including normal prenatal and perinatal period, hand apraxia, pregressed hand stereotypies (hand-mouthing and hand washing type). Postnatal microcephaly, hyperventilation and constipation are present in one and severe scoliosis in the second patient of 31 years. This phenotype, although belonging to RTT spectrum, does not fit with the congenital variant because

of the absence of severe microcephaly and the quite good motor abilities. In one patient the OFC is even in the normal range and both are able to walk, the younger unsupported and the older with support. The overall clinical picture of these two patients fits well with that described in the old literature as *"forme fruste"* of RTT as cases partially fulfilling the classic inclusion criteria [6], [20], [7]. In summary, the phenotype is undoubtedly milder than the congenital RTT variant previously associated with *FOXG1* mutations. It is worth nothing that among the 10 patients previously reported with *FOXG1* mutations the only one without the severe phenotype of congenital RTT variant has the same mutation of patient 2, p.Tyr400X. Therefore, we hypothesize that some specific *FOXG1* mutations may correlate with a milder phenotype. In order to clarify, the different pathogenic role we decided to investigate the relationship between FoxG1 and the chromatin. Since the crucial event at the basis of FoxG1 action is its binding to chromatin, it is essential to know whether the binding of FoxG1 to chromatin is static or dynamic, and whether pathological mutations of the gene modify this binding and the distribution of the protein in other cell compartments. Results obtained in strip FRAP experiments show that GFP-FoxG1 WT is strongly and reversibly bound to chromatin and a significant fraction of the total protein is irreversibly bound. It is tempting to speculate that these two binding states, reversibly and stably bound to chromatin, reflect two different roles of FoxG1: the reversibly bound fraction might be associated with the modulation of gene expression, while stably bound FoxG1 might operate as a structural protein involved in chromatin organization and long

term gene repression. Moreover these chromatin binding properties of FoxG1 explain the unambiguous capacity of FoxG1 to maintain a nuclear or cytoplasmatic localization. Indeed the affinity for chromatin drops down from t2 3.08 s in the cells where FoxG1 is nuclear to t2 0.79 s in the chromatin of cells in which FoxG1 is prevalently cytoplasmic, indicating that the protein localization depends primarily on the affinity for chromatin. All this being considered we tested and compared the distribution, binding and immobile fraction of three FoxG1 derivatives, the two mutations reported here and a previously reported mutation associated with congenital variant [8]. It is interesting to observe that even a small deletion of FoxG1, like that seen in Tyr400X, caused a dramatic reduction in chromatin affinity.

However the decrease of chromatin binding further increased with the extension of the protein deletion but does not seem to be related with the severity of symptoms in Rett patients. Intriguingly the immobile fraction is not related with the decrease of the chromatin affinity and appeared significantly higher for mutation Ser323fsX325 that is associated with the most severe Rett phenotype [8]. These data clearly indicate that; (i) the protein integrity is crucial to determine chromatin binding; (ii) several portion of the protein contribute to chromatin binding; (iii) the change in chromatin affinity is not a relevant read-out for the severity of Rett syndrome symptoms. This evidence is strongly supported by the fact that the non sense mutation Gln46X totally impairs binding to chromatin, but maintains a small but detectable immobile fraction, and corresponds to a patient exhibiting a mild Rett phenotype. To reconcile these findings with the patho-

physiological scenario it is worth reminding that Rett patients carrying mutations on *FOXG1* are heterozygotes and in the same cell both the mutated and wild type proteins coexist. Each with its specific feature in reversible and stable binding to chromatin. It is then tempting to speculate that the severity of symptoms, at least for the conditions herein examined, could be attributed to that fraction of protein which is not anymore able to be exchanged and that stably remains bound to chromatin. Mutation Ser323fsX325 presenting a higher immobile fraction as compared to Gln46X ad Tyr400X (Fig 4E and 5E) can act by excluding the access of the wild type FoxG1 protein (encoded by the normal chromosome) to chromatin thus preventing its normal action. This hypothesis is further supported by data obtained in +/- *Foxg1* mouse that with a single dose of the protein, show normal viability and are in fact commonly used as cre/loxP recipients [21]. The Gln46X mutation that almost abolishes the protein and exhibits a human mild Rett phenotype can somehow be assimilated to the +/- *Foxg1* mouse genotype. In this prospective it is possible that *FOXG1* mutation exerts its pathogenic role also through a "dominant negative-like" by disturbing the already barely sufficient FoxG1 wt protein in its functional action. Usually, *FOXG1* mutated patients do not show peculiar facial features in contrast with those with the 14q12 microdeletion syndrome. Unexpectedly, the two patients have both peculiar facial features that are strikingly similar (Fig. 1). The facial appearance is different than that reported in the 14q12 microdeletion syndrome in which downslanting palpebral fessures, bilateral epicantal folds, depressed nasal bridge, tended

upper lip, and large ears are usual present [13]. The facial gestalt of both patients is evocative of the Kleefstra syndrome [OMIM 607001] considering that they both present flat face with anteverted nares, thickened lower lip, slight upslanting palbebral fissures. Although everted lower lip, bulbous nasal tip, tongue protrusion are present in both Kleefstra and 14q12 microdeletion syndrome, the facial gestalt of this two patients is more consistent with the *EHMT1* associated phenotypic spectrum. *EHMT1* encodes a histone methyl transferase which is known to promote heterochromatin formation and reduction of gene transcription. Although a direct interaction between FoxG1 and EHMT1 proteins has not been demonstrated yet, both proteins interact with members of JARID1 family and are involved in modulation of the chromatin structure (Fig 6). In this perspective, the overlapping phenotype described in this paper could not be completely unexpected. Further experiments are necessary in order to clarify the relationship between *FOXG1* and *EHMT1*.

Acknowledgements

This work has been supported by PRIN 2008 to Francesca Mari and by Telethon grants GTB07001 and GDP09117 to Alessandra Renieri.

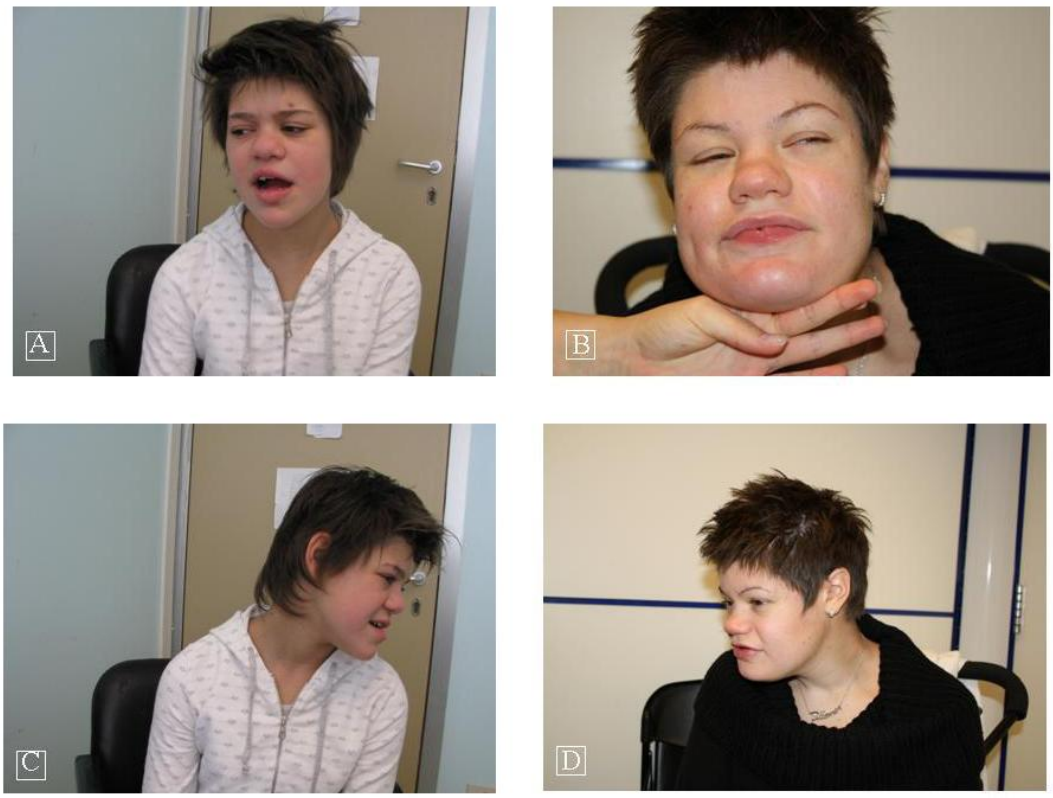

Figure 1. Pictures of the two patients Front (A) and lateral (C) view of patient 1. Front (B) and lateral (D) view of patient 2.

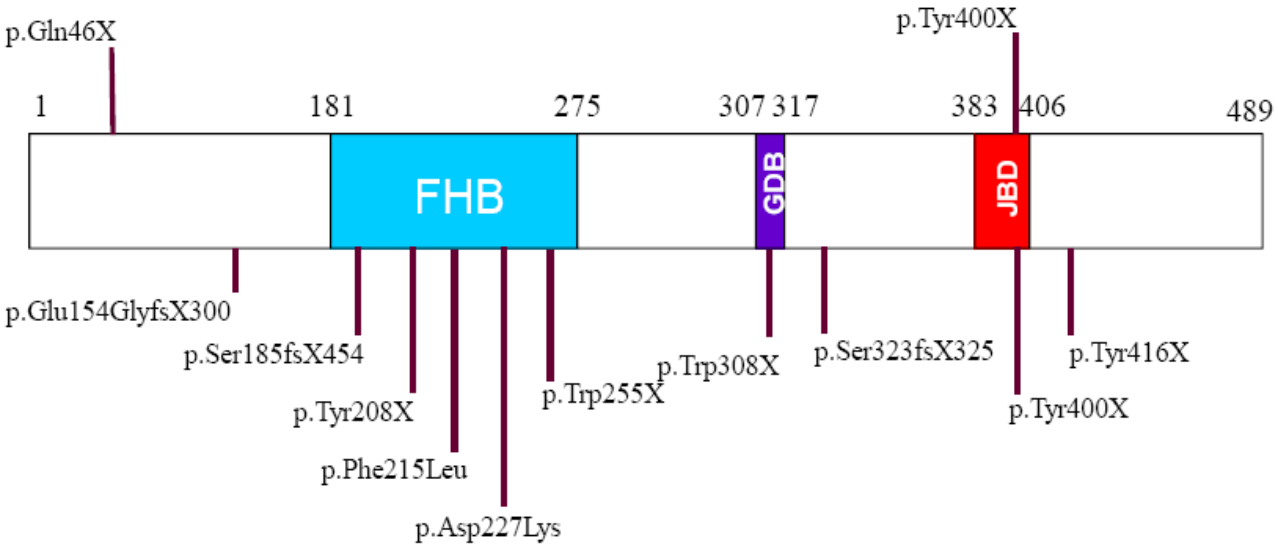

Figure 2. Schematic representation of the protein. *FOXG1* mutations already reported in the literature on the bottom; the two mutations reported in the present article on the top.

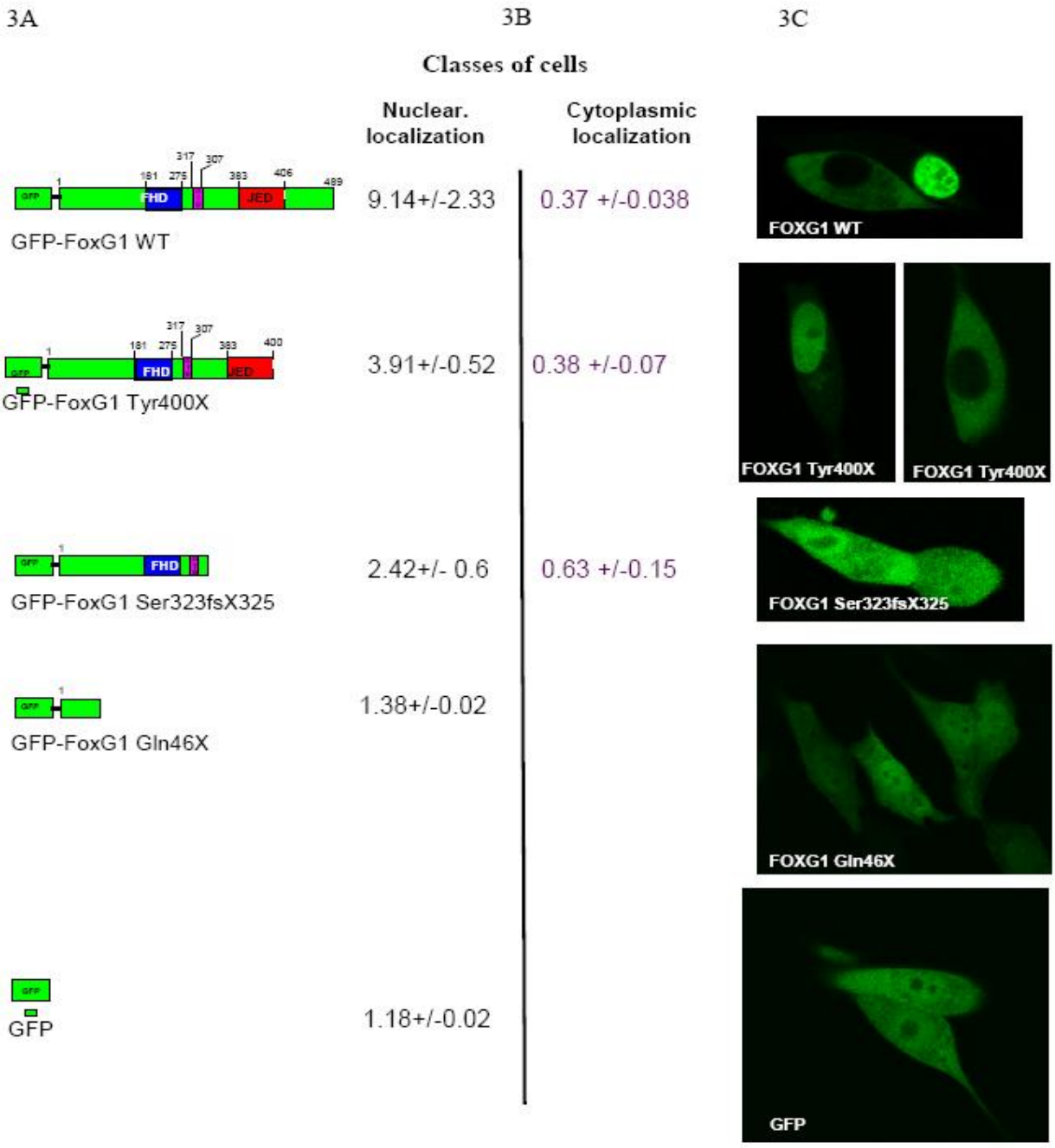

Figure 3. GFP-FoxG1 Fluorescently tagged mutants and subcellular localization.

A) Schematic representation of the constructs used in this study with the definition of the functional regions and the location of nonsense mutations. WT: Wild Type, FHD: Fork Head Domain; GTB: GROUCHO/TLE-Binding domain; JED: JARID1B Binding Domain.

B) Quantification of the two different classes of cells following the expression of the chimeric protein schematized on the left. The value indicate the nuclear/cytoplasmic (Nuc/Cyt) ratios of fluorescence intensity.

C) Picture of transfected cells showing different nuclear and cytoplasmic localization of GFPFoxG1 WT, GFP- Tyr400X, GFP- Ser323fsX325, GFP-Gln46X and GFP alone.

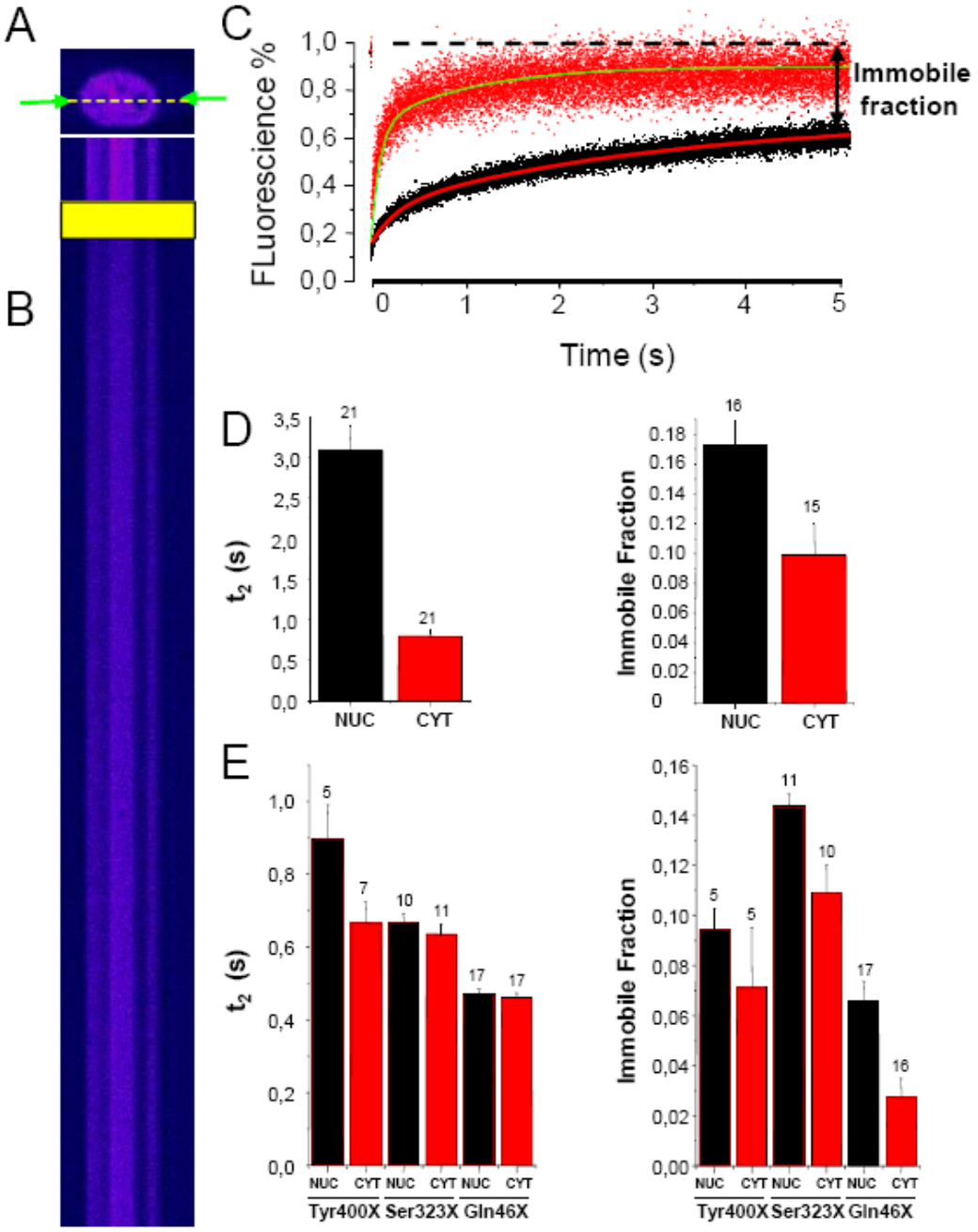

Figure 4. Relative mobility of FoxG1 in nuclear and in cytoplasmatic compartments (cells with nuclear localization of FoxG1)
A) High resolution imaging of a NIH3T3 transfected with GFP-FoxG nuclear localization. To assess the mobility of the protein at an high time resolution, repetitive line scans were performed along the line indicated by the green arrows. Pseudo colour were used to improve the readability of the image. Calibration bar 10 μm.

B) Time series showing the fluorescence intensity across the scanned line. The photobleaching, indicated by the yellow rectangle, is followed by the gradual recovery of fluorescence.
C) Quantification of the signal intensity in the nucleus and in cytoplasm (black and red line, respectively). In this case the t2 were 3.02 s and 1.29 s (nucleus and cytoplasm respectively) and the immobile fractions were 0.18 and 0.8. D) Summary of average values for t2 and immobile fraction measured in cells transfect with GFP-FoxG1 wt.
D) Summary of average values for t2 and immobile fraction measured in cells transfect with GFP-Tyr400X, GFPSer323fsX325 and GFP-Gln46X. Numbers indicate the sample size and bars are standard errors. The p values are in the tables in the supplementary materials.

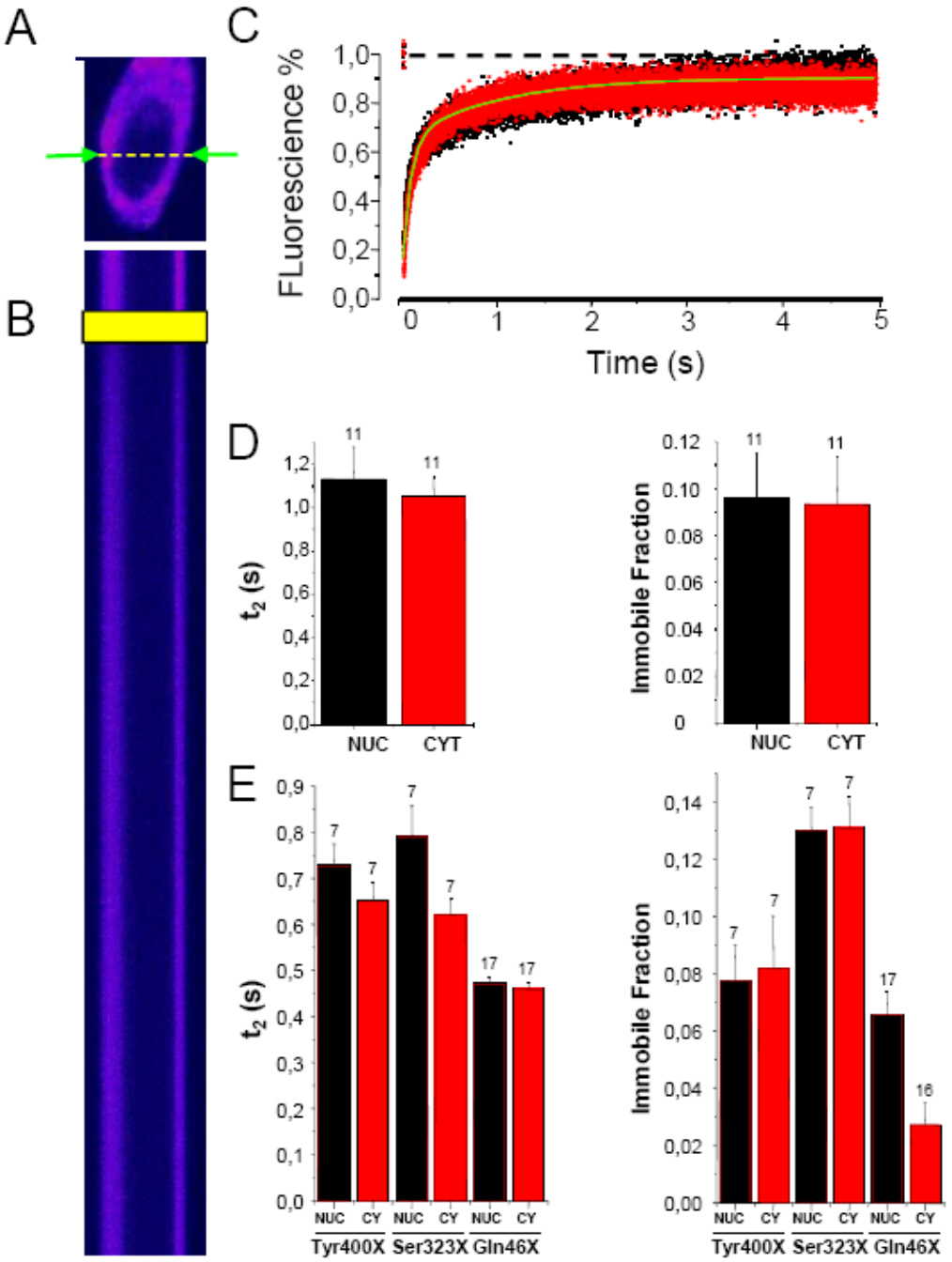

Figure 5. Relative mobility of FoxG1 in nuclear and in cytoplasmatic compartments (cells with cytoplasmic localization of FoxG1)
A) High resolution imaging of a NIH3T3 transfected with GFP-FoxG1 cytoplasmatic localization. To assess the mobility of the protein at an high time resolution, repetitive line scans were performed along the line indicated by the green arrows. Pseudo colour were used to improve the readability of the image. Calibration bar 10 μm.

B) Time series showing the fluorescence intensity across the scanned line. The photobleaching, indicated by the yellow rectangle, is followed by the gradual recovery of fluorescence.
C) Quantification of the signal intensity in the nucleus and in cytoplasm (black and red line respectively). In this case the t2 were 1.2 s and 1 s (nucleus and cytoplasm respectively) and the immobile fractions were 0.8 and 0.8. D) Summary of average values for t2 and immobile fraction measured in cells transfected with GFP-FoxG1.
D) Summary of average values for t2 and immobile fraction measured in cells transfected with GFP-Tyr400X, GFPSer323fsX325 and GFP-Gln46X. Numbers indicate the sample size and bars are standard errors. The p values are in the tables in the supplementary materials.

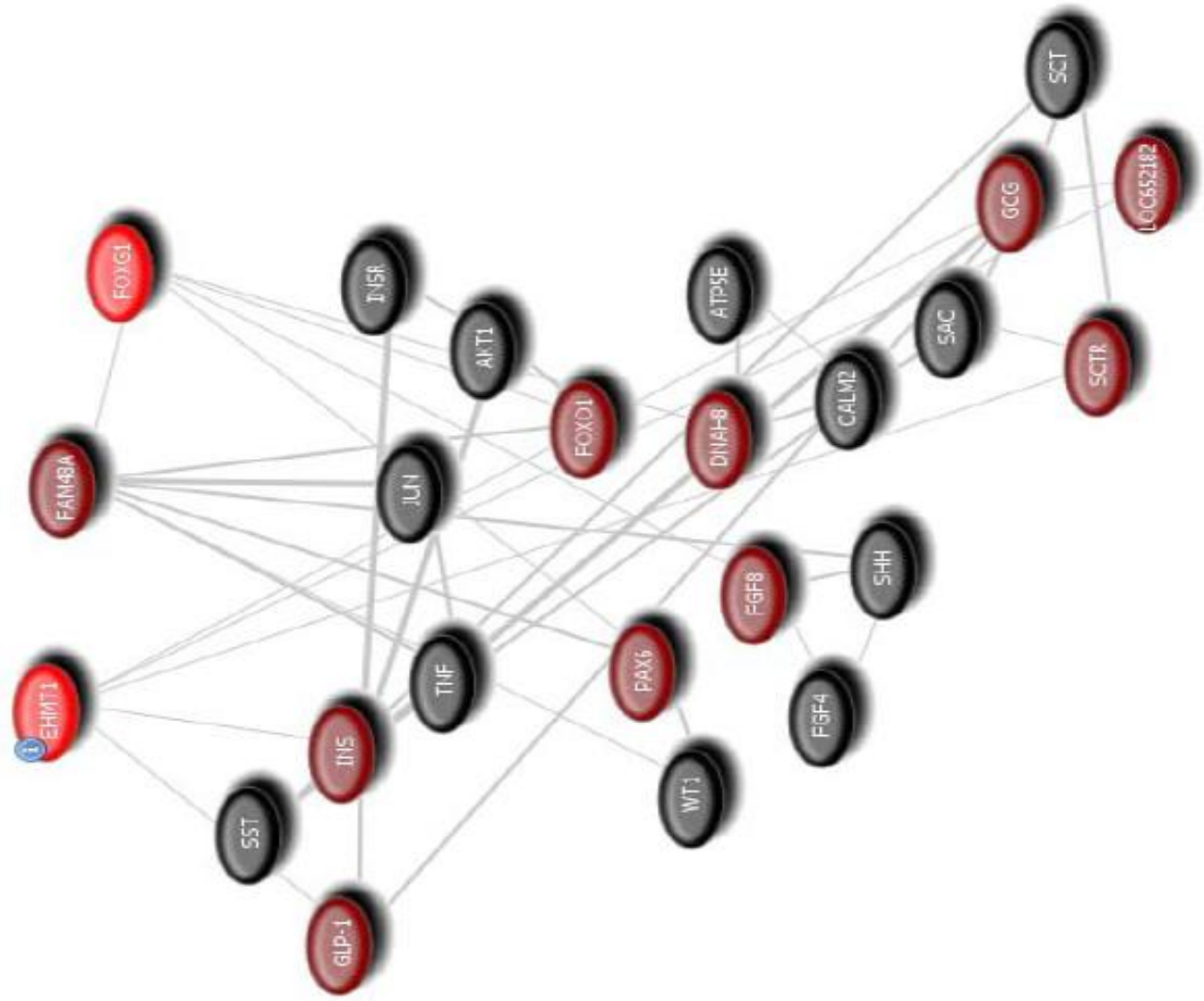

Figure 6. Graph showing the pathway connecting *FOXG1* and *EHMT1*.
The graph has been created using a tool based on co-occurrence in article (www.pubgene.org). The link between two genes/proteins represents an interaction reported at least in one article.

Table I

t-test p values of immobile fraction

immobile fraction			FOXG1 WT				FOXG1 Y400X				FOXG1 S323fsX325				FOXG1 Q46X		GFP	
			N/C ratio > 1		N/C ratio < 1		N/C ratio > 1		N/C ratio < 1		N/C ratio > 1		N/C ratio < 1		Nuc	Cyt	Nuc	Cyt
			Nuc	Cyt	Nuc	Cyt	Nuc	Cyt	Nuc	Cyt	Nuc	Cyt	Nuc	Cyt				
OXG1 WT	N/C ratio > 1	Nuc																
		Cyt	0.008															
	N/C ratio < 1	Nuc	0.007	N.S.														
		Cyt	0.006	N.S.	N.S.													
FOXG1 Y400X	N/C ratio > 1	Nuc	0.031	N.S.	N.S.	N.S.												
		Cyt	0.009	N.S.	N.S.	N.S.	N.S.											
	N/C ratio < 1	Nuc	0.003	N.S.	N.S.	N.S.	N.S.	N.S.										
		Cyt	0.006	N.S.	N.S.	N.S.	N.S.	N.S.	N.S.									
FOXG1 323fsX325	N/C ratio > 1	Nuc	N.S.	N.S.	0.024	0.028	$<10^{-4}$	$<10^{-3}$	$<10^{-4}$	0.001								
		Cyt	0.016	N.S.	N.S.	N.S.	N.S.	N.S.	N.S.	N.S.	0.008							
	N/C ratio < 1	Nuc	N.S.	N.S.	N.S.	N.S.	0.013	0.024	0.004	0.034	N.S.	N.S.						
		Cyt	N.S.	N.S.	N.S.	N.S.	0.032	0.031	0.008	0.041	N.S.	N.S.	N.S.					
FOXG1 Q46X	Nuc		$<10^{-5}$	N.S.	N.S.	N.S.	N.S.	N.S.	N.S.	N.S.	$<10^{-6}$	0.004	$<10^{-3}$	$<10^{-3}$				
	Cyt		$<10^{-7}$	0.005	0.024	0.002	$<10^{-3}$	0.032	0.002	0.004	$<10^{-10}$	$<10^{-5}$	$<10^{-7}$	$<10^{-6}$	0.002			
GFP	Nuc		$<10^{-5}$	0.018	0.002	0.006	$<10^{-4}$	0.019	$<10^{-3}$	0.003	$<10^{-10}$	$<10^{-5}$	$<10^{-7}$	$<10^{-6}$	$<10^{-3}$	N.S.		
	Cyt																	

The table reports the p values of the t-test between all the measured immobile fractions of the different proteins investigated.
N.S.: Not Significative (p>0.05)

Table II

t-test p values of T_2

T_2			FOXG1 WT				FOXG1 Y400X				FOXG1 S323fsX325				FOXG1 Q46X		GFP	
			N/C ratio > 1		N/C ratio < 1		N/C ratio > 1		N/C ratio < 1		N/C ratio > 1		N/C ratio < 1		Nuc	Cyt	Nuc	Cyt
			Nuc	Cyt	Nuc	Cyt	Nuc	Cyt	Nuc	Cyt	Nuc	Cyt	Nuc	Cyt				
OXG1 WT	N/C ratio > 1	Nuc																
		Cyt	$<10^{-8}$															
	N/C ratio < 1	Nuc	$<10^{-3}$	0.018														
		Cyt	$<10^{-4}$	0.022	N.S.													
FOXG1 Y400X	N/C ratio > 1	Nuc	0.002	N.S.	N.S.	N.S.												
		Cyt	$<10^{-3}$	N.S.	N.S.	0.021	N.S.											
	N/C ratio < 1	Nuc	$<10^{-3}$	N.S.	N.S.	0.021	N.S.	N.S.										
		Cyt	$<10^{-3}$	N.S.	0.023	0.006	0.022	N.S.	N.S.									
FOXG1 323fsX325	N/C ratio > 1	Nuc	$<10^{-5}$	N.S.	0.022	0.011	N.S.	N.S.	N.S.	N.S.								
		Cyt	$<10^{-5}$	N.S.	0.004	$<10^{-3}$	0.002	N.S.	N.S.	N.S.	N.S.							
	N/C ratio < 1	Nuc	$<10^{-3}$	N.S.	N.S.	N.S.	N.S.	N.S.	N.S.	N.S.	N.S.	0.027						
		Cyt	$<10^{-3}$	N.S.	0.016	0.003	0.011	N.S.	N.S.	N.S.	N.S.	N.S.	0.049					
FOXG1 Q46X	Nuc		$<10^{-8}$	$<10^{-4}$	$<10^{-5}$	$<10^{-7}$	$<10^{-6}$	$<10^{-4}$	$<10^{-6}$	$<10^{-4}$	$<10^{-4}$	$<10^{-5}$	$<10^{-5}$	$<10^{-4}$				
	Cyt		$<10^{-8}$	$<10^{-4}$	$<10^{-5}$	$<10^{-7}$	$<10^{-6}$	$<10^{-4}$	$<10^{-6}$	$<10^{-5}$	$<10^{-4}$	$<10^{-6}$	$<10^{-6}$	$<10^{-4}$	N.S.			
GFP	Nuc		$<10^{-4}$	0.001	0.001	$<10^{-4}$	$<10^{-4}$	0.001	$<10^{-4}$	$<10^{-3}$	0.002	$<10^{-4}$	$<10^{-3}$	$<10^{-3}$	N.S.	N.S.		
	Cyt		$<10^{-4}$	0.001	0.001	$<10^{-4}$	$<10^{-4}$	$<10^{-3}$	$<10^{-4}$	$<10^{-3}$	0.002	$<10^{-4}$	$<10^{-3}$	$<10^{-3}$	N.S.	N.S.	N.S.	

The table reports the p values of the t-test between all the measured T_2 of the different proteins investigated.
N.S.: Not Significative ($p>0.05$)

References

1. Jeffrey LN, G. Walter, E. Kaufmann, W. Daniel, G. Glaze, DG. Jhon, C. Angus, J. Clarke, A. Bahi- Buisson, N. Leonard, H. Bailey, M. Schanen, C. Zappella, M. Renieri, A. Huppke, P. Percy, A. Rett Syndrome: Revised Diagnostic Criteria and Nomenclature. Annals of Neurology 2010.

2. Huppke P, *et al.* Rett syndrome: analysis of MECP2 and clinical characterization of 31 patients. Hum Mol Genet. 2000;9:1369-1375.

3. Monros E, *et al.* Rett syndrome in Spain: mutation analysis and clinical correlations. Brain Dev 2001;Suppl 1:S251-253.

4. Smeets E, *et al.* Rett syndrome in adolescent and adult females: clinical and molecular genetic findings. Am J Med Genet A 2003;122:227-33.

5. Philippe C*, et al.* Phenotypic variability in Rett syndrome associated with FOXG1 mutations in females. J Med Genet 2009.

6. Hagberg B, *et al.* "Forme frustes" of Rett syndrome-a case report. Am J Med Genet 1986;24:175-181.

7. Hagberg BA, *et al.* Rett variants: a suggested model for inclusion criteria. Pediatr Neurol 1994;11:5-11.

8. Ariani F, *et al.* FOXG1 is responsible for the congenital variant of Rett syndrome. Am J Hum Genet 2008;83:89-93.

9. Mencarelli MA*, et al.* Novel FOXG1 mutations associated with the congenital variant of
Rett syndrome. J Med Genet;47:49-53.

10. Bahi-Buisson N, et al. Revisiting the phenotype associated with FOXG1 mutations: two novel cases of congenital Rett variant. Neurogenetics;11:241-9.

11. Bisgaard AM*, et al.* Additional chromosomal abnormalities in patients with a previously detected abnormal karyotype, mental retardation, and dysmorphic features. Am J Med Genet A 2006;140:2180-7.

12. Papa FT, *et al.* A 3 Mb deletion in 14q12 causes severe mental retardation, mild facial dysmorphisms and Rett-like features. Am J Med Genet A 2008;146A:1994-8.

13. Mencarelli MA, *et al.* 14q12 Microdeletion syndrome and congenital variant of Rett syndrome. Eur J Med Genet 2009;52:148-52.
14. Martynoga B, *et al.* Foxg1 is required for specification of ventral telencephalon and region-specific regulation of dorsal telencephalic precursor proliferation and apoptosis. Dev Biol 2005;283:113-27.
15. Yao J, *et al.* The winged-helix protein brain factor 1 interacts with groucho and hes proteins to repress transcription. Mol Cell Biol 2001;21:1962-72.
16. Roesch A, *et al.* RBP2-H1/JARID1B is a transcriptional regulator with a tumor suppressive potential in melanoma cells. Int J Cancer 2008;122:1047-57.
17. Marchi M, *et al.* Spatio-temporal dynamics and localization of MeCP2 and
pathological mutants in living cells. Epigenetics 2007;2:187-97.
18. Kumar A, *et al.* Analysis of protein domains and Rett syndrome mutations indicate that multiple regions influence chromatin-binding dynamics of the chromatinassociated protein MECP2 *in vivo*. J Cell Sci 2008;121:1128-37.
19. Regad T, *et al.* The neural progenitor-specifying activity of FoxG1 is antagonistically regulated by CKI and FGF. Nat Cell Biol 2007;9:531-40.
20. Hagberg BA, ed. Rett Syndrome - Clinical & Biological aspects. London: McKeith Press, 1993.
21. Shen L, *et al.* FoxG1 haploinsufficiency results in impaired neurogenesis in the postnatal hippocampus and contextual memory deficits. Hippocampus 2006;16:875-90.

Result 4.4

The smallest Microdeletion involving *FOXG1* and *C14orf23* is associated with the Congenital Variant of Rett syndrome plus mild dysmorphic features.

Ariele Spanhol-Rosseto* [1,2], Sheila Unger* [1], Uta Tacke [1], Tanja Velten [1], Bernhard Zabel [1], Ekkehart Lausch [1]

* *This manuscript submitted to the American Journal of Human Genetics*

The smallest Microdeletion involving *FOXG1* and *C14orf23* is associated with the Congenital Variant of Rett syndrome plus mild dysmorphic features.

Ariele Spanhol-Rosseto* [1,2], Sheila Unger* [1], Uta Tacke [1], Tanja Velten [1], Bernhard Zabel [1], Ekkehart Lausch [1]

[1] Centre for Pediatrics and Adolescent Medicine, University of Freiburg, Freiburg, Germany

[2] Medical Genetics, Department of Molecular Biology, University of Siena, Siena, Italy

* Both authors contributed equally to the work and are joint first authors

Corresponding author:

Dr. Ekkehart Lausch

Sektion Pädiatrische Genetik

UNIVERSITAETSKLINIKUM FREIBURG

Zentrum für Kinderheilkunde und Jugendmedizin

Tel +49 761 270-4391 / Fax -4471

Mathildenstraße 1, 79106 Freiburg

ekkehart.lausch@uniklinik-freiburg.de

Running title: Microdeletion involving *FOXG1* and *C14orf23*

Abstract

Rett syndrome is a severe neurodevelopment disorder and it is the second most common cause of mental retardation in females. Beside the most common classic form, due to *MECP2* mutations, a number of variants have been described such as the congenital variant. Recently, mutations of the *FOXG1* gene, located in 14q12, have been identified in patients affected by the congenital variant of Rett syndrome. To date, eleven cases with *FOXG1* point mutations and 7 patients with deletions of variable extension involving *FOXG1* have been reported. Here, we describe the smallest 14q12 microdeletion, involving only two genes *FOXG1* and *C14orf23,* in a patient affected by the congenital variant of Rett and showing additional mild dysmorphic features. Our patient has a phenotype overlapping the congenital variant of Rett and the 14q12 microdeletion syndrome. Given that no additional characteristics have been reported in patients with *FOXG1* point mutations, we could hypothesize that the mild facial dysmorphic features present in our patient are due to the *C14orf23* gene disruption.

Key words: *FOXG1,* Rett syndrome, congenital variant, array-CGH, 14q12 deletion, *C14orf23*

Introduction

Rett syndrome (RTT, OMIM#312750) is a neurodevelopmental disorder that represents one of the most common genetic causes of mental retardation in girls with an estimated prevalence of 1/7000-10000 female births [1-3]. In addition to the classic form, due to mutations in the *MECP2* gene, a number of variants have been described including the congenital variant [18, 22]. In 2008, mutations in the *FOXG1* gene, located in 14q12 have been identified as the cause of this phenotype [17, 59].

So far 11 *FOXG1* point mutations and 7 deletions of variable extension involving this gene have been reported in the literature [17, 37, 56, 59-64]. Patients with point mutations show a phenotype consistent with the diagnosis of congenital variant of RTT except one patient who is reported affected by classic RTT.

Beside the congenital RTT due to *FOXG1* point mutations, a 14q12 microdeletion syndrome has been described [17, 56]. These patients in addition to the severe neurological phenotype show peculiar facial features including downslanting palpebral fessures, bilateral epicantal folds, depressed nasal bridge, bulbous nasal tip, tended upper lip, everted lower lip and large ears [60].

Here we report on a new case with the smallest 14q12 microdeletion involving the *FOXG1* gene, identified by array-CGH, showing congenital RTT with additional characteristic facial features. We discuss the clinical correlation of cases with 14q12 deletion syndrome

Materials and methods

Genomic DNA isolation

Blood samples were obtained from patient and available parents after informed consent. Genomic DNA of the patient was isolated from an EDTA peripheral blood sample by using a QIAamp DNA Blood Kit according to the manufacturer protocol (Qiagen, www.qiagen.com). The Hoechest dye binding assay was used on a DyNA Quant™ 200 Fluorometer (GE Healthcare) to determine the appropriate DNA concentration. Genomic DNA from normal female 46,XX was obtained from Promega.

Array-CGH analysis

Array based CGH analysis was performed using a commercially available oligonucleotide microarray containing about 244.000 60-mer probes (Human Genome CGH Microarray 244A Kit, Agilent Technologies, Santa Clara, California).

FISH analysis

Chromosomal preparations for the analysis were obtained according to standard techniques. Fluorescent in situ hybridization (FISH) was performed with TelVision 14q12 probe (Vysis). Each experiment was carried out according to the manufacturer's instructions.

Results

Patient Description

A 4 year old female patient was recently referred to the Pediatric Unit of the Centre for Pediatrics and Adolescent Medicine of Freiburg University for severe developmental delay and postnatal microcephaly (Fig. 1). The patient is the second child of non consanguineous and healthy parents of Vietnam's origin. The older sister is healthy. At birth (39 weeks), auxological parameters were in the normal range (2865 gr, 10-25 cnt; OFC 32.5, 10-25 cnt, length 48 cm, 25-50 cnt) and Apgar score was 10 at 1' and 5'. She was noticed to be abnormal at 4 weeks of age with reduced spontaneous movements, disturbed sleep and long periods of crying and screaming. At 7 months she was not able to hold the head and to sit. At that time microcephaly was evident with length and weight in the normal range (length 69 cm, 90th cnt; weight 7.6kg, cnt and OFC 39cm, <3° cnt). The baby showed repetitive protruding tongue movements. At 15 months she was hypotonic, she was not able to sit, she showed severe feeding difficulties and she was easily frightened by the noise. At that time seizures occurred for the first time and they were characterized by myoclonus, eye rolling and hypersalivation. Currently, she is under therapy with Sultiam. EEG was normal aside from increased background activity. A brain MRI showed corpus callosum hypoplasia. At the time of the last examination she was 4 years. She showed microcephaly (OFC 43.5 cm, <<3° cnt) with normal weight (13.5kg) and length (96 cm), she presented severe developmental delay (never walking not sitting, poor head control, no speech), axial

hypotonia and seizures. Bruxism and sialorrhea were present. She was referred often to have wake periods at night. The patient showed hand apraxia, stereotypic hand movements and jerky movements of the 4 limbs. Tongue was always out of mouth and she showed good eye contact. She also showed some dysmorphic features such as anteverted large ears, tented upper lip, epichantal folds, short palpebral fissures. The Karyotype, 15q11.2 region analysis and *MECP2* molecular analysis resulted normal.

Array-CGH analysis

Whole array-based CGH analysis (Agilent 244K) with a spatial resolution of 8.9Kb (functional resolution of about 27 Kb) identified a deletion of approximately 640 Kb in 14q12 between 28.5 Mb and 29.2 Mb (proximal breakpoint: last oligonucleotide present at 28.58Mb and first deleted at 28.62Mb; distal breakpoint: last deleted oligonucleotide at 29.26 and first present at 29.27). Only two genes were present in the deleted region: *FOXG1* and *C14orf23* (Fig 2). The result was confirmed by FISH analysis. The same analysis did not reveal the deletion in parents' DNA confirming its *de novo* origin.

Discussion

Up to now 7 patients with the 14q12 microdeletion are reported. Two of them are large rearrangements extending beyond the 14q12 band (from q11.2 to q13) identified by karyotype [55]. One of them was reported in the Proceedings of the 2009 ESHG Meeting [63]. The deletion of this case extends for 2.8 Mb but its exact localization is unknown. The remaining four

are reported in figure 2 and extend from 2.6 Mb to 3.6 Mb [17, 56, 60, 62]. The present case represents the smallest 14q12 microdeletion reported up to now extending for only 640 Kb and including only tow genes. One of these genes is *FOXG1* previously associated with the congenital variant of RTT.

A number of features of the patient suggest the diagnosis of the congenital variant of RTT. These include severe developmental delay with normal perinatal period, severe postnatal microcephaly, stereotypic hand and tongue movements, hand apraxia, jerky movements of limbs, seizures, bruxism, sialorrhea, and corpus callosum hypoplasia. In particular, the presence a normal prenatal and perinatal period followed by a severe psychomotor delay with absence of speech and deambulation, postnatal micrcephaly with hand apraxia and stereotypic hand movements are the key elements for the diagnosis according to the last revised criteria of Rett syndrome variants [65].

In addition to signs typical of congenital RTT variant, the patient reported here presents additional dysmorphic features including anteverted large ears, tented upper lip, epichantal folds, short palpebral fissures. These peculiar facial features have been previously reported in the 14q12 microdeletion syndrome. Given that no additional characteristics have been reported in patients with FOXG1 point mutations, we could hypothesize that the mild facial dysmorphic features present in our patient are due to the disruption of the second gene present in the region, namely *C14orf23*.

C14orf23 is an homo sapiens chromosome 14 open reading frame 23, transcript variant 2, non-coding RNA. The role of non-coding genes in the

pathogenesis and potentially the treatment of several human diseases is increasingly being confirmed. Variations in non coding RNAs have been demonstrated to have a role in determining disease susceptibility [66]. Very recently, non coding RNA have been confirmed to cause human disease.

Interestingly, the patient reported by Jacob, although showing a larger deletion of about 2.6 Mb, lacks only the two genes deleted in our patient. Her phenotype was described as congenital RTT with dysmorphic features [62]. Although the facial phenotype of this patient is grossly described, this observation is in accordance with the hypothesis of the involvement of the gene *C14orf23* in the development of dysmorphic features.

This case confirms that the phenotype related to the *FOXG1* gene is specific and it is consistent with a congenital RTT.

Acknowledgements

We are grateful to the family for the participation to the study.

References

Ariani F, Hayek G, Rondinella D, Artuso R, Mencarelli MA, Spanhol-Rosseto A, Pollazzon M, Buoni S, Spiga O, Ricciardi S, Meloni I, Longo I, Mari F, Broccoli V, Zappella M, Renieri A. 2008. FOXG1 is responsible for the congenital variant of Rett syndrome. Am J Hum Genet 83(1):89-93.

Bahi-Buisson N, Nectoux J, Girard B, Van Esch H, De Ravel T, Boddaert N, Plouin P, Rio M, Fichou Y, Chelly J, Bienvenu T. 2009. Revisiting the phenotype associated with FOXG1 mutations: two novel cases of congenital Rett variant. Neurogenetics 11(2):241-9.

Bisgaard AM, Kirchhoff M, Tumer Z, Jepsen B, Brondum-Nielsen K, Cohen M, Hamborg-Petersen B, Bryndorf T, Tommerup N, Skovby F. 2006. Additional chromosomal abnormalities in patients with a previously detected abnormal karyotype, mental retardation, and dysmorphic features. Am J Med Genet A 140(20):2180-7.

Boute O. A 2,8Mb 14q12 deletion with severe encephalopathy and Rett-like features; 2009; Vienna. nature publishing group. p 96.

Chahrour M, Zoghbi HY. 2007. The story of Rett syndrome: from clinic to neurobiology. Neuron 56(3):422-37.

Hagberg B, Aicardi J, Dias K, Ramos O. 1983. A progressive syndrome of autism, dementia, ataxia, and loss of purposeful hand use in girls: Rett's syndrome: report of 35 cases. Ann Neurol 14:471-9.

Hagberg BA, Skjeldal OH. 1994. Rett variants: a suggested model for inclusion criteria. Pediatr Neurol 11:5-11.

Jacob FD, Ramaswamy V, Andersen J, Bolduc FV. 2009. Atypical Rett syndrome with selective FOXG1 deletion detected by comparative genomic hybridization: case report and review of literature. Eur J Hum Genet 17(12):1577-81.

Kamnasaran D, O'Brien PC, Schuffenhauer S, Quarrell O, Lupski JR, Grammatico P, Ferguson-Smith MA, Cox DW. 2001. Defining the breakpoints of proximal chromosome 14q rearrangements in nine patients using flow-sorted chromosomes. Am J Med Genet 102(2):173-82.

Knight JC. 2003. Functional implications of genetic variation in non-coding DNA for disease susceptibility and gene regulation. Clin Sci (Lond) 104(5):493-501.

Le Guen T, Bahi-Buisson N, Nectoux J, Boddaert N, Fichou Y, Diebold B, Desguerre I, Raqbi F, Daire VC, Chelly J, Bienvenu T. 2010. A FOXG1 mutation in a boy with congenital variant of Rett syndrome. Neurogenetics.

Mencarelli MA, Kleefstra T, Katzaki E, Papa FT, Cohen M, Pfundt R, Ariani F, Meloni I, Mari F, Renieri A. 2009. 14q12 Microdeletion syndrome and congenital variant of Rett syndrome. Eur J Med Genet 52(2-3):148-52.

Neul J, Kaufmann WE, Glaze D, Christodoulou J, Clarke A, Bahi-Buisson N, Leonard H, Bailey M, Schanen N, Zappella M, Renieri A, Huppke P,

Percy A. 2010. Rett Syndrome: Revised Diagnostic Criteria and Nomenclature. Ann Neurol in press.

Papa FT, Mencarelli MA, Caselli R, Katzaki E, Sampieri K, Meloni I, Ariani F, Longo I, Maggio A, Balestri P, Grosso S, Farnetani MA, Berardi R, Mari F, Renieri A. 2008. A 3 Mb deletion in 14q12 causes severe mental retardation, mild facial dysmorphisms and Rett-like features. Am J Med Genet A 146A(15):1994-8.

Philippe C, Amsallem D, Francannet C, Lambert L, Saunier A, Verneau F, Jonveaux P. 2010. Phenotypic variability in Rett syndrome associated with FOXG1 mutations in females. J Med Genet 47(1):59-65.

Rett A. 1966. Ueber ein eigenartiges hirnatrophisches Syndrom bei Hyperammonaemie im Kindesalter. WienMedWochenschrift 116:723-26.

Rolando S. 1985. Rett syndrome: report of eight cases. Brain and Development 7:290-296.

Figures legends

Figure 1. Patient pictures at the time of last examination are shown. Front (left) and profile (right). Note the severe microcephaly, tongue protrusion, the large and anteverted ears. Informed consent for pictures was obtained from the parents.

Figure 2. The deletion indicated by the array CGH experiment is mapped against the corresponding genomic region in the UCSC genome browser (a). In the lower part (b), the extent of the deletion in the patient described in this report is compared with that in the already reported patients.

Fig.1

Fig. 2

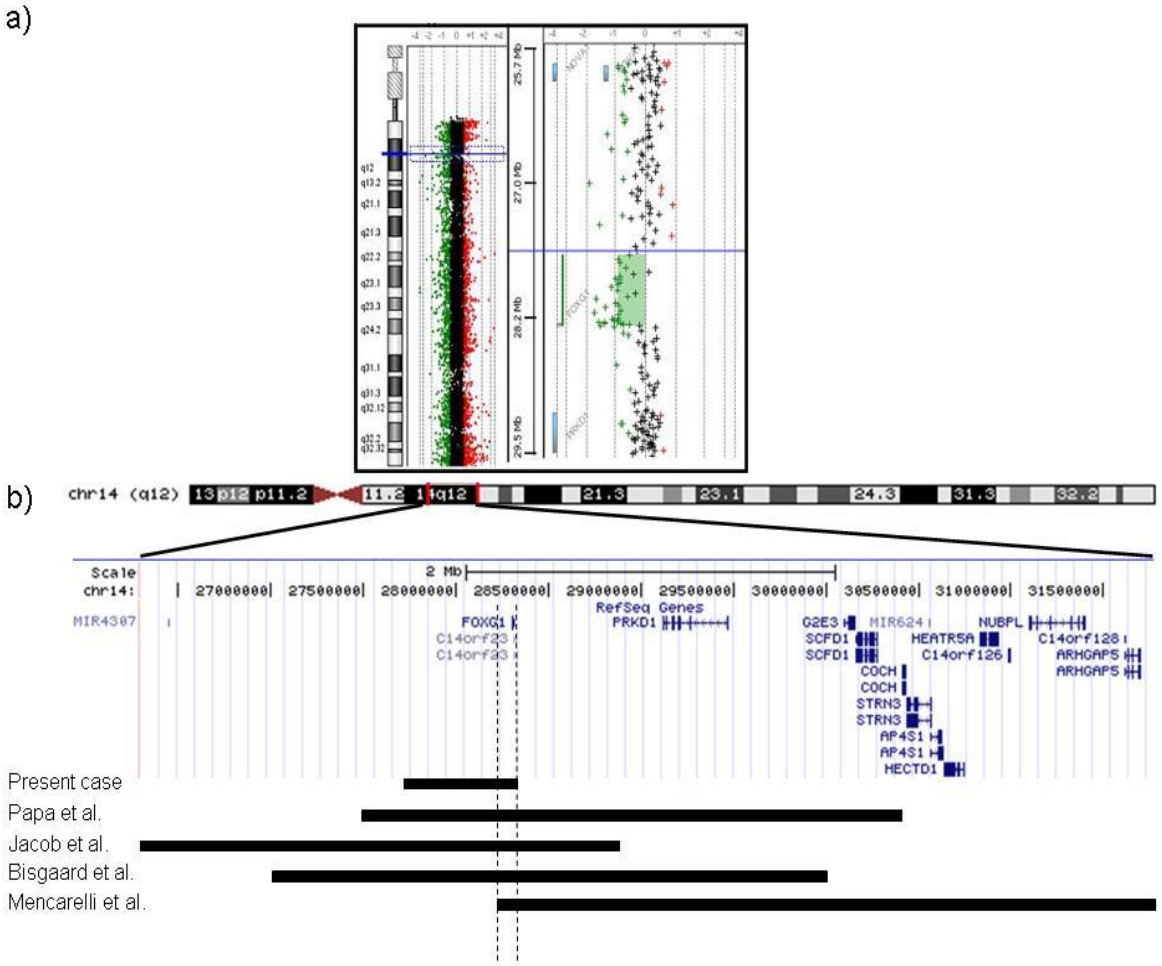
a)
b)
chr14 (q12)
Scale
chr14:
2 Mb
RefSeq Genes
MIR4307
FOXG1
C14orf23
PRKD1
G2E3
MIR624
NUBPL
SCFD1
HEATR5A
C14orf128
C14orf126
ARHGAP5
COCH
STRN3
AP4S1
HECTD1
Present case
Papa et al.
Jacob et al.
Bisgaard et al.
Mencarelli et al.

5. Conclusions and future perspectives

5. Conclusions and future perspectives

During the four years of the PhD course my research project has been focused mainly on searching for new genes involved in Rett syndrome.

In 2008 our group identified a girl with severe encephalopathy, postnatal microcephaly and Rett-like features with a 3 Mb deletion in 14q12 [17]. The region included only five genes. Among them we focused our attention on *FOXG1B* gene, because it is known to promote neuronal progenitor proliferation and to suppress premature neurogenesis; moreover, a possible association of the gene with mental impairment had been already reported [54, 55]. Mutation analysis, in a first cohort of 53 *MECP2/CDKL5*-mutation negative patients allowed us to identify the first two mutated patients classified (Result 3.1). Both patients had a clinical diagnosis of congenital variant of RTT. Subsequently, we decided to expand the analysis to other patients obtained through an international collaboration; in this second cohort, we identified five additional *FOXG1B* mutated cases (4 point mutations and a genomic deletion), all compatible with a diagnosis of congenital variant (Result 3.2 and 3.4). finally, we recently identified 2 more cases that displayed a milder phenotype and had been diagnosed as “forme fruste” RTT variants (Result 3.3).

Considering also cases reported by other groups, up to now 22 cases with a *FOXG1* alteration have been reported in literature: 8 deletions, one duplication, one inversion and 12 point mutations (table 1). Among those patients with a point mutation, 9 have a congenital phenotype while one is a classic RTT and the last two have a forme fruste variant. Therefore it seems

that the phenotype predominantly associated with *FOXG1* mutations is the congenital variant of RTT. However, the reported cases are still too few to draw definitive conclusions. Moreover, the identification of 2 patients with a "*forme fruste*" phenotype suggest the possibility that some *FOXG1* mutations could be associated with milder phenotypes. In agreement with this hypothesis, it is worth noting that, the only other patient without the severe phenotype of congenital RTT variant (case 8 in Table 1 with a classic RTT) has the same mutation identified in one of our *forme fruste* patients (p.Tyr400X, patient 12 in Table 1).

Regarding patients with chromosomal aberrations, we can distinguish four categories: i) patients with complex rearrangements; ii) patients with deletions larger than 3 Mb and involving more than 3 genes; iii) 2 patients with a small deletion involving only *FOXG1* and a putative gene with unknown function; iv) one patient with a large duplication. Not for all patients a detailed clinical description is available; it is thus difficult to draw a conclusion on their phenotypic category. The two patients with a smaller deletion have a congenital phenotype (case 18 and 21 in table 1), reinforcing the idea that this might be the main phenotype associated with *FOXG1*. Patients with larger deletions still have RTT features associated with a dysmorphic facies including downslanting palpebral fessures, bilateral epicantal folds, depressed nasal bridge, bulbous nasal tip, tended upper lip, everted lower lip and large ears. This condition is defined as "14q12 deletion syndrome" [60]. For those patients having a complex

rearrangement the phenotype is more variable and genotype-phenotype correlation is difficult to define.

FOXG1 encodes for a transcription factor that plays an essential role in the development of mammalian ventral telencephalon. Accordingly, *Foxg1* knock-out (KO) mouse brain shows a remarkable reduction of the telencephalic vesicles due to a severely compromised growth of the telencephalon and absence of ventral tissue [40, 44, 46, 47]. FoxG1 continues to be strongly expressed in brain areas known to undergo postnatal neurogenesis, namely the subventricular zone (SVZ) of the lateral ventricle and the dentate gyrus (DG) of the hippocampus. This suggests that it is also involved also in post-natal neurogenesis in these areas [67]. Accordingly, it has been demonstrated that FoxG1+/- mice have a 60% decrease in the total number of hippocampal dentate granule cells that is related to a loss of DG neurogenesis [67]. Consistent with these findings, heterozygous animals survive into adulthood but they display microcephaly, and behavioural and cognitive deficiencies consistent with an impairment of hippocampal function [67-69]. Our data show that, apart from the SVZ and DG, FoxG1 expression is maintained, although at lower levels, also post–mitotic neurons of post-natal cerebral cortex. Little is known about the potential function FoxG1 might exert in these cells. A glimpse might come from data reporting that, upon specific Foxg1 inactivation in the post–mitotic cerebral cortex compartment, neurons fail to localize correctly and cortical layers are disorganized (Fishell G., Cortical Development Meeting, Chaina, Greece, 2008). This raises the possibility that FoxG1 might

be involved in neuronal migration and layers organization. It is interesting to note that our data show that post-natal areas of FoxG1 expression overlap to those of Mecp2, the first gene involved in RTT. Moreover, similar to Mecp2, Foxg1 protein can bind to histone deacetylase 1 protein and it is involved in the regulation of chromatin organization [3, 32]. It is thus tempting to speculate that the 2 proteins might participate to a common molecular pathway involved in the regulation of chromatin dynamics. This would explain the phenotypic overlap between patients with mutations in the two genes. However, further experiments will be necessary in order to confirm/exclude this hypothesis.

At the cellular level, Foxg1 protein is located inside the nucleus in a diffuse pattern that excludes heterochromatic foci in both neuronal and non-neuronal cells (Result 3.1). We thus hypothesized that the protein is probably not stably associated to heterochromatin. To address this point, and define the consequences of pathogenic mutations, we used an in vitro expression system that allowed us to study FoxG1 sub-cellular localization and the dynamics of its association to chromatin (Result 3.3). Our experiments demonstrated that wild type FoxG1 binds to chromatin in a reversible way; however, a significant fraction of the total protein is stably bound. It is tempting to speculate that these two FoxG1 fractions (the reversible and the stably bound ones) might reflect two different functional roles of FoxG1 inside the nucleus: the reversibly bound protein might be associated to a dynamic modulation of gene expression. On the contrary, stably bound FoxG1 might act as a structural protein involved in chromatin

organization and long term gene repression. Analysis of pathological derivatives revealed a progressive impairment of FoxG1 nuclear localization indicating that larger truncations results in a dramatic reduction in chromatin affinity, with the Gln46X mutation resulting in a diffuse and homogeneous protein localization. This indicates that protein integrity is essential for nuclear localization; however, different portions of the protein are involved in controlling protein FoxG1 nuclear localization and thus chromatin affinity.

It is interesting to note that the extension of FoxG1 deletion and localization impairment do not correlate with the severity of the clinical phenotype. Indeed, the mutation resulting in the shorter protein (only 46 aminoacids) leads to milder phenotype (*forme fruste*) respect to the mutation that results in the more severe congenital RTT variant. These results could be explained if we consider that RTT patients with *FOXG1* mutations are heterozygotes presenting in the same cell both mutated and wild type proteins. Therefore, the severity of phenotype could be ascribed to the fraction of protein which is stably bound to chromatin (immobile fraction). In fact, the protein with p.Ser323fsX325 mutation presenting a higher immobile fraction respect to Gln46X and Tyr400X can act as dominant negative by excluding the access of FoxG1 wt to chromatin. In the case of Gln46X mutation, that almost abolishes the protein, the competition with FoxG1 wt is absent. FoxG1 wt protein encoded by the second allele can thus exert its normal function. As concerns the Tyr400X mutation, it is important to note that, compared to the other 2 mutations, both the DNA-

binding Forkhead domain and the Groucho-binding domain are intact and that it preserves almost the entire JARID1 domain. As expected its immobile fraction is higher respect to Gln46X but it is lower if compared to Ser323fsX325 mutant protein that represent a somehow intermediate condition between the more N-terminal (Gln46X) mutation and the C-terminal one (Tyr400X). Therefore, it is tempting to speculate that there might be a "critical length" of the protein that influences its tridimensional structure and thus its interaction with chromatin: longer proteins might maintain a certain ability to bind chromatin while shorter ones might have a tridimensional structure that does not allow the interaction anymore. Further experiments using different mutants that disrupt the protein at different levels are required to test this hypothesis.

The first glimpse on the molecular mechanisms of RTT was obtained in 1999 with the identification of *MECP2* as the main gene responsible for the disorder [6]. Subsequently, we and others showed that another X-linked gene, *CDKL5*, is responsible for atypical RTT, namely the early onset seizures variant [16]. Now with the work described in this thesis we added another important piece to this intriguing puzzle with the identification of the third gene involved in this complex disorder. Further studies will be necessary to both define the phenotype associated with mutations in this gene and the mechanisms leading from *FOXG1* deficiency to RTT phenotype.

Table I. *FOXG1* mutated patients identified until now (august 2010)

PATIENTS	PHENOTYPE	*FOXG1* MUTATION
1- Ariani *et al*; 2008	Congenital	c.765G>A; p.W255X
2- Ariani *et al*; 2008	Congenital	c.969delC; p.S323fsX325
3- Mencarelli *et al*; 2009	Congenital	c.681C>G; p.N227K
4- Mencarelli *et al*; 2009	Congenital	c.643T>C; p.F215L
5- Mencarelli *et al*; 2009	Congenital	c.551_552insC; p.S185fsX454
6- Mencarelli *et al*; 2009	Congenital	c.624C>G; p.Y208X
7- Philippe *et al* ; 2009	Congenital	c.924A>G; p.Trp308X
8- Philippe *et al;* 2009	Classic	c.1200C>G; p.Tyr400X
9- Bahi-Buisson *et al*; 2009	Congenital	c.C1248G; p.Y416X
10- Bahi-Buisson *et al*; 2009	Congenital	c.460_461dupG; p.E154GfsX300
11- De Filippis et al (manuscript submitted)	RTT forme fruste	c.136C>T; p.Gln46X
12- De Filippis et al (manuscript submitted)	RTT forme fruste	c.1200C>A; p.Tyr400X
13- Shoichet *et al ; 2005*	RTT features	46,XX,t(2;14)(p.22;q12), Inversion with FOXG1 at breakpoint [28.956-28.959Mb]-[27.534-27.695Mb]
14- (Case 5) Bisgaard *et al*; 2006	RTT features and dysmorphic face	46,XX,t(2;14), with 14q deletion 2.65-3.5Mb [27.2-29.8Mb]
15- (Case3) Kamnasaran *et al; 2001*	Not available	14q Deletion 46,XY,del(14)(q11.2q13) Identified at karyotype
16- (Case5) Kamnasaran *et al; 2001*	Developmental delay, agenesis corpus callosum	14q Deletion, 46,XY,del(14)(q11.2q13) Identified at karyotype
17- Papa *et al*; 2008	RTT features and dysmorphic face	14q deletion, 3Mb [27.5-30.4Mb]
18- Boute *et al; 2010*	RTT features and dysmorphic face	14q deletion, 2.8Mb
19- Mencarelli *et al*; 2009	RTT features and dysmorphic face	14q deletion, 3.6Mb [28.2-31.8Mb] + 10q21.1 deletion, 4.8Mb [52.9-57.7Mb]
20- Jacob *et al*; 2009	Congenital	14q deletion, 2.6Mb [26.3-28.9Mb]
21- Freiburg case report (unpublished case)	Congenital	14q deletion, 0.64 Mb [27.7-28.34Mb]
22- Yeung *et al*; 2009	Developmental delay, early onset seizures	14q duplication, 4.45Mb [25.9-30.4Mb]

6. Personal contribution

6. Personal contribution

During the first three years of Ph.D. course, my research activity was focused on the molecular diagnosis of Rett syndrome patients. To this aim, I used a combination of DHPLC, Sequencing analysis, MLPA and Real Time quantitative PCR in order to identify point mutations and deletions/duplications in both *CDKL5* and *MECP2* genes.
I have been also involved in the identification of the gene responsible for the Congenital variant of RTT through a collaboration with international laboratories

In the last year I spent a research period in the laboratory of Human Genetics, Pediatric Neurology Unit of University Hospital of Freiburg studying a cohort of Rett-like patients in order to identify new *FOXG1* mutations. This experience led to the identification of the patient described in Results 3.4. A manuscript reporting this patient is presently in preparation.

Concerning work data, I contributed to the project as follows:

Result 3.1 [59]: I performed *FOXG1* mutational analysis by DHPLC and direct sequencing and searched for gene deletions/duplications by real time qPCR. I also searched for literature data about FoxG1 function for manuscript preparation.

Result 3.2 [60]: I performed *FOXG1* molecular analysis in an international cohort of Rett patients by DHPLC, direct sequencing and real time qPCR. Moreover, I collaborated to write the manuscript; in particular, I reviewed literature data, I wrote the introduction and the results of patients molecular analysis and I prepared the figures.

Result 3.3 (manuscript submitted): I performed *FOXG1* mutational analysis by DHPLC, direct sequencing and real time qPCR.

Result 3.4 (unpublished case): I collaborated to perform molecular analysis by direct sequencing and I collaborated to write the manuscript.

7.References

7.References

1. Rett A. **Ueber ein eigenartiges hirnatrophisches Syndrom bei Hyperammonaemie im Kindesalter**. Wien.Med.Wochenschrift 1966;116:723-26.
2. Hagberg B, *et al.* **A progressive syndrome of autism, dementia, ataxia, and loss of purposeful hand use in girls: Rett's syndrome: report of 35 cases.** Ann Neurol 1983;14:471-9.
3. Chahrour M, *et al.* **The story of Rett syndrome: from clinic to neurobiology**. Neuron 2007;56:422-37.
4. Renieri A, *et al.* **Diagnostic criteria for the Zappella variant of Rett syndrome (the preserved speech variant)**. Brain Dev 2009;31:208-16.
5. Zappella M. **The preserved speech variant of the Rett complex: a report of 8 cases,**. Eur Child Adolesc Psychiatry 1997;6:23-25.
6. Amir RE, *et al.* **Rett syndrome is caused by mutations in X-linked MECP2, encoding methyl-CpG-binding protein 2**. Nat Genet 1999;23:185-8.
7. D'Esposito M, *et al.* **Isolation, physical mapping, and Northern analysis of the X-linked human gene encoding methyl CpG-binding protein, MECP2**. Mammalian Genome 1996;7:533-535.
8. Meloni I, *et al.* **A mutation in the Rett syndrome gene, *MECP2*, causes X-linked mental retardation and progressive spasticity in males**. Am J Hum Genet 2000;67:982-985.
9. Artuso R. **Early-onset seizure variant of Rett syndrome: Definition of the clinical diagnostic criteria.** Brain and Development 2010;32:17-24.
10. Beyer KS, *et al.* **Mutation analysis of the coding sequence of the MECP2 gene in infantile autism**. Hum Genet 2002;111:305-9.
11. Hagberg BA, ed. *Rett Syndrome - Clinical & Biological aspects*. London: McKeith Press, 1993.
12. Christodoulou J, *et al.* MECP2-Related Disorders. In: Pagon RA BT, Dolan CR, Stephens K, ed. *GeneReviews*. Seattle (WA): University of Washington, 2001.
13. Sampieri K, *et al.* **Italian Rett database and biobank**. Hum Mutat 2007;28:329-35.
14. Scala E, *et al.* **MECP2 deletions and genotype-phenotype correlation in Rett syndrome**. Am J Med Genet A 2007;143:2775-84.
15. Mari F, *et al.* **CDKL5 belongs to the same molecular pathway of MeCP2 and it is responsible for the early-onset seizure variant of Rett syndrome.** Hum Mol Genet. 2005;14:1935-46.
16. Scala E, *et al.* **CDKL5/STK9 is mutated in Rett syndrome variant with infantile spasms.** J Med Genet 2005;42 (2):103-7.
17. Papa FT, *et al.* **A 3 Mb deletion in 14q12 causes severe mental retardation, mild facial dysmorphisms and Rett-like features**. Am J Med Genet A 2008;146A:1994-8.
18. Hagberg BA, *et al.* **Rett variants: a suggested model for inclusion criteria**. Pediatr Neurol 1994;11:5-11.

19. Hagberg B. **Clinical delineation of Rett syndrome variants**. Neuropediatrics 1995;26:62.
20. Hagberg B, *et al.* **Rett females: patterns of characteristic side-asymmetric neuroimpairments at long-term follow-up**. Neuropediatrics 2002;33:324-6.
21. De Bona C, *et al.* **Preserved speech variant is allelic of classic Rett syndrome**. Eur J Hum Genet 2000;8:325-330.
22. Rolando S. **Rett syndrome: report of eight cases**. Brain and Development 1985;7:290-296.
23. Zappella M, *et al.* ***Study of MECP2 gene in Rett syndrome variants and autistic girls***. Am J Med Genet (Neuropsychiatr Genet) 2003;119B:102-107.
24. Kriaucionus S, *et al.* **The major form of MeCP2 has a novel N-terminus generated by alternative splicing.** Nucleic Acids Res. 2004;32:1818-23.
25. Mnatzakanian GN, *et al.* **A previously unidentified MECP2 open reading frame defines a new protein isoform relevant to Rett syndrome.** Nat Genet 2004;36:339-341.
26. Jonce P. **Methylated DNA and MeCP2 recruit histone deacetylase to repress transcription.** Nat Genet 1998;19:187-91.
27. Nan X, *et al.* **Transcriptional repression by the methyl-CpG-binding protein MeCP2 involves a histone deacetylase complex.** Nature 1998;393:386-389.
28. Kokura K, *et al.* **The Ski protein family is required for MeCP2-mediated transcriptional repression.** J Biol Chem. 2001;276:34115-34121.
29. Kaludov NK, *et al.* **MeCP2 driven transcriptional repression in vito: selectivity for methylated DNA, action at a distance and contacts with the basal transcription machinery**. Nucleic Acids Research 2000;28:1921-1928.
30. Ng H, *et al.* **MBD2 is a transcriptional repressor belonging to MeCP1 histone deacetylase complex**. Nat Genet 1999;23:5-6.
31. Horike S, *et al.* **Loss of silent-chromatin looping and impaired imprinting of DLX5 in Rett syndrome.** Nat Genet 2005;37:31-40.
32. Yao J, *et al.* **The winged-helix protein brain factor 1 interacts with groucho and hes proteins to repress transcription**. Mol Cell Biol 2001;21:1962-72.
33. Ricciardi S, *et al.* **CDKL5 influences RNA splicing activity by its association to the nuclear speckle molecular machinery**. Hum Mol Genet 2009;18:4590-602.
34. Chahrour M, *et al.* **MeCP2, a key contributor to neurological disease, activates and represses transcription**. Science 2008;320:1224-9.
35. Bertani I, *et al.* **Functional consequences of mutations in CDKL5, an X-linked gene involved in infantile spasms and mental retardation**. J Biol Chem 2006;281:32048-56.
36. Nemos C. **Mutational spectrum of CDKL5 in early-onset encephalopathies: a study of a large collection of French patients and review of the literature.** Clin Genet 2009;76:357-71.

37. Bahi-Buisson N, *et al.* **Revisiting the phenotype associated with FOXG1 mutations: two novel cases of congenital Rett variant**. Neurogenetics 2009;11:241-9.
38. Rusconi L, *et al.* **CDKL5 expression is modulated during neuronal development and its subcellular distribution is tightly regulated by the C-terminal tail**. J Biol Chem 2008;283:30101-11.
39. Kameshita I, *et al.* **Cyclin-dependent kinase-like 5 binds and phosphorylates DNA methyltransferase 1**. Biochem Biophys Res Commun 2008;377:1162-7.
40. Xuan S, *et al.* **Winged helix transcription factor BF-1 is essential for the development of the cerebral hemispheres**. Neuron 1995;14:1141-52.
41. Dou C, *et al.* **BF-1 interferes with transforming growth factor beta signaling by associating with Smad partners**. Mol Cell Biol 2000;20:6201-11.
42. Hanashima C, *et al.* **Brain factor-1 controls the proliferation and differentiation of neocortical progenitor cells through independent mechanisms**. J Neurosci 2002;22:6526-36.
43. Hanashima C, *et al.* **Foxg1 suppresses early cortical cell fate**. Science 2004;303:56-9.
44. Martynoga B, *et al.* **Foxg1 is required for specification of ventral telencephalon and region-specific regulation of dorsal telencephalic precursor proliferation and apoptosis**. Dev Biol 2005;283:113-27.
45. Muzio L, *et al.* **Foxg1 confines Cajal-Retzius neuronogenesis and hippocampal morphogenesis to the dorsomedial pallium**. J Neurosci 2005;25:4435-41.
46. Tao W, *et al.* **Telencephalon-restricted expression of BF-1, a new member of the HNF-3/fork head gene family, in the developing rat brain**. Neuron 1992;8:957-66.
47. Hebert JM, *et al.* **The genetics of early telencephalon patterning: some assembly required**. Nat Rev Neurosci 2008;9:678-85.
48. Danesin C, *et al.* **Integration of telencephalic Wnt and hedgehog signaling center activities by Foxg1**. Dev Cell 2009;16:576-87.
49. Manuel M, *et al.* **The transcription factor Foxg1 regulates the competence of telencephalic cells to adopt subpallial fates in mice**. Development 2010;137:487-97.
50. Huh S, *et al.* **Dorsal-ventral patterning defects in the eye of BF-1-deficient mice associated with a restricted loss of shh expression**. Dev Biol 1999;211:53-63.
51. Hanashima C, *et al.* **The role of Foxg1 and dorsal midline signaling in the generation of Cajal-Retzius subtypes**. J Neurosci 2007;27:11103-11.
52. Dou CL, *et al.* **Dual role of brain factor-1 in regulating growth and patterning of the cerebral hemispheres**. Cereb Cortex 1999;9:543-50.
53. Seoane J. **p21(WAF1/CIP1) at the switch between the anti-oncogenic and oncogenic faces of TGFbeta**. Cancer Biol Ther 2004;3:226-7.

54. Shoichet SA, *et al.* **Haploinsufficiency of novel FOXG1B variants in a patient with severe mental retardation, brain malformations and microcephaly**. Hum Genet 2005;117:536-44.
55. Kamnasaran D, *et al.* **Defining the breakpoints of proximal chromosome 14q rearrangements in nine patients using flow-sorted chromosomes**. Am J Med Genet 2001;102:173-82.
56. Bisgaard AM, *et al.* **Additional chromosomal abnormalities in patients with a previously detected abnormal karyotype, mental retardation, and dysmorphic features**. Am J Med Genet A 2006;140:2180-7.
57. Hagberg B, *et al.* **An update on clinically applicable diagnostic criteria in Rett syndrome. Comments to Rett Syndrome Clinical Criteria Consensus Panel Satellite to European Paediatric Neurology Society Meeting, Baden Baden, Germany, 11 September 2001**. Eur J Paediatr Neurol 2002;6:293-7.
58. Ariani F, *et al.* **Real-time quantitative PCR as a routine method for screening large rearrangements in Rett syndrome: Report of one case of MECP2 deletion and one case of MECP2 duplication**. Hum Mutat 2004;24:172-7.
59. Ariani F, *et al.* **FOXG1 is responsible for the congenital variant of Rett syndrome**. Am J Hum Genet 2008;83:89-93.
60. Mencarelli MA, *et al.* **14q12 Microdeletion syndrome and congenital variant of Rett syndrome**. Eur J Med Genet 2009;52:148-52.
61. Philippe C, *et al.* **Phenotypic variability in Rett syndrome associated with FOXG1 mutations in females**. J Med Genet 2009.
62. Jacob FD, *et al.* **Atypical Rett syndrome with selective FOXG1 deletion detected by comparative genomic hybridization: case report and review of literature**. Eur J Hum Genet 2009;17:1577-81.
63. Boute O. A 2,8Mb 14q12 deletion with severe encephalopathy and Rett-like features. *European Human Genetics Conference 2009*. Vol 17. Vienna: nature publishing group, 2009:96.
64. Le Guen T, *et al.* **A FOXG1 mutation in a boy with congenital variant of Rett syndrome**. Neurogenetics 2010.
65. Neul J, *et al.* **Rett Syndrome: Revised Diagnostic**
Criteria and Nomenclature. ANNALS of Neurology 2010;in press.
66. Knight JC. **Functional implications of genetic variation in non-coding DNA for disease susceptibility and gene regulation**. Clin Sci (Lond) 2003;104:493-501.
67. Shen L, *et al.* **FoxG1 haploinsufficiency results in impaired neurogenesis in the postnatal hippocampus and contextual memory deficits**. Hippocampus 2006;16:875-90.
68. Eagleson KL, *et al.* **Disruption of Foxg1 expression by knock-in of cre recombinase: effects on the development of the mouse telencephalon**. Neuroscience 2007;148:385-99.

69. Siegenthaler JA, *et al.* **Foxg1 haploinsufficiency reduces the population of cortical intermediate progenitor cells: effect of increased p21 expression**. Cereb Cortex 2008;18:1865-75.

8. Acknowledgements

My first “thank you!” goes to my family and friends who gave me strength and courage to leave everything and everyone in my home country and to come to Italy for a new great intellectual and cultural experience. Here I could learn a lot, not only about medical genetics; I learned a new language and came in contact with a new culture, I learned how to work in a group and take my responsibilities.

I would like to thank Professor Alessandra Renieri for the great opportunity she gave me to make the work I like. Thanks for your help also to all the medical doctors, the nurses and the technicians of the laboratory. A special thank to Ilaria Meloni, Francesca Mari, and Francesca Ariani who guided me during the four years of my PhD . I am also very grateful to all my colleagues from the laboratory. Some of them became great friends that I will always bring in my heart. I want to thank those who always supported me and gave me strength in the most difficult moments, especially Ilaria M, Elisa, Viria, Roberta, Mariangela,Gabriella,Francesca Sc.

A special thank to Professors A Superti-Furga, B Zabel, S Unger and E Lausch for their kind collaboration and for making me feel good even if I was very far of my house ...in Freiburg. They also gave me the opportunity to make a great new research experience. I want to thank also the new friends I met in the Freiburg laboratory: Karstin, Maren, Tanja, Romy, Christoph and a special thank to Sophia.

I am very grateful to my boyfriend Federico; he had the patience to wait when I was far from him for months, and he gave me support in the moments of stress and anxiety.

Finally, “thankyou!” to all the families of RETT syndrome patients. You are the ones that allow our research to go on!

In memory of my brother Honorato Spanhol who always encouraged me…

9. Appendix

9.1 Curriculum Vitae

Name: Ariele

Last name: Spanhol Rosseto

Date of Birth: 28/05/1984

Place of Birth: Cachoeiro de Itapemirim, Espirito Santo, Brazil

Study:

August 2006: Degree in Biological Science at the University of Sao Pedro, *FAESA*, Vitoria, Espirito Santo, Brazil.

Research Project:

October 2006 – today: worked as Ph.D. student in the Research Project focused on the molecular diagnosis of Rett syndrome for the identification and characterization new genetic lesions involved in Rett syndrome under the supervision of prof. Alessandra Renieri, Medical Genetics, University of Siena.

List of Publications:

FOXG1 is responsible for the congenital variant of Rett syndrome
Ariani F, Hayek G, Rondinella D, Artuso R, Mencarelli MA, **Spanhol-Rosseto A,** Pollazzon M, Buoni S, Spiga O, Ricciardi S, Meloni I, Longo I, Mari F, Broccoli V, Zappella M, Renieri A. Medical Genetics, Molecular Biology Department, University of Siena, 53100 Siena, Italy. Am J Hum Genet. 2008 Jul;83(1):89-93.

Novel FOXG1 mutations associated with the congenital variant of Rett syndrome.

Mencarelli M, **Spanhol-Rosseto A**, Artuso R, Rondinella D, De Filippis R, Bahi-Buisson N, Nectoux J, Rubinsztajn R, Bienvenu T, Moncla A, Chabrol B, Villard L, Krumina Z, Armstrong J, Roche A, Pineda M, Gak E, Mari F, Ariani F, Renieri A.

J Med Genet. 2010 Jan;47(1):49-53

**FOXG1* mutation leading to reduced chromatin affinity causes *"Rett fruste"* overlapping with *EHMT1* phenotype.

De Filippis R , Pancrazi , Bjørgo K , **Rosseto A** , Kleefstra T , Grillo E , Panighini A , Meloni I , Ariani F , Mencarelli MA , Hayek J , Renieri A , Costa M , Mari F .

* *This manuscript has been submitted to the Human Mutation.*

*The smallest Microdeletion involving *FOXG1* and *C14orf23* is associated with the Congenital Variant of Rett syndrome plus mild dysmorphic features.

Ariele Spanhol-Rosseto* [1,2], Sheila Unger* [1], Uta Tacke [1], Tanja Velten [1], Bernhard Zabel [1], Ekkehart Lausch [1]

**This manuscript submitted to American Journal of Human Genetics*.

9.2 List of abbreviations

RTT- Rett Syndrome

MECP2 - Methyl-CpG-binding Protein 2

FOXG1B - Forkhead box protein G1

CDKL5 - Cyclin-Dependent Kinase Like 5

PSV - Preserved Speech Variant

XLMR - X-Linked Mental Retardation

AS - Angelman Syndrome

PPM-X - X-linked mental retardation syndrome with Psychosis, Pyramidal signs, and Macroorchidism maps to Xq28

I.Q.- Intelligence Quotient

Ensembl - Is a joint project between EMBL - EBI and the Wellcome Trust Sanger Institute to develop a software system which produces and maintains automatic annotation on selected eukaryotic genomes

ISSX - X-linked Infantile Spasms

EEG - Electroencephalography

MBD - Methyl-CpG Binding Domain

TRD - Trascriptional Repression Domain

NLS - Nuclear Localisation Signal

C-ter - C-terminal domain

FHD - Fork-Head Domain

JBD - JARID1B Binding Domain

GTBD - Groucho-Binding Domain

BF-1 - Brain Factor 1

YB1 - Y box-binding protein 1

SHH - Sonic Hedgehog Homolog

GFP - Green Fluorescent Protein

FRAP - Fluorescence Recovery After Photobleaching

DHPLC - Denaturing High Performance Liquid Chromatography

PCR - Polymerase Chain Reaction

9.3 List of figures and tables

Introduction

the serine–threonine protein kinase active site (black box). The Thr-Glu-Tyr (TEY) motif in this domain is indicated by a black dashed line. The Putative NLS are indicated with blue lines. The MECP2 interaction domain (green box), and the DNMT1 interaction domain (yellow box) are also indicated. The orange square corresponds to the nuclear export signal. The signal peptidases I Serine active site, located in the C-terminal region of the protein, is represented by the striped box. Numbers at the top refer to the amino acid positions.

Figure 5. FoxG1 protein Functional Domains:
The three main functional domains of FoxG1 protein are shown: the DNA binding fork-head domain in light blue (FHD), the Groucho-binding domain in violet (GTBD), and the JARID1B binding domain in red (JBD). The numbers at the top refer to amino acid positions.

Result 3.1

Figure 1. FOXG1 Mutations and Alterations of the Functional Domains (A) Sequence tracing of FOXG1 mutations in the two patients. Mutated bases are indicated above the line. (B) Schematic representation of FoxG1 protein. The three main functional domains are shown: the DNA binding fork-head domain
in light blue (FHD), the Groucho-binding domain in violet (GTBD), and the JARID1B binding domain in red (JBD). The numbers at the top refer to the

amino acid positions. Mutations are indicated by zigzag lines. (C and D) Ribbon representation of the tertiary structure obtained with Phyre v.0.2 software. (C) shows the structure of the region containing the three functional domains of wild-type protein (amino acids 180–489). Arrows highlight the two mutations. The FHD domain (cyan) consists of three alpha helices and one beta hairpin (two beta strands and one loop), whereas the GTBD (violet) and JBD (red) domains are random coiled. (D) shows structural modification after p.W255X (left) and p.S323fsX325 (right) mutations. The p.W255X mutation determines a protein truncation just after the second beta strand leading to the loss of the beta hairpin and thus preventing DNA binding. The p.S323fsX325 mutation leaves the FHD domain intact and truncates the protein just after GTBD, inducing conformational changes that lead to its misfolding.

Figure 2. Pictures of the Two Congenital RTT Patients Case 1 (#156) is shown on the left; case 2 (#868) is shown on the right. They show peculiar jerky movements of the upper limbs frequently pushed in different directions accompanied by continuous flexionextension, wringing movements of the fingers of the hands. The hands were brought together in hand-washing and hand-mouth stereotypic activities, which were intense and present all the time they were awake. Similar flexion-extension movements of the toes were noticed in the feet. The double scoliosis of case 1 is clearly evident, whereas the other girl maintained a straight vertebral

column as often occurs in RTT in the first decade. Teeth grinding was present, and the tongue often protruded out from the mouth.

Figure 3. FoxG1 and MeCP2 Expression Domain in Postnatal Cortex and Neuronal Subnuclear Localization (A and B) Expression analysis by in situ hybridization of Foxg1 and MeCP2 on P8 postnatal forebrain tissue. As shown in (A), Foxg1 expression is found in differentiating and mature cortical neurons in the definitive cortical plate (indicated by arrows in [A]) similar to the MeCP2 expression pattern (indicated by arrows in [B]). In (A0), the inset shows background staining with a sense cRNA for Foxg1 in the same in situ hybridization conditions used for (A) and (B).

(C–J) FoxG1 and MeCP2 sub-cellular localization in non-neural and primary neurons. As shown in (C)–(F), in NIH 3T3 cells, MeCP2-GFP exogenous protein has a diffuse nuclear localization with accumulation in the heterochromatic foci (indicated by arrows in [D]) as identified when compared with DAPI staining (indicated by arrows in [C]). (E) and (F) show that conversely, FoxG1-flag exogenous protein displays a widespread nuclear localization without enrichment in heterochromatic sites. (G)– (J) show FoxG1 and MeCP2 localization in 12DIV (days in vitro) primary hippocampal neurons. In (G), MeCP2 endogenous protein is accumulated in heterochromatic foci (indicated by arrows). As shown in (H), FoxG1-flag exogenous nuclear localization is excluded from heterochromatic puncta (indicated by arrowheads). As shown in (I), MeCP2 and FoxG1-flag

colocalize in the nuclear compartment outside the heterochromatic foci. As shown in (J), Nuclear FoxG1-flag localization is detected in a differentiated b-III-tubulin-positive neuron. The following abbreviations are used: cx, cerebral cortex; se, septum; str, striatum; and v, ventricle.

Result 3.2

Table 1. Clinical features of patients with FOXG1 mutations.

Figure 1. Pictures of three of the new patients with FOXG1 mutations. Panel A, case 4; panel B, case 1; panel C, case 2. Note in patient 4 the constant and intense hand to mouth stereotypic activities. The severe microcephaly of case 1 is clearly evident. Patient 2, presently aged 6 years 6 months, is able to stand up only with support but she cannot walk. Parental/guardian consent has been obtained.

Figure 2. FOXG1 mutations and alterations of the functional domains. Schematic representation of FoxG1 protein. The three main functional domains are shown: the DNA binding fork-head domain, the Groucho binding domain and the JARID1B binding domain is red. The numbers at the top refer to the amino acid positions. The frameshift and stop mutations are showed below by zigzag lines. The missense mutations are indicated at the top. The asterisks indicate the two mutations previously reported in Ariani *et al.*[3]

Result 3.3

Figure 1. Pictures of the two patients Front (A) and lateral (C) view of patient 1. Front (B) and lateral (D) view of patient 2.

Figure 2. Schematic representation of the protein. *FOXG1* mutations already reported in the literature on the bottom; the two mutations reported in the present article on the top.

Figure 3. GFP-FoxG1 Fluorescently tagged mutants and subcellular localization.

A) Schematic representation of the constructs used in this study with the definition of the functional regions and the location of nonsense mutations. WT: Wild Type, FHD: Fork Head Domain; GTB: GROUCHO/TLE-Binding domain; JED: JARID1B Binding Domain.

B) Quantification of the two different classes of cells following the expression of the chimeric protein schematized on the left. The value indicate the nuclear/cytoplasmic (Nuc/Cyt) ratios of fluorescence intensity.

C) Picture of transfected cells showing different nuclear and cytoplasmic localization of GFPFoxG1 WT, GFP- Tyr400X, GFP- Ser323fsX325, GFP-Gln46X and GFP alone.

Figure 4. Relative mobility of FoxG1 in nuclear and in cytoplasmatic compartments (cells with nuclear localization of FoxG1)

A) High resolution imaging of a NIH3T3 transfected with GFP-FoxG nuclear localization. To assess the mobility of the protein at an high time resolution, repetitive line scans were performed along the line indicated by

the green arrows. Pseudo colour were used to improve the readability of the image. Calibration bar 10 μm.

B) Time series showing the fluorescence intensity across the scanned line. The photobleaching, indicated by the yellow rectangle, is followed by the gradual recovery of fluorescence.

C) Quantification of the signal intensity in the nucleus and in cytoplasm (black and red line, respectively). In this case the t2 were 3.02 s and 1.29 s (nucleus and cytoplasm respectively) and the immobile fractions were 0.18 and 0.8. D) Summary of average values for t2 and immobile fraction measured in cells transfect with GFP-FoxG1 wt.

D) Summary of average values for t2 and immobile fraction measured in cells transfect with GFP-Tyr400X, GFPSer323fsX325 and GFP-Gln46X. Numbers indicate the sample size and bars are standard errors. The p values are in the tables in the supplementary materials.

Figure 5. Relative mobility of FoxG1 in nuclear and in cytoplasmatic compartments (cells with cytoplasmic localization of FoxG1)

A) High resolution imaging of a NIH3T3 transfected with GFP-FoxG1 cytoplasmatic localization. To assess the mobility of the protein at an high time resolution, repetitive line scans were performed along the line indicated by the green arrows. Pseudo colour were used to improve the readability of

the image. Calibration bar 10 μm.

B) Time series showing the fluorescence intensity across the scanned line. The photobleaching, indicated by the yellow rectangle, is followed by the gradual recovery of fluorescence.

C) Quantification of the signal intensity in the nucleus and in cytoplasm (black and red line respectively). In this case the t2 were 1.2 s and 1 s (nucleus and cytoplasm respectively) and the immobile fractions were 0.8 and 0.8. D) Summary of average values for t2 and immobile fraction measured in cells transfected with GFP-FoxG1.

D) Summary of average values for t2 and immobile fraction measured in cells transfected with GFP-Tyr400X, GFPSer323fsX325 and GFP-Gln46X. Numbers indicate the sample size and bars are standard errors. The p values are in the tables in the supplementary materials.

Figure 6. Graph showing the pathway connecting *FOXG1* and *EHMT1*.

The graph has been created using a tool based on co-occurrence in article (www.pubgene.org). The link between two genes/proteins represents an interaction reported at least in one article.

Table I. t-test p value of immobile fraction

Table II. t-test p value T_2

Result 3.4

Figure 1. Patient face picture are shown. This is a picture of the patient at the time of the last examination. Informed consent for pictures was obtained from the parents.

Figure 2. DNA Analytics, software resolution 4.0 [CGH], Array -CGH results showing the 14q12 deletion. Chromosome ideograms and array CGH chromosomal profile of chromosome 14 are shown on the left. On the right, an enlargement showing the deleted segment of chromosome 14 [28.585.459-292.69.201].

Figure 3. Detailed view of the deleted region by Ensembl genome browser. The region contains only 2 genes: FOXG1B and C14orf23.

Conclusions and future perspectives

Table I. *FOXG1* mutated patients identified until now (august 2010)